NTNU

Norwegian University of
Science and Technology

Effect of Mechanical Recycling on the Hydrolytic Degradation of PLA used in Food Packaging

Anne Marthe Solvoll

Chemical Engineering and Biotechnology
Submission date: July 2016
Supervisor: Gisle Øye, IKP
Co-supervisor: Joaquín Martínez Urreaga, Spania-UPM

Norwegian University of Science and Technology
Department of Chemical Engineering

Preface

This thesis completes my Master of Science degree at the Department of Chemical Engineering at the Norwegian University of Science and Technology (NTNU). This project is built on a research internship completed the fall of 2015, and experimental work carried out at ETSII UPM at the Department of Environmental and Industrial Chemical Engineering. The experimental work was performed under the supervision of Professor Joaquín Martínez Urreaga, who was my main supervisor.

First, I would like to thank my supervisor, Professor Joaquín Martínez Urreaga, for great guidance, always being positive, and for giving me the opportunity to write this thesis. Second, I want to thank PhD student Freddys Beltran and Professor Maria Ulagares de la Orden, for teaching me everything I needed to know in the laboratory and for answering all of my questions. Third, I want to thank the Department of Environmental and Industrial Chemical Engineering at UPM for the treatment I have received and also I would like to thank my co-supervisor Professor Gisle Øye.

Finally, I would like to thank my family, friends and my boyfriend, Fernando for all the support and love they have given me. I could never have done it without you.

I declare that this is an independent work according to the exam regulations of the Norwegian University of Science and Technology (NTNU).

Madrid, Spain 17.07.2016

Anne Marthe Solvoll

Abstract

The demand for plastic continues to increase, and the search for sustainable solutions has become crucial for the large demand the world is facing today. The biopolymer polylactic acid (PLA) has generated special interest, especially for packaging in the food industry, due to its optical and mechanical properties, biocompatibility, and biodegradability.

The aim of this Master`s thesis was to examine the water uptake of mechanically recycled PLA, and consequently the hydrolytic degradation with the prospect of using the material as packaging material. It was compared with virgin PLA, to obtain information about the behaviour of the material in the recycled state.

The primary challenge with PLA regarding its use in different applications is its facility to undergo hydrolytic degradation in the presence of water. In hydrolytic degradation the ester bonds of the molecules undergo hydrolysis, leading to a decrease in average molecular weight and a worsening of mechanical properties and the stability of the material, which may render it useless for some applications. Therefore, it was necessary to test the utility of mechanical recycling of PLA and its nanocomposites by studying its resistance to hydrolytic degradation in comparison with the virgin material.

Commercial PLA pellets were purchased, which could be used just as they were, but a 2% Cloisite 30B™ clay was added to half of the PLA material. The pellets were prepared by extrusion and, half of the samples were exposed to accelerated ageing, cleaning and finally, mechanically reprocessed to simulate the recycling process. The PLA was immersed for different times in a buffer solution to maintain neutral conditions concerning hydrolytic degradation.

UV-Vis spectroscopy of the immersion liquid presented spectra that illustrated three bands located at 228, 246 and 290 nm. These bands grow with increasing immersion time and can be assigned to oligomers of low molecular weight, lactide, lactic acid and lactoyllactic acid that are formed during the hydrolytic degradation of PLA. The PLA endured hydrolytic degradation, and the small molecules formed migrated to the liquid during this process. The FTIR analysis presented the existence of four types of interactions between water and polymer that can be distinguished as very strongly-, strongly-, weakly- and very weakly absorbed water.

Fickian behaviour was assumed for the water diffusion up until two days of immersion and by this assumption, the diffusion coefficients were calculated. The diffusion coefficients for the recycled materials with and without clay were calculated to be $3.5 \cdot 10^{-12}$ and $7.1 \cdot 10^{-12}$ m^2/s respectively. Clay caused increased water absorption in the material, due to its hydrophilicity, and when dispersed as layers in the polymer it acts as a barrier preventing the passage of water. Thus, the material with clay has a lower diffusion coefficient, which may be important to slow the absorption of water in early stages, extending the life of the materials made with PLA. The recycling of the material caused a small degradation, altering the molecular structure of the polymer and thus, providing faster diffusion of water.

The measured intrinsic viscosity decreased with immersion time, and the degradation occurred more rapidly in the recycled material compared to the virgin material and even faster in the material with clay. Thermogravimetric analysis indicated that the thermal stability of the material is reduced with immersion time due to degradation and that the stability of the recycled material, is slightly inferior to the virgin material. The material with clay also showed to be inferior regarding the thermal stability, compared to the material without clay.

The results obtained in this project provided information on the water absorption and hydrolytic degradation of PLA, and about the effect on factors such as the presence of a layered clay or mechanical recycling of the plastic. Recycling has a slight negative effect on the material, where it increases the diffusion coefficient compared to the virgin material. The presence of clay sheets well dispersed in the polymer may slow the absorption of water, which can slow the first stages of the hydrolytic degradation.

The mechanical recycling, when no demanding cleaning steps are included in the process, gives materials with good properties, very similar to those corresponding to the virgin materials. The results obtained in this work appear to indicate that these recycled materials could be used in packaging. When a demanding cleaning step is included in the recycling process, the recycled materials show decreased stability, although the difference is small. These results support the feasibility of the mechanical recycling of PLA.

Abbreviations

PLA	Poly(lactic acid)
302	Cloisite™ 30B
PLAV	Virgin poly(lactic acid)
PLAV-302	Virgin poly(lactic acid) nanocomposites with 2% Cloisite™ 30B
PLAR	Recycled poly(lactic acid)
PLAR-302	Recycled poly(lactic acid) nanocomposites with 2% Cloisite™ 30B
PLARC	Recycled poly(lactic acid) that has undergone a cleaning step
PLARC-302	Recycled PLA nanocomposites with 2% Cloisite™ 30B that has undergone a cleaning step
PHA	Polyhydroxyalkanoates
PBS	Poly(butylene succinate)
PBAT	Polybutyrat
PE	Polyethylene
PP	Polypropylene
PET	Polyethylene terephthalate
PCL	Polycaprolactone
PTT	Polytrimethylene terephthalate
PVC	Polyvinyl chloride
PS	Polystyrene
LDPE	Low-density polyethylene
LLDPE	Linear low-density polyethylene
PLLA	Poly(L-lactide)
PDLA	Poly(D-lactide)
PDLLA	Poly(DL-lactide)
FTIR	Fourier transform infrared spectroscopy
ATR	Attenuated Total Reflection
UV-Vis	Ultraviolet-Visible spectroscopy
TA	Thermal Analysis
TGA	Thermogravimetric Analysis
MMT	Montmorillonite

List of symbols

M_t	Mass absorbed at a time, t
M_{inf}	Absorbed water mass at equilibrium
τ	$h^2/D\pi^2$
D	Apparent diffusion constant
D_c	Corrected apparent diffusion coefficient
h	Polymer thickness
n	Number of terms of the series
M_∞	Final mass at equilibrium
$[\eta]$	Intrinsic viscosity
η_r	Relative viscosity
η_{sp}	Specific viscosity
η_{red}	Reduced viscosity
η_{inh}	Inherent vicosity
M_v	The viscosity average molecular weight
K	Constant in Mark-Houwink-Sakurada equation for a given polymer-solvent pair dependent on temperature
α	Constant in Mark-Houwink-Sakurada equation for a given polymer-solvent pair dependent on temperature
T_g	Glass transition temperature
m	Mass
A	Absorbance

Contents

1. Introduction

The impact of 50 years of rampant plastics fabrication, disposal and use is now well recognised and documented. The fact that plastics made from non-renewable natural gas and petroleum resources threaten the environment is no secret. It threatens the human health, the very life of the ocean and species maintenance.

There is an increasing demand for plastics to be used for packaging and therefore an increase in the search for sustainable solutions to the large demand the world is facing today. Development of biodegradable plastics is part of the long-term solution to the damaging environmental consequences of plastic pollution (Dusselier et al., 2015). Polymers present several of desired properties like lightness, transparency and softness, and have been the most common supplier of packaging materials. Biobased and biodegradable plastics have a broad range of applications in biomedical, agriculture and packaging fields. The non-biodegradability of synthetic packaging materials and the increase in demand has led to a series of severe environmental problem. Using biodegradable polymers, especially in food packaging, can offer a solution to this issue (Siracusa et al., 2008).

Bioplastics can either be biodegradable, biobased or both. The fact that a plastic is biobased does not necessarily mean it is biodegradable. If a plastic is biodegradable, biobased or both it is defined as a bioplastic according to European Bioplastics.

Bioplastic can be divided into three different groups, and illustrated in figure 1.1:

- Both biobased and biodegradable bioplastics:
  - Polylactic acid (PLA), polyhydroxyalkanoates (PHA), polybutylene succinate (PBS) and starch blends
- Fossil resources based and biodegradable:
  - Polybutyrat (PBAT)
- Biobased/Partly biobased non-degradable plastics:
  - Polyethylene (PE), polypropylene (PP) and polyethylene terephthalate (PET) (Perstorp Winning Formulas).

Blends of thermoplastic starch (TPS) and aliphatic/aromatic polyesters are the most common of the biodegradable materials, such as polylactic acid (PLA), polycaprolactone (PCL) and polyhydroxy butyrate (PHB) (Bastioli, 2005; Soroudi & Jakubowicz, 2013). The terms biodegradable and bioplastic do not mean the same: biodegradable materials refer to materials that can be degraded by microbes by fermentation in a bioactive environment under specific conditions. But some materials degrade at such slow rates, that they are considered non-biodegradable. Plastic that is produced from a biological source with a short carbon cycle is defined as a bioplastic (Soroudi & Jakubowicz, 2013).

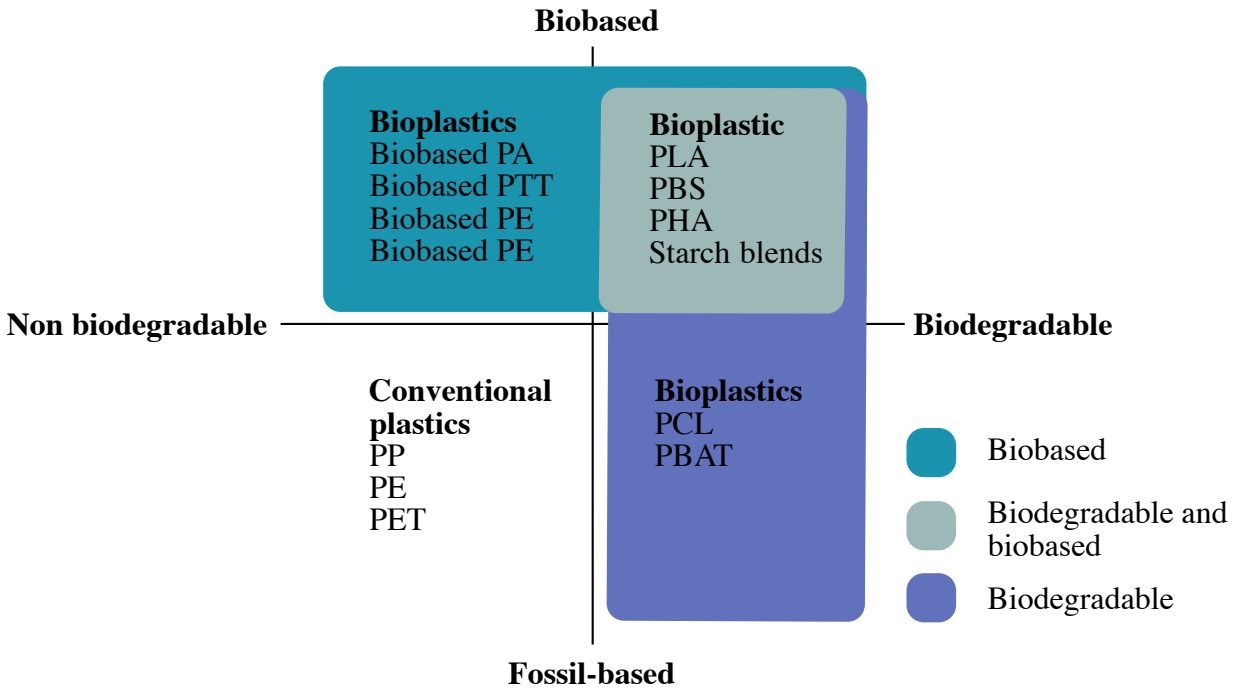

Figure 1.1: Division of different types of bioplastics (Perstorp Winning Formulas).

The market for biopolymers and biocomposites is growing, and according to European Bioplastics, the total production capacity of bioplastics will increase from 1.5 Mtons in 2012 to 6.7 Mtons in 2018 (European Bioplastics, 2014). Bioplastic can make major contributions to a solution in the environmental crisis since they reduce CO_2 and are biodegradable. Biopolymers and their blends can be recycled using both mechanical and chemical methods, but for biocomposites, the focus has been on mechanical recycling.

Biobased plastics require being recycled separately in separate streams for each material, like the established plastics. For those plastics that already have a recycling stream, like PET, the biobased counterpart can be recycled in the existing stream, like bio-PET. A current stream for PLA does to this day not exist (European Bioplastics). If and when compostable plastics ends up in the conventional plastics recycling streams, the existing sorting technology can sort the two types out with little residual waste (Remar, 2011). Bioplastics produced for food applications have to meet strict criteria to be approved for such use, and it is important that none of the components leading to possible health risks are released.

Polylactic acid (PLA) has achieved considerable interest in the food application industry and is one of the most valuable bio-based plastic on the market. PLA is an aliphatic polyester that is produced from food starches such as potatoes and corn, which are both renewable sources. PLA compared to petroleum-based plastics offers many advantages and is one of the few plastics appropriate for use in 3D printers, as well as being biocompatible so that it can be utilized in the medical industry. Furthermore, in certain environments, the period of biodegradation will range from 6 months to two years, depending on the environment. It is also industrially recyclable and compostable (Dusselier et al., 2015).

The first step in the current PLA production is the anaerobic fermentation of renewable carbohydrates to aqueous lactic acid. The industrial path from lactic acid to PLA depends on the intermediate synthesis of the cyclic dimer of lactic acid, the lactide. Through a controlled ring-opening polymerization the dimer is converted to quality PLA (Auras et al., 2010; Dusselier et al., 2015). It can also be synthesized by direct condensation polymerization. PLA entails some properties that may propose disadvantages in many applications such as lower thermal stability and impact resistance compared to other conventional polymers. However, a quick solution to this issue can be the addition of nanoclays, which can improve properties like the rigidity, crystallinity, permeability, and thermal stability. It is also interesting regarding degradation because it is important to know how it degrades to know if it can be recycled. In this project, it was worked with montmorillonite, which is a laminar clay.

The degradation of polymers occurs either chemically or physically, and the degradation rate is important to know for the shelf-time of the polymer for when it is being used in the industry. However, after the material has been recycled, it may be reused, and the same efficiency is

desired. Mechanical recycling of PLA will lead to less usage of raw materials and energy, and lower emission of gasses into the atmosphere.

To be able to understand the effects of mechanical recycling and if it is feasible, it is necessary to compare the properties of the virgin with the recycled material. If the material is going to be used in food applications, it is also important to see if it endures cleaning. In this study, the properties of the cleaned and mechanically recycled material was compared to those of the virgin and the recycled material without the cleaning step, with emphasis on the resistance to hydrolytic degradation, since PLA probably will be in contact with moist food and due to their chemical nature. The hydrolytic degradation limits the application of PLA considerably since it produces a reduction in the mechanical properties and the stability of the material. The resistance against hydrolytic degradation has been studied by using experimental techniques such as Ultraviolet visible spectrophotometry (UV-Vis), Fourier transform infrared spectroscopy (FTIR), gravimetric analysis, intrinsic viscosity measurements and thermogravimetric analysis (TGA). The water absorption was investigated by using a gravimetric method.

The objective/purpose of this study was to examine the water uptake of mechanically recycled PLA, and consequently the hydrolytic degradation with the prospect of using the material as packaging material. It was to be compared with virgin PLA, to obtain information about the behaviour of the material in the recycled state.

The primary objective was answered, by breaking it down into the following specific objectives:

- The virgin material was exposed to accelerated ageing by ultraviolet light and heat to simulate an effect of use and mechanical recycling of the studied material. Thus, the recycled material is obtained.
- Characterise the virgin and the recycled material.
- Determine the hydrolytic degradation of PLA by viscosity measurements.
- Quantify the water absorption at initial and final stage of the hydrolytic degradation of the recycled material by gravimetric analysis at different immersion times.
- Evaluate changes in chemical nature of the material due to absorption of water by FTIR analysis.
- Study the types of water in the material after absorption.

- Study the applicability of UV-Vis spectroscopy in providing information on the hydrolytic degradation of the materials.
- Analyse the effect of mechanical recycling on the water absorption of the material.
- Determine the thermic stability of the materials by thermogravimetric analysis.
- Compare the obtained results for the recycled material, including the cleaning step, with the corresponding results of the virgin material and the recycled material without the cleaning step.

2. PLA

Polylactic acid (PLA) is the most commonly used bioplastic today due to low cost and availability, and a sustainable solution to the increasing demand for plastic that the world is facing today.

PLA is a biodegradable polymer that belongs to the family of aliphatic polyesters and is derived from renewable resources, such as corn starch, sugarcane, tapioca roots or starch. In 2010, PLA had the second highest consumption volume of any bioplastic of the world (Garlotta, 2001). The chemical structure of PLA is illustrated in figure 2.1.

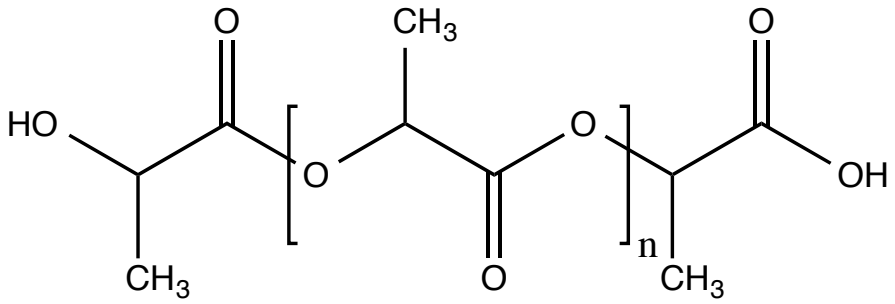

Figure 2.1: Chemical structure of PLA.

Lactic acid, the monomer of PLA, is the most extensively occurring and the simplest hydrocarboxylic acid, where the carbon atom is asymmetric and exists in two optically active configurations. The monomer is a naturally occurring organic acid. The PLA structure can be modified under polymerization of a controlled mixture of D(-) and L(+) enantiomers, reaching an amorphous or crystalline structure of high-molecular weight, thus being suitable as packaging material in the food industry. Depending on which monomer the PLA is obtained from, there exists three stereochemical varieties of PLA; poly(L-lactide) (PLLA), poly(D-lactide) (PDLA) and poly(DL-lactide) (PDLLA). PDLLA is obtained from a mixture, usually a 50:50 ratio, of D- and L- isomers (Garlotta 2001; Nampoothiri et al., 2010).

The production of PLA ranges from carbohydrate fermentation to chemical synthesis, like condensation reactions and the polymerization of lactic acid by ring-opening of the lactide,

although fermentation predominates (Benninga, 1990; Garlotta, 2001; Nampoothiri et al., 2010). Both fermentation and chemical synthesis yield high-molecular weight polymers with high-performance properties.

2.1 Properties

PLA is a transparent thermoplastic that is visually very similar to polystyrene and polyethylene terephthalate (PET). The properties of PLA are administrated by essential parameters such as the chemical structures of PLA, including the chain structure, conformation, and tacticity. They are also dependent on factors such as the temperature of polymerization and the annealing time, which determines characteristic parameters of the polymer like the molecular weight, the purity, and composition of the polymer and crystallinity (Belgacem & Gandini, 2008).

The enantiomeric purity of the lactic acid stereo-copolymers has a clear relation to the physical properties of PLA. The PLA properties will vary depending on from which isomer it is obtained, and the crystallinity structure will rely on the three possible configurations; PLLA, PDLA, and PDLLA. L(+) or D(-) PLA have a crystallinity of about 37%, which the amorphous portion has a glass transition temperature of around 53°C, whereas the crystalline portion has a melting point at about 175°C. In comparison, a racemic mix of the two isomers is amorphous and has no crystalline melting point. However, it softens or has a sticking point of about 50-75°C (Bonsignore, 1995).

The mechanical properties of lactic acid based polymers can vary to a large extent, ranging from stiff and high strength materials to soft and elastic plastics. One way to modify the properties is the addition of plasticizers. Commercial PLA, which consists of 98% L-lactide and 2% D-lactide, has a modulus of 2.1 GPa and an elongation break of 9%. Following plasticization, the elongation at break rises to 200% and its Young's modulus decreases to 0.7 MPa. A corresponding glass transition temperature shift from 58 to 18°C also follows (Södergård & Stolt, 2002; Visakh et al., 2013).

When a polymer is used in food packaging, the barrier properties are of great importance so that contamination can be avoided from outside and inside oxygen that can contribute to degradation of the content. It is in the amorphous regions of the polymer that the diffusion occurs. Thus an

increase in crystallinity will cause a decrease in the permeability of the polymer. PLA exhibits barrier properties that are considerably good, for oxygen, carbon dioxide and water (Belgacem & Gandini, 2008).

PLA is a biocompatible polymer, which is an important property that allows contact of PLA with cell tissues, which gives multiple applications in the biomedical sector (Nampoothiri et al., 2010).

2.2 Synthesis

The basic building block/The single monomer of PLA, lactic acid, is produced via chemical synthesis or carbohydrate fermentation. Lactic acid (2-hydroxy propionic acid) is the simplest hydroxy acid, and it occurs naturally in two optically active configurations, the L(+) and D(-) stereoisomers and are both produced by fermentation of carbohydrates. In industrial scale, it is more common to utilize the lactic fermentation than chemical synthesis. Lactic fermentation predominates because chemical synthesis has limitations regarding the inability to only make the wanted L-lactic acid stereoisomer and high manufacturing expenses (Datta & Henry, 2006; Jamshidian et al., 2010; Garlotta, 2001). In the fermentation, homolactic organisms are used the same way as an optimized strain of Lactobacillus, which solely form lactic acid (Garlotta, 2001; Hartmann, 1998). Then carbohydrates such as cornstarch, which is an inexpensive source, can be converted into lactic acid (Dorgan et al., 2000; Gupta et al., 2007). The carbohydrates that can be applied depend on the strain of Lactobacillus, but in general, most of the simple sugars that are obtained from agricultural byproducts can be used, like lactose, sucrose, glucose, maltose, and dextrose. The reaction is illustrated in figure 2.2.

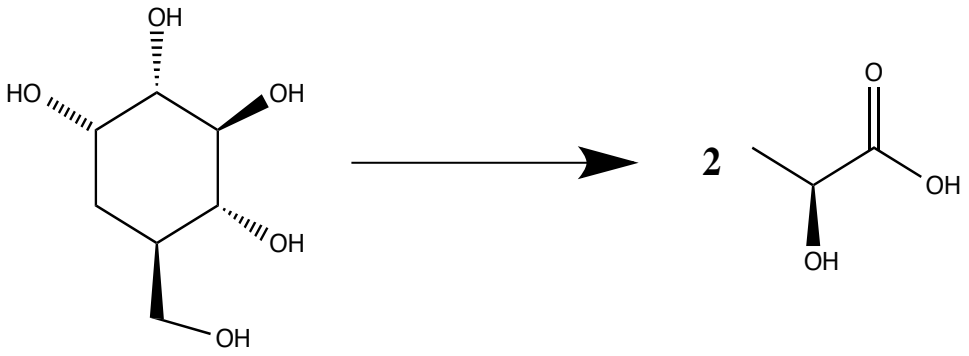

Glucose Lactic Acid

Figure 2.2: Lactic acid production by fermentation

The weight of PLA can vary, but it is only its high molecular weight polymer that can be used for packaging because grades with low molecular weight have poor mechanical properties and poor resistance to hydrolysis. There are three different pathways for the polymerization of PLA, and they are illustrated in figure 2.3;

- **Direct condensation polymerization***: in which a fragile, low molecular weight polymer is obtained, making it unusable.*
- **Direct polycondensation in an azeotropic solution:** *in which a high molecular weight polymer is obtained, with excellent properties.*
- **Polymerization through lactide formation:** *where the intermediate, denominated lactide, is obtained and is a high molecular polymer.*

2.2.1 Direct condensation polymerization

PLA consists of both a carboxyl and a hydroxyl group making it able to be converted directly into polyester via polycondensation reaction. The conventional condensation polymerization of lactic acid does not increase the molecular weight satisfactorily, leading to fragile, low molecular weight polymers with a molecular weight between 2.000-10.000 g/mole, due to, among other reasons, the presence of water and impurities. It's hard to obtain high molecular weight polymers with excellent mechanical properties using this method, making it unusable for industrial applications, unless external coupling agents that either reacts with the hydroxy or the carboxyl

group are used and therefore increase the molecular weight of the polymers (Jamshidian, 2010; Garlotta, 2001).

2.2.2 Direct polycondensation in an azeotropic solution

The second pathway to produce PLA is the azeotropic condensation polymerization, and this method yields high-molecular weight polymers, MW>100.000, without the use of chain extenders or external coupling agents. The lactic acid is condensed by azeotropic distillation at low pressure in the presence of a catalyst, thus avoiding the presence of water.

To have an acceptable reaction rate, high levels of a catalyst is required, which can lead to catalyst impurities. The residual catalyst can result in degradation and irreproducible hydrolysis rates. This pathway generates a polymer suitable for a various range of applications. However, the produced catalyst residue may limit their use in biomedical applications (Garlotta, 2001; Nampoothiri, 2010).

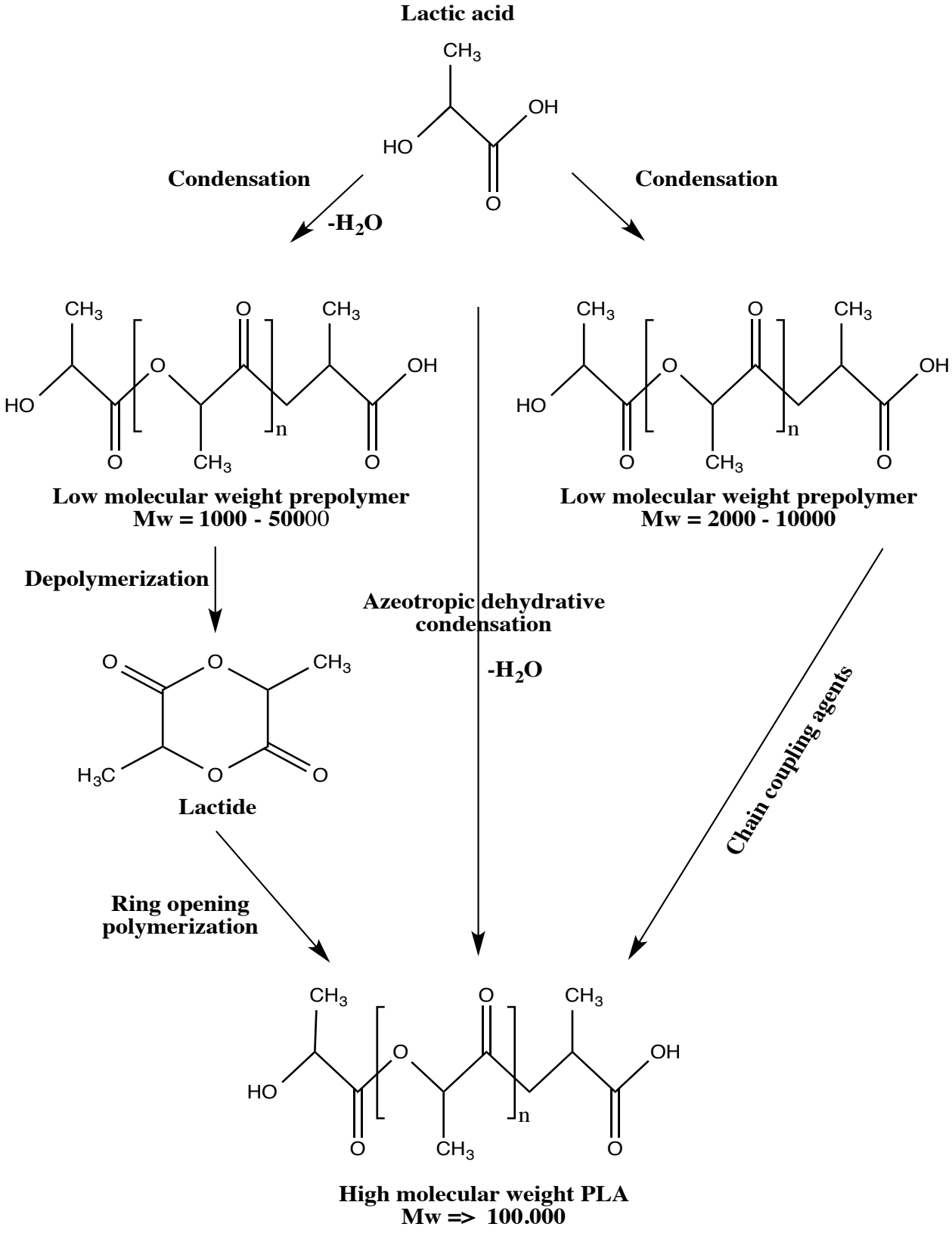

Figure 2.3: PLA synthesis (Lunt, 1998).

2.2.3 Polymerization through lactide formation

The most common way to obtain high-molecular weight PLA is by ring-opening polymerization. In ring-opening polymerization, an intermediate, denominated lactide, is obtained by depolymerization of low molecular weight PLA. This lactide possesses three stereoisomers, and the polymerization occurs under reduced pressure so that a mixture of L-lactide, D-lactide or DL-lactide polymers is produced. The stereoforms are illustrated in figure 2.4. The component percentage of the mix depends on the feedstock, catalyst, and temperature (Garlotta, 2001; Hartmann, 1998).

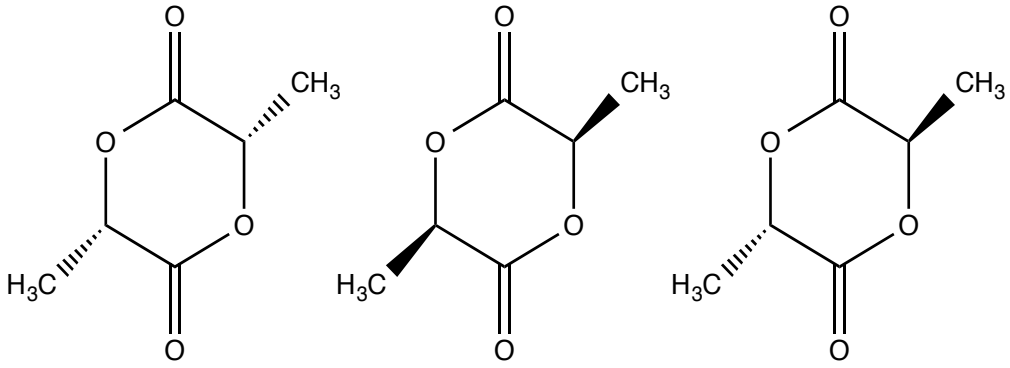

L-lactide D-lactide DL-lactide

Figure 2.4: Stereoforms of lactides.

Initially, lactic acid is condensed in the presence of water to obtain the cyclic dimer of lactic acid, which is a prepolymer of low molecular weight. This lactide is produced by depolymerization of PLA by applying pressure, resulting in conversion of the lactide by using a catalyst in a mixture of stereoisomers of lactide (Garlotta, 2001). The obtained lactide ring is illustrated in figure 2.4.

The mixture is purified and then subjected to a process of ring-opening polymerization in the presence of a catalyst, resulting in a high molecular weight polymer suitable for multiple applications. The ring-opening can either be done in the anionic or cationic form, and these initiations are usually done in solvent systems, and due to their high reactivity, are susceptible to racemization, transesterifications, and especially impurity levels. Cationic compounds used for such polymerization are triflic acid and methyl triflate, and proceeds via triflate ester end groups instead of free carbenium ions. At low temperatures, <100°C, this process yields an optically

active polymer without racemization (Garlotta, 2001; Henton et al., 2005; Gupta et al., 2007). Anionic compounds used for such polymerization are bases like potassium benzoate. The process proceeds by the nucleophilic reaction of the anion with the carbonyl and the subsequent acyl-oxygen cleavage, producing an alkoxide end group, which remains to propagate (Garlotta 2001).

This process produces high molecular weight PLA, and is used to modify the properties by adjusting the ratio and the sequence of the L- and D-lactic acid enantiomers. Thus, with this method, it is possible to control the chemistry accurately, and vary the properties of resulting polymers in a controlled environment making ring-opening polymerization one of the most used method for preparing polymers like PLA, and because of this, broadening the field of applications (Södergård & Stolt, 2002).

To eliminate the expensive and polluting solvents used in this process, "Cargill Dow Polymers LLC" has developed a continuous and economical industrial process for PLA production, which is illustrated in figure 2.5. This process uses tin catalysts and a system of vacuum distillation for the purification of lactide (Henton et al., 2005).

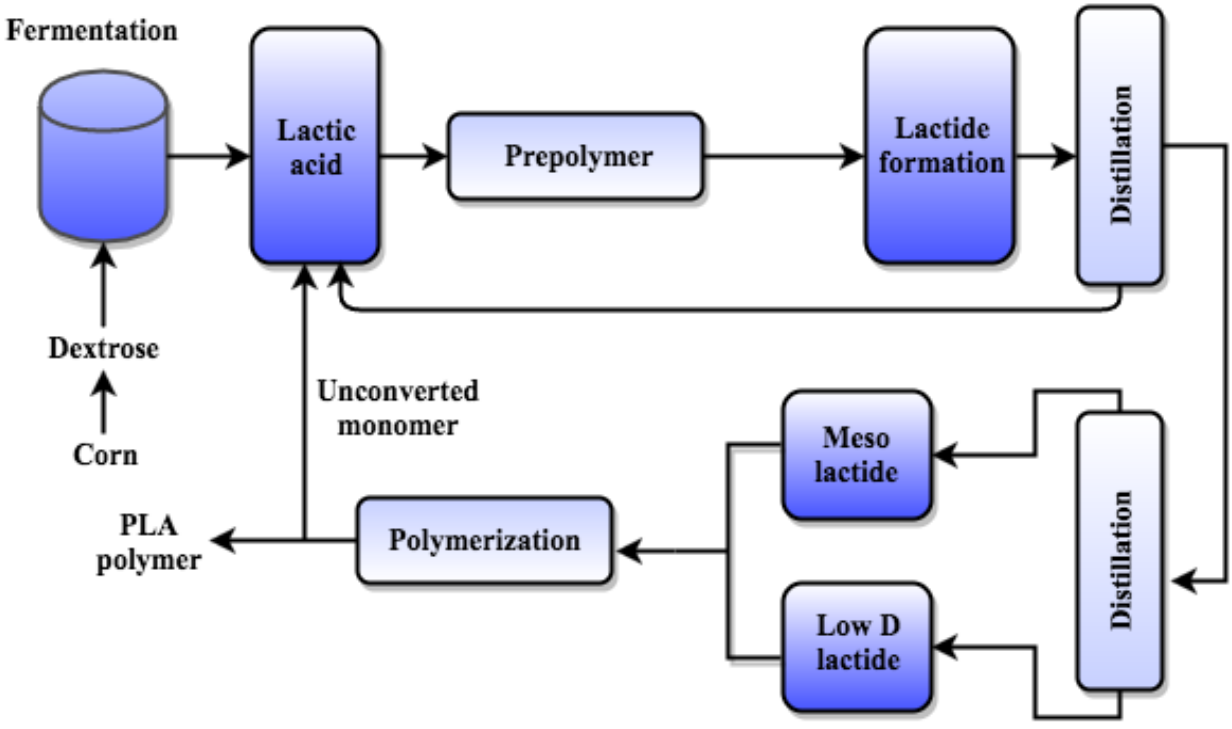

Figure 2.5: Scheme of the "Cargill Dow Polymers LLC" PLA production process (Gruber and O'Brien, 2005).

2.3 Applications

PLA has the potential of being used in a wide range of applications, where three stands out as the primary fields, like packaging, biomedicine, and industrial textile. In the packaging sector, PLA has a market capacity that is unlimited and is the major PLA application today with 70 % of the total consumption of PLA being used in packaging (Jamshidian et al., 2010). PLA is an economically viable material whose consumption is a huge demand in the market for biodegradable packaging. The demand for PLA has increased due to the need to improve food safety and environment quality and to find options to petrochemical plastics.

When plasticized, PLA possesses properties that make it a possible substitute for polymers such as PET, polyvinyl chloride (PVC), polystyrene (PS), low-density polyethylene (LDPE), and linear low-density polyethylene (LLDPE). PLA is an excellent choice for products that often end up in the landfill and food containers, being a non-toxic and biodegradable compound (Xiao et al., 2012). PLA has potential in the field of biomedicine due to its biocompatibility that allows contact with cellular tissues. It also degrades naturally in lactic acid, which is quickly eliminated by the human body Examples can be for fine suture, bone fixation material, drug delivery microsphere and tissue engineering (Zhao et al., 2004; Nampoothiri et al., 2010; Xiao et al., 2012). Other potential uses for PLA are upholstery, disposable garments, awnings, feminine hygiene products, and nappies.

Drawbacks such as limited barrier and mechanical properties, hydrolytic degradation by water and heat resistance must be overcome to meet market expectations and to substance, the increasing demand of PLA, so that the world production can be considerably increased (Belgacem & Gandini, 2008).

2.4 Recycling of PLA

Bioplastic blends can be recycled either by chemical or mechanical recycling methods. Mechanical recycling refers to processes that target to recuperate the plastic waste through mechanical processes such as grinding, washing, separating, drying, re-granulating and compounding. The aim of this is to produce recycled material that can be converted into new plastics products, often replacing virgin plastics (Plastics Recyclers Europe). Mechanical recycling of plastics is the most favourable technology for the industry and PLA is one of the

most reviewed bioplastics regarding recyclability. PLA can biodegrade under certain conditions, such as the presence of moisture and oxygen (Helfenbein, D., 2011; Soroudi & Jakubowicz, 2013), which significantly lowers the harmful environmental impact of PLA waste. However, it still has some limitations.

When PLA is processed in its molten state, it has a tendency to undergo thermal degradation, which is related to the processing temperature, the residence time in the extruder and, in some cases the moisture content of the granules (Taubner & Shishoo, 2001). These drawbacks also affect the recyclability of PLA. However, by using polymer blends the mechanical properties can be improved, which can overcome the disadvantages. Other limitations by mechanical recycling are the need for sorting, sensitivity to material impurities and thermo-mechanical degradation of polymers. Due to contamination in the recycling stream, the polymers usually need to be separated before this step. An example is the contamination of PLA water bottles in the PET recycling stream that will contaminate the stream even at very low levels of PLA and will lead to increasing the cost (Soroudi & Jakubowicz, 2013).

PLA has also been recovered by chemical recycling, but it requires complicated and expensive processes. Mechanical recycling may be cheaper than the chemical recycling, uses more conventional and easier methods (NatureWorks LLC; Chariyachotilert et al., 2012). The optimal conditions for mechanical recycling are unknown, as well as the final properties of articles produced with postconsumer PLA. Chariyachotilert et al. studied if poly(L-lactic acid) bottles could be successfully flaked and cleaned for blending with PLLA resin to create PLLA sheets and thermoformed containers, with promising results (Chariyachotilert et al., 2012). Thus, one of the objectives of this project was to include a cleaning step in the mechanical recycling process of PLA.

3. Clay

Recently, there has been a growing interest in polymer nanocomposites that are based on clay minerals, because they often display concurrent improvement in numerous properties of the neat polymer. These can lead to an enhanced barrier, mechanical and thermal properties of the virgin polymer. Properties like increased strength and heat resistance, high moduli, increased gas flammability and permeability, and increased degradability of biodegradable polymers (Ray, 2010; Lan and Pinnavaia, 1994; Kojima et al., 1993; Meneghetti and Qutubuddin, 2006).

Clay is a naturally occurring material composed primarily of fine-grained minerals with traces of metal oxides and organic matter. Upon drying or firing, it will become hard, brittle and non-plastic, but is generally plastic when wet. Clays usually contain minor amounts of impurities such as calcium, sodium, potassium, magnesium or iron. Chemically, they are hydrous aluminium silicates (Guggenheim and Martin, 1995). Clays can best be identified and studied using the following methods: Infrared spectroscopy, electron microscopy, differential thermal analysis, electron diffraction, X-ray diffraction, X-ray fluorescence and energy-dispersive X-ray analysis.

In the atomic structure of most clay minerals, there are two units involved, according to Grim (Grim, 1968). In one unit the oxygens or hydroxyls are tightly packed, where Mg, Al or Fe atoms are fixed in octahedral coordination, so that they are located in equidistant from six hydroxyls or oxygens. The second unit is formed of silica tetrahedrons. Both units are illustrated in figure 3.1.

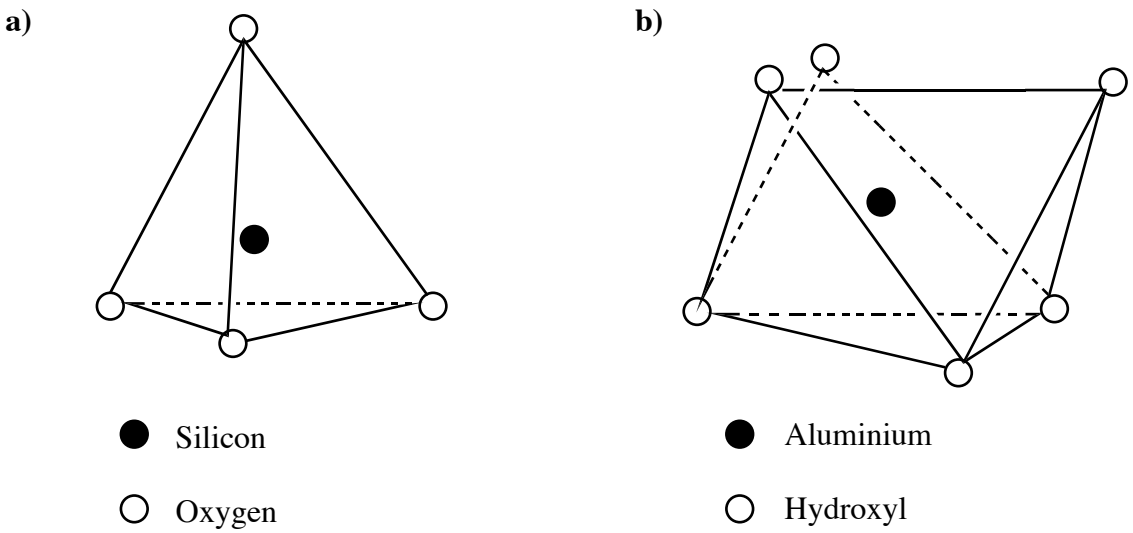

Figure 3.1: The basic structural units, which most clay consists of, are a) a silicon-oxygen tetrahedron and b) an aluminium hydroxyl octahedron.

A silicon atom is equidistant from four hydroxyls or oxygens in each tetrahedron, arranged in the form of a tetrahedron with the silicon atom at the center. Arranged silica tetrahedral groups form a hexagonal network (Obaje et al., 2013). The network is repeated indefinitely so that the formation of a sheet of the composition Si_2O_6 occurs.

The clay structure consists of three layers; oxygen, silicon, and hydroxyl atoms respectively. The first layer is the base of the tetrahedral groups and is made up of oxygen atoms; in the second layer, silicon atoms that occupy the cavity at the junction of three oxygen atoms form a hexagonal network. The third layer consists of hydroxyl atoms lying straight on top of the silicon at the tip of the tetrahedrons (Obaje et al., 2013).

Clays' raw materials have many industrial applications such as construction, textile, paper, ceramic, agricultural, pharmaceutical, nuclear energy, and petroleum industries (Obaje et al., 2013).

3.1 Montmorillonite

The most typically mineral clays used to prepare polymer nanocomposites are montmorillonites, along with hectorites and saponites. Cloisite 30B™ is a montmorillonite clay, which is organically modified layered silicate, and the one used in this project. Cloisite 30B™ is a type of phyllosilicate, which belongs to the montmorillonite family that is organically modified with bis(2-hydroxy-ethyl)methyl alkyl quaternary ammonium ions chains.

Montmorillonite is a 2:1 layered phyllosilicates, whose structure consists of two tetrahedral layers in which an octahedral layer is inserted in-between. Metal in this octahedral structure was entirely Al^{3+} and uncharged. Montmorillonite is produced during isomorphic substitution of Mg^{2+} for Al^{3+} in the octahedral layer (Beall and Powell, 2011). In tetrahedral substituted layered silicates the negative charge is located on the surface of silicate layers, and for that reason, the polymer matrices can interact more readily with these than with octahedral substituted material. The thickness of these layers is about 1 nm, and the lateral dimensions may vary from 30 nm to several microns larger. The thickness depends on the particular layered silicate (Ray & Okamoto, 2003). A crystalline structure of montmorillonite clay mineral is illustrated in figure 3.3.

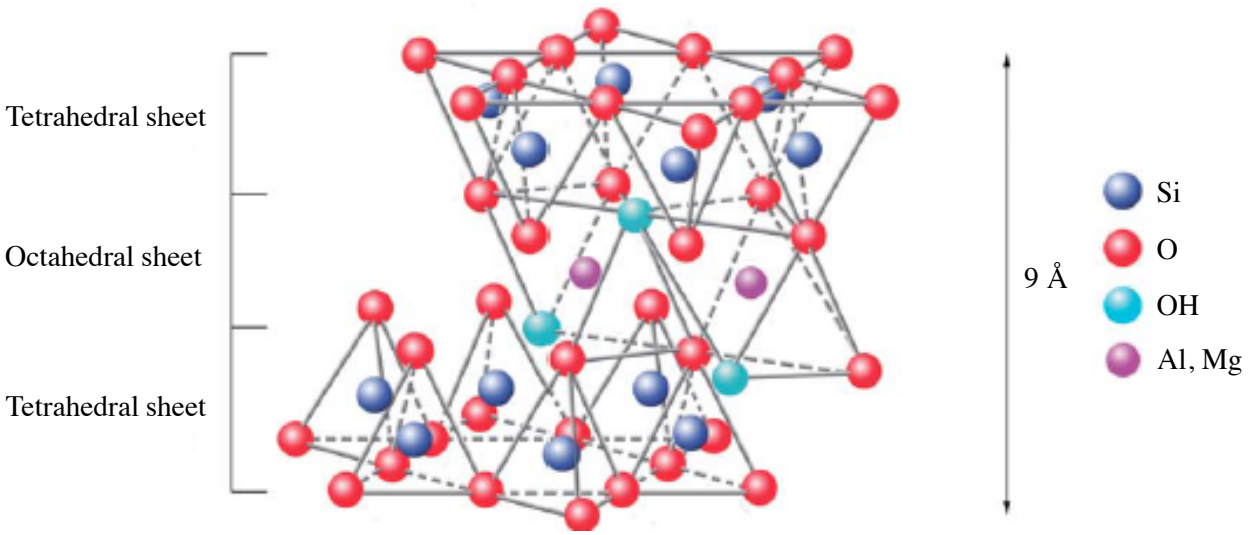

Figure 3.3: The montmorillonite structure consists of two tetrahedral sheets and one octahedral sheet. Thus, forming a 2:1 sheet structure. The 2:1 sheet has a thickness of 9 Å. The clay sheets originate by stacking alternate planes of ions (O and OH) and cations (Si^{4+}, Mg^{2+}, and Al^{3+}) (Franco Urquiza and Maspoch Rulduá, 2009).

When preparing nanocomposites, two characteristics of clays should be taken into account:

- The ability of the silicate particles to disperse between individual layers.
- Capacity to modify the surface chemistry through ion exchange reactions with organic and inorganic cations.

The degree of dispersion of silicate layers in a particular polymer matrix depends on the interlayer cations, thus making these two characteristics are interrelated (Auras et al., 2010). The clays should be organically modified because montmorillonites quickly swell in an aqueous medium. Montmorillonites are highly hydrophilic, thus have difficulty to disperse in the polymer matrix. The characteristics of montmorillonite can be modified through more or less simple procedures. Some of these proceedings involve the transformation of the natural zeolite structure and between pillars, thus generating new structures where their texture properties and structure varies on the starting material. The material properties are in this way optimized according to the needs of the application for which they are intended (Krstić, 2005).

Montmorillonite has a set of surface properties such as adsorption capacity, large surface area and homogeneity in the distribution of surface sites. Thus, making it of great importance in the industry, due to its role as a catalyst and an adsorbent. Montmorillonite is primarily used in the petroleum industry, as an adsorbent for removing suspended impurities in the products from the fraction distillation of crude oil, and as catalysts or catalysts supports in transformation reactions derivates (Krstić, 2005).

The preparation of nanocomposites with organically modified layer silicates provides increased biodegradability. The improved biodegradability may be because these silicates act as catalysts on the mechanism of biodegradation by the presence of terminal hydroxyl groups in their sheets, which can initiate hydrolytic degradation in polymers (Auras et al., 2010; Ray et al., 2003; Paul and Robeson, 2008).

4. Characterisation techniques

Experimental techniques such as FTIR, UV-Vis, gravimetric analysis, viscosity measurements and thermogravimetric analysis were used for the characterisation of the properties of PLA.

4.1 Fourier transform infrared spectroscopy (FTIR)

FTIR is used to obtain an infrared spectrum of absorption or emission of gas, liquid or solid, and it measures how well a sample absorbs light at different wavelengths. It is commonly used to show the presence or absence of functional groups which have specific vibration frequencies like C=O, NH_2, OH, CH, C-O.

Infrared spectroscopy measures the changes in bond lengths and bond angles. In this method, the changes in the vibrational and rotation movements of the molecules are measured. These changes are caused by the fact that the atoms within a molecule always oscillate around an equilibrium position. When there is absorption in the infrared region (1-100 μm) it results in changes in the vibrational- and rotational status of the molecules and the vibrational frequency of the molecules. These changes are what the absorption depend on. Absorption intensity will depend on the efficiency of the transfer of infrared photon energy to the particles, and this will rely on the change in the dipole moment, which occurs as a result of molecular vibration. For this reason, the absorption that causes a change in the dipole moment will be the only infrared light absorbed by the molecule. The greater the dipole change, the stronger the intensity of the band in an IR spectrum (Åmand & Tullin, 1997; Van de Weert et al., 2005; Griffiths & De Haseth, 2007). The infrared spectrum covers that part of the electromagnetic spectrum that lies between the visible and the microwave region, shown in figure 4.1. An increase in wavenumber leads to an increase in energy. The IR region can be subdivided into three areas recognized as near-IR, mid-IR and far-IR with the wavenumber ranges of respectively 14000-4000, 4000-400 and 400-20 cm^{-1} (Dept. of Chem and Biochem, UC, 2007).

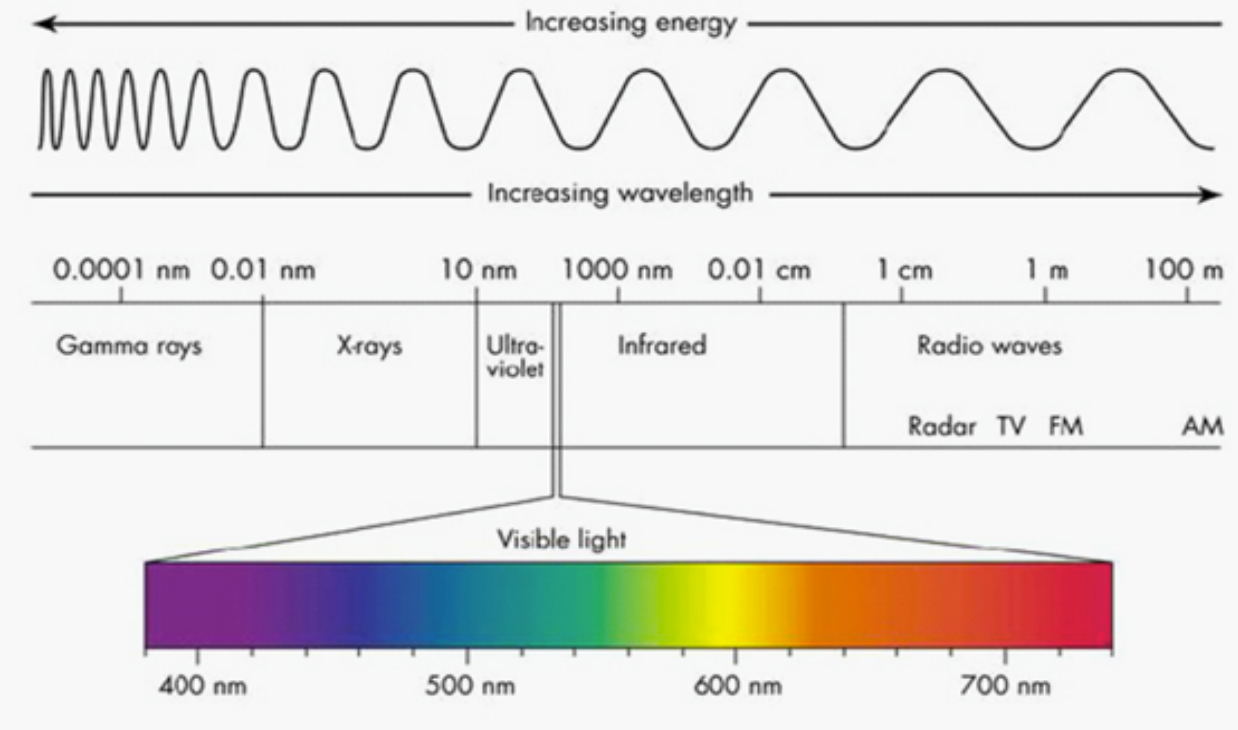

Figure 4.1: Electromagnetic spectrum (Cole-Parmer, 2015).

Electromagnetic spectrum refers to the seemingly diverse collection of radiant energy, from cosmic rays to X-rays to visible light to microwaves. All of which individually can be considered as a wave or particle traveling at the speed of light. These waves vary from each other in the length and frequency, as illustrated in figure 4.1 (Dept. of Chem and Biochem, UC, 2007). All the resolution elements are measured at all times during the measurements.

A molecule maintains their atoms in a certain bond distance and placement, due to the attractive forces and the repulsions of the electrons. The energy that is required to keep this distance will lead to a production of vibrations of the atoms. Of all the atomic movements of the molecule, it can mainly be divided into two types of molecular vibrations; stretching, which is a change in bond length, and bending, which is a change in bond angle, as illustrated in figure 4.2 (Stuart, 2005).

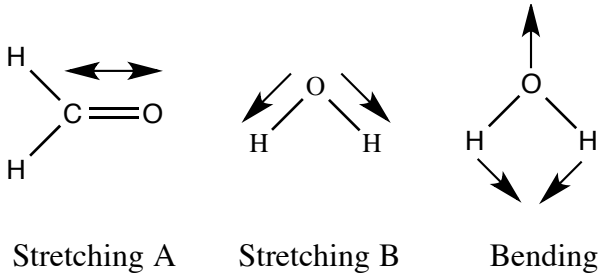

Figure 4.2: Stretching and bending vibrations.

The change in bond length is due to tension between atoms so that the interatomic distance is increased and decreased. Asymmetric vibrations of similar bonds will occur, when the molecule has different terminal atoms, such as HCN, and then the two stretching modes will no longer be symmetric, as illustrated in figure 4.3.

Figure 4.3: Symmetric and Asymmetric stretching.

Bending vibrations will also subsidise to infrared spectra, and the different types are called "deformation", "rocking", "wagging" and "twisting" and are illustrated in figure 4.4.

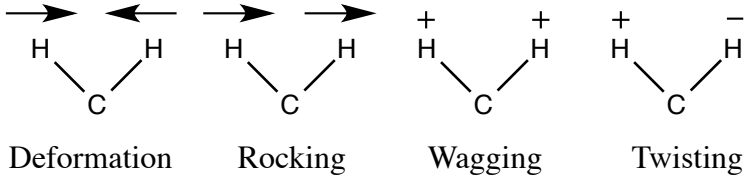

Figure 4.4: Bending vibrational modes for a CH_2 molecule.

For more complex molecules, the hydrogen atoms can be considered in isolation since it is usually attached to a bigger chain, making the molecule more rigid. Thus, making the analysis more straightforward, and this result in in-plane and out-of-plane bending, which is illustrated in figure 4.5.

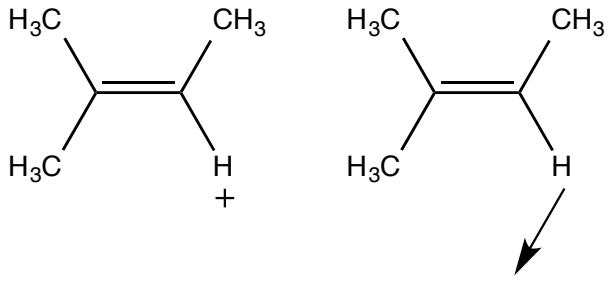

Out-of-plane bending In-plane bending

Figure 4.5: Bending vibrations.

The frequencies at which the organic molecule absorbs the infrared light can tell which functional groups that are present in the molecule. Depending on the distance between atoms and the movement occurring in the bonds between the atoms, the molecule gives rise to bands at approximately the same frequencies, which are associated with their bonds, allowing detection of which functional groups that are present in the molecule. The spectrum is then analysed with a comparison of tables, which correlate frequencies with functional groups. Thus, making infrared spectroscopy a useful tool in the qualitative analysis of organic compounds (Dept. of Chem and Biochem, UC, 2007).

4.2 Ultraviolet - Visible Spectroscopy (UV-Vis)

For qualitative and quantitative analyses, UV-Vis spectrophotometry is commonly used in analytical laboratories. The method is very easy to use, and not very time-consuming (Chan, 2004). UV-Vis spectroscopy provides information about electronic transitions and types of bonds in the analyte. Electronic transitions are associated with high energy that is high enough to dissociate some molecules. This high energy causes changes in electron energy and can also lead to vibrational changes and rotation (Ortega, 2015; López-Mayorga, 2012). The spectra are

measured from 200-800 nm for UV-Vis spectroscopy, and it studies the alterations in electronic energy levels within the molecule developing due to a transfer of electrons from π- or non-bonding orbitals. The method can provide knowledge about conjugated unsaturation, aromatic compounds, π-electron systems and conjugated non-bonding electron systems to name a few (Royal Society of Chemistry, 2009; Owen, 1996).

During analysis, the UV-Vis light will pass through the sample with continuously changing wavelength. The sample absorbs the light with the wavelength, which corresponds to the energy level required to excite an electron to a higher level (McMurry, 2008). In each possible case, an electron is excited from a full orbital into an empty anti-bonding orbital, where the full orbital has little energy and is in a ground state, and the empty non-bonding orbital has higher energy and is in an excited state. Each wavelength of light has a certain amount of energy that is just enough to do this electron transition, then that wavelength will be absorbed. The energy required for π- and σ-orbital to promote the electron to the higher energy level is dependent on the gap between the energy levels, and the larger the gap, the greater amount of energy is required. This will result in light of higher frequency, and therefore shorter wavelength will absorb (Royal Society of Chemistry, 2009; Owen, 1996). The excited molecule returns to ground state after absorption, by returning the excess energy as heat, or as fluorescent radiation of higher wavelengths. The visible spectrum is only a minor part of the total radiation spectrum, most of the radiation around us, cannot be seen but only detected by sensing instruments. The electromagnetic spectrum is illustrated in figure 4.1 (William Reusch, 2013).

Valence electrons can commonly be found in three different types of electron orbitals:

1. Single bonding orbitals, σ
2. Triple or double bonding orbitals, π
3. Non-bonding orbitals (lone pair electrons), n

The interaction between n- and π-electrons and π- and π-electrons is considerable, while the interaction between σ- and π-electrons can be neglected. The non-bonding electrons are bound more weakly than the bonding electrons, and among the bonding electrons σ- are linked stronger than π-electrons. For the antibonding levels, the σ*-level has a higher energy level than the π*-level. The electron density of the different types of orbitals is illustrated in figure 4.6. These

various types of electrons give rise to several electron transitions that can be observed in the UV-Vis spectra.

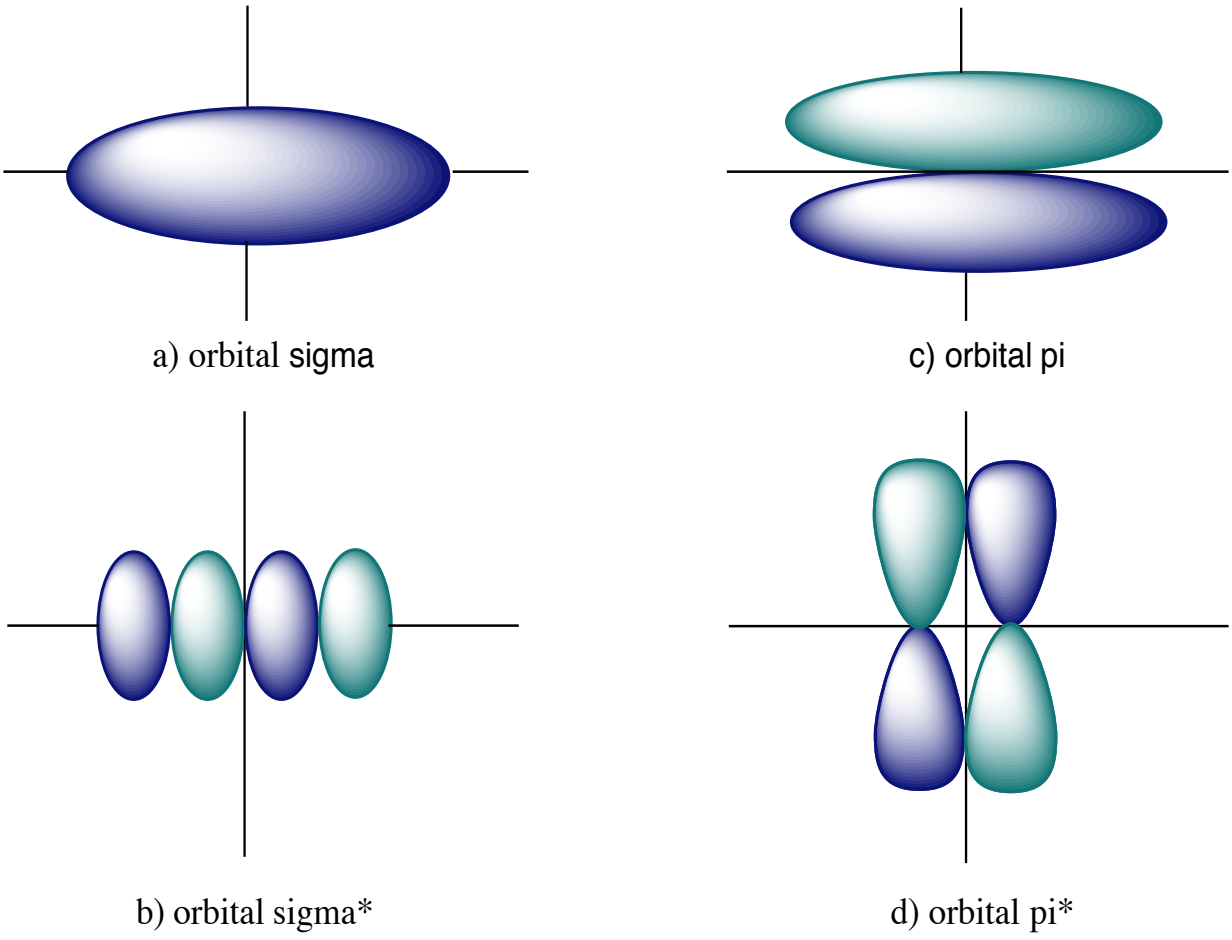

Figure 4.6: Distribution of the density charges of π, σ, π* and σ* electrons.

The molecule absorbs energy, and an electron is promoted from an occupied molecular orbital, usually a non-bonding n or bonding π orbital, to a vacant molecular orbital, usually an antibonding π* or σ* orbital, of greater potential energy, which is illustrated in figure 4.7

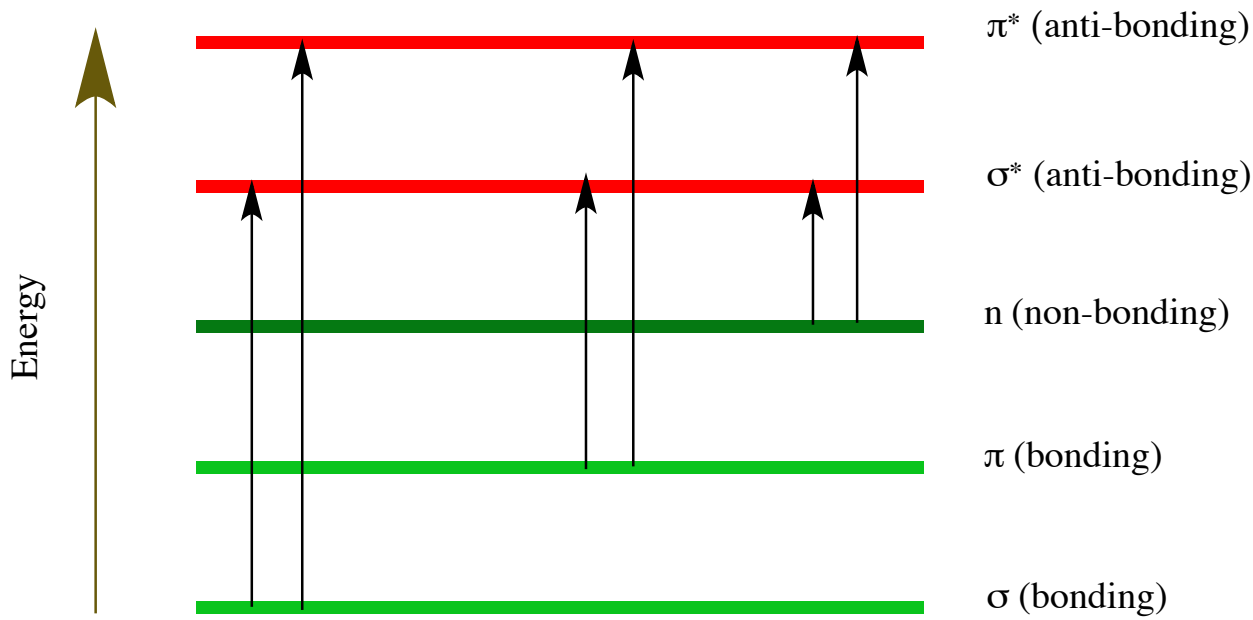

Figure 4.7: Electron energy level in the molecules with possible energy transitions between the electrons.

The energy level of a nonbonding electron is between the bonding and antibonding orbitals π and σ. There are six possible transitions in organic molecules, which are illustrated by arrows in figure 4.7. In the transitions σ → σ* and π → π* an electron passes a ground state to a bonding orbital, which is one type of transitions. Another type involves the passage of a delocalized electron (in an antibonding orbital) to an antibonding orbital, like in the n → π* transition, and it is weaker than the other type, and commonly found in the region of the far or near ultraviolet. It also appears at slightly higher wavelengths in the near ultraviolet or the visible part of the spectrum. The last type is produced from one fundamental state to another of very high energy near the ionization of the molecule, and can not be seen in the UV-Vis spectrum, and those are the π → σ* and σ → π* transitions (López-Mayorga, 2012).

In the transitions from σ → σ*, an electron from a molecule in a σ-bonding orbital is excited to the corresponding σ*-antibonding orbital. These are high-energy transitions, which include very short wavelength ultraviolet light (<150 nm), and will therefore usually fall outside of the measurable UV-Vis range. Saturated compounds containing atoms with pairs of nonbonding electrons can generate n → σ* transitions, which requires less energy than σ → σ* transitions, and can be produced by radiation in the region between 150 and 250 nm, frequently generating peaks below 200 nm (López-Mayorga, 2012).

Only occurring π to π* and n to π* transitions in the UV-Vis region can be observed. Thus, the majority of the UV-Vis spectroscopy absorptions are based on transitions of the electrons, n or π, to the excited state π*. The energy required for the transitions n → π* and π → π* will produce peaks in a spectral region that are convenient experimentally (200-700 nm). Both of these transitions require a presence of a functional group that provides the π orbital. Strictly speaking, the term chromophore is applied for these unsaturated absorbent centers (López-Mayorga, 2012).

4.3 Viscosity

The viscosity of a solution is a measurement of its resistance to flow and describes the internal friction of a moving fluid. When a polymer is dissolved in a solvent, it allows it to measure the viscosity, which is associated with the molecular weight of the polymer. The intrinsic viscosity of a solution is related to the ability of the polymer to increase the viscosity of the solvent and is dependent on the polymer concentration and the size and shape of their molecules (Lu et al., 2013; Lyulin et al., 2000). Through measuring the viscosity, the viscosity average molecular weight, M_v, can be obtained. The viscosity depends on the solvent used and temperature, and if different solvents are being used it will lead to different results, thus it is important knowing the relationship between the viscosity and the viscosity average molecular weight at each temperature and in each solvent (Wagner, 1985).

The intrinsic viscosity can be calculated by finding the relative viscosity, η_r and the specific viscosity, η_{sp}, which is done by using equations 4.1 and 4.2 respectively.

$$\eta_r = \frac{\eta}{\eta_0} = \frac{t}{t_0} \tag{4.1}$$

$$\eta_{sp} = \frac{\eta - \eta_0}{\eta_0} = \frac{t - t_0}{t_0} \tag{4.2}$$

Where the fall time through a capillary of the solution is denominated as t, and for the pure solvent is designated as t_0. η and η_0 are the viscosities of the solution and the pure solvent, respectively.

The viscosity is dependent on the concentration of the polymer and therefore influences the two next parameters, the reduced and the inherent viscosity. The reduced viscosity, η_{red}, and the inherent viscosity, η_{inh}, are calculated by using equation 4.3 and 4.4 respectively.

$$\eta_{red} = \frac{\eta_{sp}}{C} \tag{4.3}$$

$$\eta_{inh} = \frac{\ln(\eta_r)}{C} \tag{4.4}$$

Where C denominates the concentration of the polymer sample given in mg/L.

The presence of the polymer in the solution contributes to the variation of the viscosity by movement of isolated molecules in the solvent and the interaction between the polymer molecules and solution. The polymers ability to modify the viscosity of the solution in the absence of molecular interactions can be identified by calculating the intrinsic viscosity. The intrinsic viscosity can be calculated by linearly extrapolating the inherent and reduced viscosity to a zero concentration, which is done by equation 4.5 and illustrated in figure 4.8 (Najafi et al., 2012).

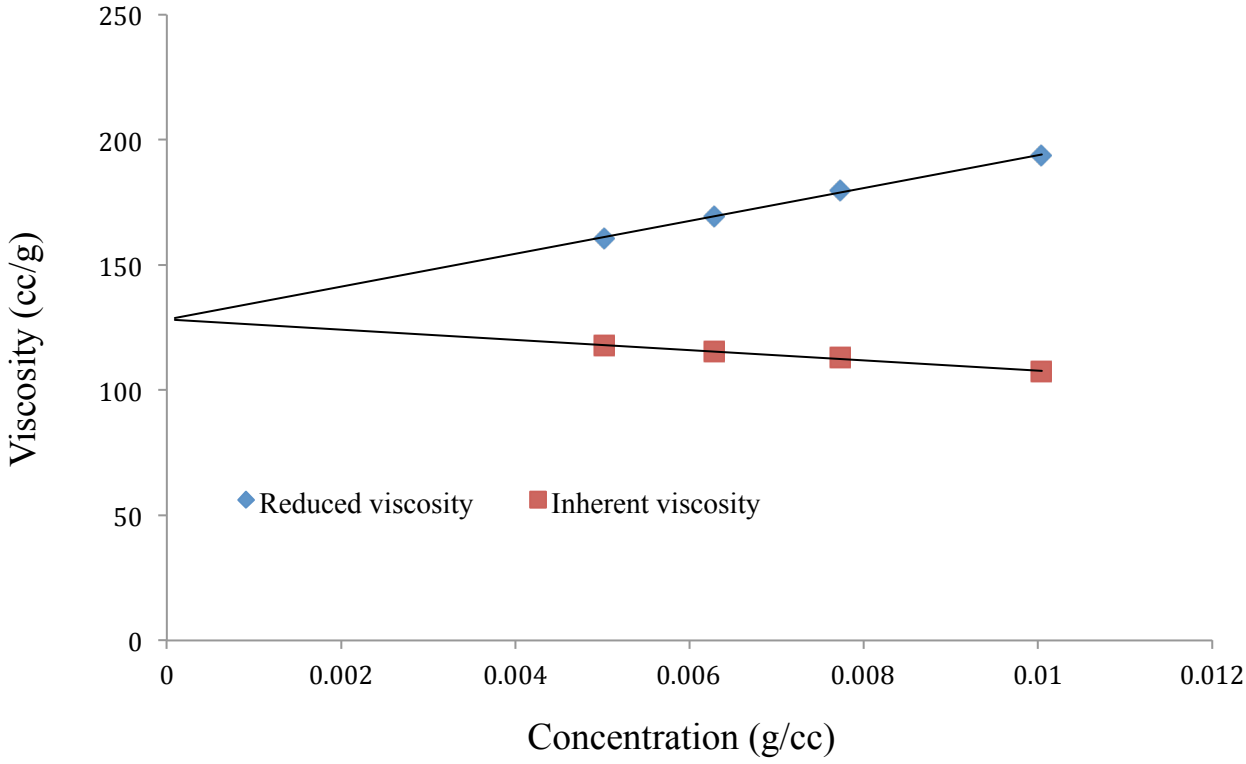

Figure 4.8: Representation of the inherent and reduced viscosity as a function of concentration.

$$[\eta] = \lim_{c \to 0}(\eta_{red)} = \lim_{c \to 0}(\eta_{inh}) \qquad (4.5)$$

The molecular weight can be associated with the intrinsic viscosity by the empirical Mark-Houwink-Sakurada equation, which is given in equation 4.6.

$$[\eta] = K \cdot (\mathrm{M}_v)^{\alpha} \qquad (4.6)$$

Where K and α are constants for a given polymer-solvent pair and are dependent on the temperature (Lu et al., 2013). The constants for $CHCl_3$-PLA at 25°C are $k=5.45 \cdot 10^{-4}$ and $\alpha=0.73$ (Badia et al., 2012).

4.5 Thermal Analysis (TA)

Thermal analysis (TA) is usually defined, as a group of different experimental techniques, were a physical property of an element, and its reaction products are measured as a function of time and temperature, while the element is exposed to a controlled temperature program. The international confederation for thermal analysis and calorimetry (ICTAC) has defined TA as an analysis of a change in a property of a sample, which is related to an imposed temperature alteration (Warrington and Höhne, 2008).

4.5.1 Thermogravimetric analysis (TGA)

Thermogravimetric analysis (TGA) is a technique for analysing the variations of the mass of a sample and is dependent on time and temperature. A thermobalance is used to carry out the thermogravimetric analysis. The thermobalance can vary the temperature in a controlled atmosphere while measuring a change in mass, usually a reduction, in the sample.

Thermogravimetric analysis measures processes that leads to variations in mass, such as reduction, decomposition, sublimation, desorption or absorption (Hatakeyama and Quinn, 1994). The thermobalance allows the temperature to be manipulated by either increasing or decreasing the temperature continuously. To evaluate the thermal stability of polymers in oxidizing and inert atmospheres, the atmosphere needs to be either static or dynamic with a flow of determined gases. The gases often used are N_2, Ar, CO_2 and air.

The technique allows the characterisation of various properties like the thermal stability of the materials under a wide range of conditions, decomposition, flammability and the amount of free or bound water in crystallization (Hatakeyama and Quinn, 1994). A thermal method like TGA will not provide specific results for each compound, and the results may vary depending on the conditions under which each experiment was carried out. Conditions such as the dynamic nature of the processes involved, heat transfer systems and the interaction of the sample in its surroundings are what it is mainly dependent on. Thus, making it important to document all the different parameters in each measurement (Warrington and Höhne, 2008).

5. Water absorption

The hydrolytic degradation of PLA in aqueous solutions occurs through the random cleavage of the ester bonds. This process is regulated by four elementary parameters: the amount of water absorbed, the rate constant, the diffusion coefficient of chain fragments within the polymer and the solubility of degradation products (Schliecker et al., 2003: Proikakis et al., 2006).

Degradation of a solid polymer matrix can either happen by heterogeneous or surface or, bulk or homogeneous erosion. The polymer degradation is much quicker than water intrusion into the polymer bulk in the first scenario and takes place in the outer polymer layers instead of the inner parts of the matrix. For bulk eroding polymers, the water is rapidly absorbed while the polymer degrades slowly. Hydration takes places very quickly and then the polymer chains are cleaved along the process. It is important to note that all degradable polymers can erode through two processes when the erosion conditions or the geometry of the specimens are chosen appropriately. Thus, the thickness of the material is a key factor that can determine the type of mechanism that works, because if it is high, degradation will be faster (Proikakis et al., 2006; Grizzi et al., 1995).

The hydrolytic degradation of PLA happens mainly in the bulk of the material instead of from its surface (Grizzi et al., 1995). The hydrolytic chain cleavage will occur favourably in the amorphous regions, thus leading to an increase in the global polymer crystallinity. The slower hydrolysis rate of the semi-crystalline P(L,L-LA) compared to amorphous P(D,L-LA) can be explained by this phenomenon (Hakkarainen, 2001: Paul et al., 2005)

The hydrolysis of the ester bonds occurs homogeneously through the polymer matrix for PLA, but as time passes, two factors become of primary importance. First, the degradation causes an increase of terminal groups of carboxylic acids, which catalyse the hydrolysis of the ester groups. Secondly, only oligomers soluble in an aqueous medium can escape from the matrix, which means that the oligomers located in the core region of the array are retained, while the soluble oligomers close to the surface can be released before degrading completely. Because of these events the pH in the core is lower, which means that the degradation will be faster (Proikakis et al., 2006).

De Jong et al. studied the hydrolytic degradation of monodisperse PLA, and concluded that at

low pH values, hydrolysis occurs, by cleaving the chain end groups whereas in an alkaline medium, a dimer of lactic acid, which is hydrolysed, is formed, and then separated so that lactoyl lactate splits off (Proikakis et al., 2006). Both mechanisms are illustrated in figure 5.1. It has also been demonstrated that the hydroxyl group of lactic acid plays a vital role when the polymer is in both acidic and alkaline medium. The hydrolysis of D,L-PLA occurs randomly in an alkaline environment, whereas in an acidic medium it will lead to excision of the chain ends.

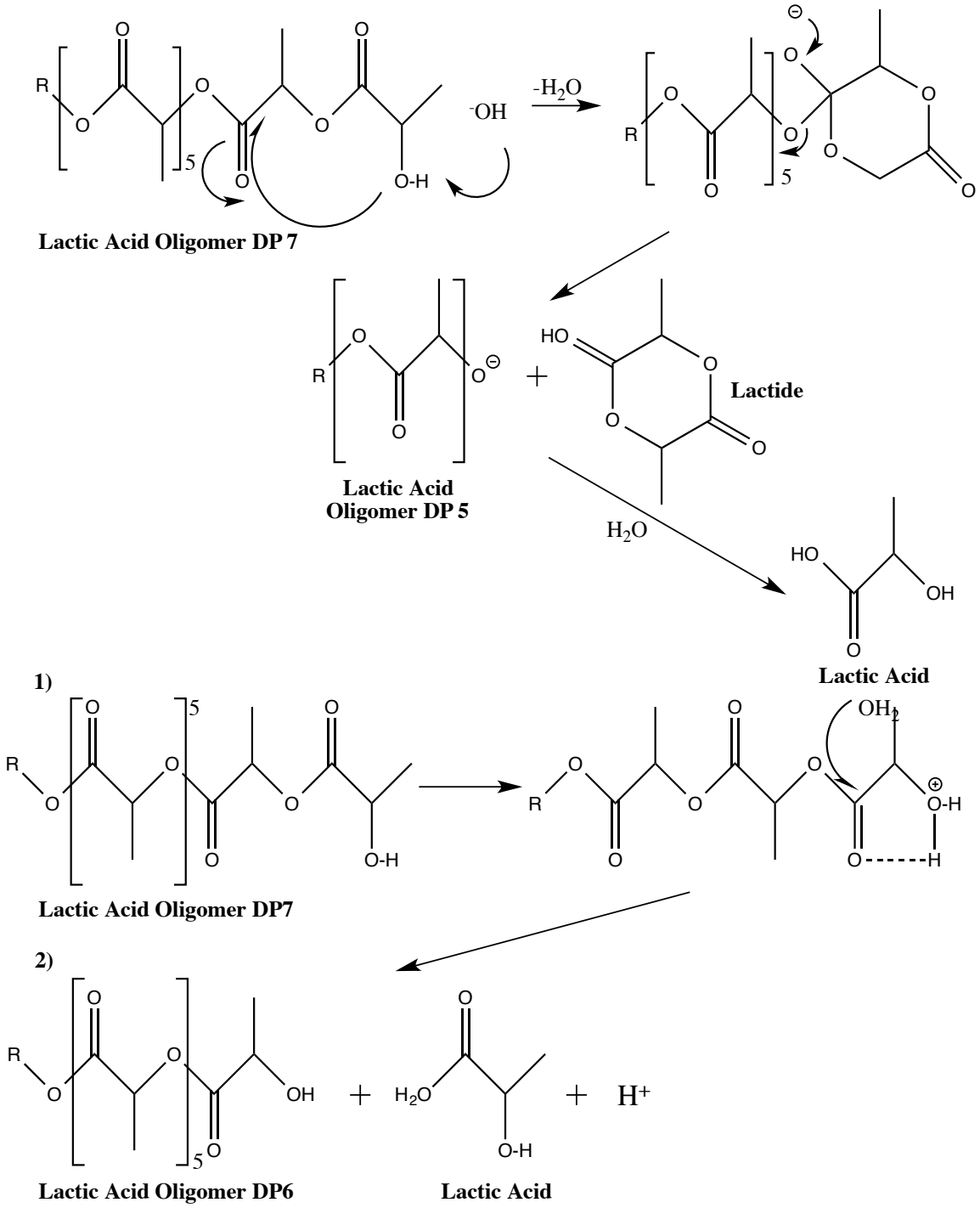

Figure 5.1: Mechanisms of hydrolytic degradation of PLA, where, in A) it is in alkaline medium and, in B) in acidic medium (de Jong et al., 2001).

When studying the hydrolytic degradation of the polymer the temperature is necessary to take into account. In conditions close to the glass transition temperature, which corresponds to a temperature of 55-60°C, degradation is based on a mechanism of erosion volume. At temperatures below the glass transition temperature, the degradation will only occur at the surface.

It is possible to measure the evolution of degradation by weighing the mass loss of the samples, which is carried out by measuring the decrease in molecular weight using an analytical balance.

Andreopoulus (Andreopoulus et al., 1999) found a relationship between the molecular weight of the used material and the hydrolytic degradation. In the cases where the materials have a low molecular weight, degradation begins in a few days, whereas for the materials that have a higher molecular weight, it takes longer for degradation to start

The introduction of additives, such as clay, can alter the PLA hydrolysis rate and affect the degradation. Thus, when comparing the oligomers of lactic acid the ones in PLA were longer compared to the ones where montmorillonite was added to the polymer. Greater mass loss has also been observed when adding montmorillonite (Roy et al. 2012).

5.1 Types of water

Materials should be exposed to a humid environment so that water absorption can occur. Hydration, in general, is a field that has gotten lots of interest because of the effects the water can have on the polymer and the role that the interactions between the one and the other plays in the biological processes.

Different approaches consider the water transport in glassy polymers. Free volume is an important term for glassy or semicrystalline polymers regarding water transport. Free volume refers to the difference between the measured volume of a polymer and the occupied volume. Thermally induced motion causes each molecular segment to move from the equilibrium position, thus occupying more space than its actual mass volume. The amount of available free volume determines the level of water absorption and the diffusivity of a polymer. This theory is

based on entirely mechanistic arguments and can give an explanation on some issues. It is not enough to predict the ultimate moisture absorption, nor the variation of sorption parameters when the temperature is increasing, and therefore the water-induced plasticization effects in polymers cannot be explained by this theory (Starkova et al., 2013). Another approach is based on the interaction concept, where polarity and interactions between the polymer and the water are taken into account. Water transport is possibly related to both theories; hydrophilicity, meaning the polymer-water affinity, and the free volume characteristics. The water diffusivity is primarily related to the free volume of the polymer, whereas the amount of water is determined by both hydrogen bonds in the polymer and free volume (Nogueira et al., 2001; Merdas et al., 2002; Starkova et al., 2013). However, experimental observations indicate that the diffusion coefficient is related to the hydrophilicity of a polymer, and it has been shown that the higher the hydrophilicity of a polymer, the lower the diffusion coefficient (Merdas et al., 2002).

According to Zhou and Lucas (Zhou & Lucas, 1999), there exists two fundamental types of water; water of type I and type II. Type I water diffuses into the polymer network and breaks the initial interchain Van der Waals and hydrogen bonds, which leads to plasticization of the polymer and an augmentation of chain segmental mobility. Type II water is related to water molecules that form multiple hydrogen bonds with the resin network. These complexes in the water molecules do not act as a plasticizer but is rather characterised as being more strongly bound to the polymer molecules with a higher amount of bridges between structural segments resulting in secondary crosslinking (Starkova et al., 2013). Type I water is often associated with the “free” water, while type II is referred to as “bound” water. In this connection, the two types of water contribute to the transportation properties of a polymer that is often related to the free volume and polymer-water affinity characteristics (Starkova et al., 2013).

The particular volume that a polymer has will increase with temperature, while the excess free volume will decrease due to augmented fluctuations of polymer chains and therefore requires more space for their distribution. The diffusion, which is a kinetic process, is dependent on the mobility of water molecules in the polymer matrix. The molecular segments of the polymer have significantly less mobility when the temperature is under the glass transition temperature, and the diffusivity is determined by the pre-existing quantity of free volume. When the temperature rises, the movement of the polymer chains will also increase and the water molecules will diffuse easier within the network. The available free volume in the polymer matrix and the number of active polar sites determines the amount of absorbed water. Thus, water can reorder the polymer

network and “open up” excluded polar sites for the association, thus, forming hydrogen bonds between water and matrix. Therefore the contribution of type II bound water has greater influence in the diffusion process at temperatures above the glass transition temperature (Soles et al., 1998; Starkova et al., 2013).

5.2 Quantitative analysis of water absorption

Quantitative analysis of water absorption often begins with assuming Fickian behavior. That is if it is considered that the diffusion constant of the material is one-dimensional, non-steady-state and with a constant diffusion coefficient, D. In this case, the second law of Fick can be applied, which is expressed in equation 5.1.

$$\frac{\partial C}{\partial t} = D\frac{\partial^2 C}{\partial x^2} \tag{5.1}$$

This equation illustrates the rate of change in the composition of the sample over time is equal to the diffusion coefficient by the rate of change in the concentration gradient and depends on upon the geometry of the material.

Crank ordered the solutions to Fick’s law of diffusion for different geometries, boundary, and initial conditions. The solution provided by the model for Crank Fick’s law for flat sheets, assuming the material is a sheet of negligible thickness compared to its two other dimensions and is illustrated in equation 5.2 and 5.3. This model assumes homogeneous diffusion in all directions, even when working with materials that are semicrystalline (Crank, 1975).

$$\frac{M_t}{M_\infty} = 1 - \frac{8}{\pi^2}\sum_{n=0}^{\infty}\frac{1}{(2n+1)^2} = \exp\left(\frac{-(2n+1)^2\pi^2 Dt}{h^2}\right) \tag{5.2}$$

$$\frac{M_t}{M_\infty} = \frac{4}{\pi}\left(\frac{Dt}{\pi}\right)^{0.5} + \frac{8}{h}(Dt)^{0.5}\sum_{n=1}^{\infty}(-1)^n\, ierfc\left(\frac{nh}{2(Dt)^{0.5}}\right) \quad (5.3)$$

Where Mt is the mass that has absorbed at time t, M∞ is the mass absorbed at t = ∞, n is the number of terms of the series, h is the polymer thickness, ierfc is the integral of the matching error function, and D is the diffusion coefficient. Equation 5.3 converges rapidly at short times, whereas equation 5.2 converges quickly at long times, and the methods for obtaining a diffusion coefficient from absorption data are based on one of these two equations (Balik, 1996).

To be able to evaluate if the behavior is Fickian or not, it is mostly common to look at the values of the measurements done at short times and by using equation 5.3. In measurements done at very short time intervals, the terms of the series are negligible, and an approximation of equation 5.4 can be employed. The approximation is given in equation 5.5.

$$\frac{M_t}{M_\infty} = \frac{4}{h}\left(\frac{Dt}{\pi}\right)^{0.5} \quad (5.4)$$

$$\frac{M_t}{M_\infty} = kt^n \quad (5.5)$$

Where the constant n indicates the mode of diffusion and the constant k shows the interaction between polymer and water and are determined by experimental data representing Ln (M_t/M_∞) versus Ln (t). When the value of n = 0.5, the diffusion is Fickian, whereas to when the value is between 0.5-1 the diffusion is non-Fickian and n > 1 it is said to be anomalous (Balik, 1996; Thomas & Pothan, 2008).

When the behavior is Fickian (approximately), the diffusion coefficient, D, can be calculated for the absorption process using equations 5.1-5.4 as proposed by Balik (Balik, 1996). The method used depends on the amount of experimental data and on whether or not it has reliable values of

M_∞. Often, these values are non-existing for many materials at room temperature, because the experimental values are over a longer period. In this case, it is reasonable to determine values of D and M_∞ by using all available data for a nonlinear fitting. By using the SorptExp function in Origin® it allows this adjustment, and the values can be determined by using these three parameters;

- Tau, τ, which is determined by equation 5.6.
- M_∞, final mass at equilibrium.
- n, number of terms of the series that are used, and should be left as a fixed number in each setting.

$$\tau = \frac{h^2}{D\pi^2} \tag{5.6}$$

This way the initial n can be determined, which should be considered to achieve a tolerable adjustment for a reasonable time interval. Once n is defined, the values D and M_∞ can be determined with generally good adjustments. The experimentally obtained values of the diffusion coefficients should be corrected, and can be done by following equation 5.7, as long as the sample does not coincide with the ideal method of being a two-dimensional sheet of negligible thickness. Thus, the samples used have a non-negligible thickness compared with the dimensions x and y.

$$D_c = D\left(1 + \frac{h}{x} + \frac{h}{y}\right)^{-2} \tag{5.7}$$

Where x is the longitude, y the width and h the thickness of the polymer sample.

So far it has been considered that the material does not suffer chemical or physical transformations during the absorption of water and that it is stable over time. Whereas to, in

reality, there are important changes and different curves can be obtained in some cases, and is illustrated in figure 5.2.

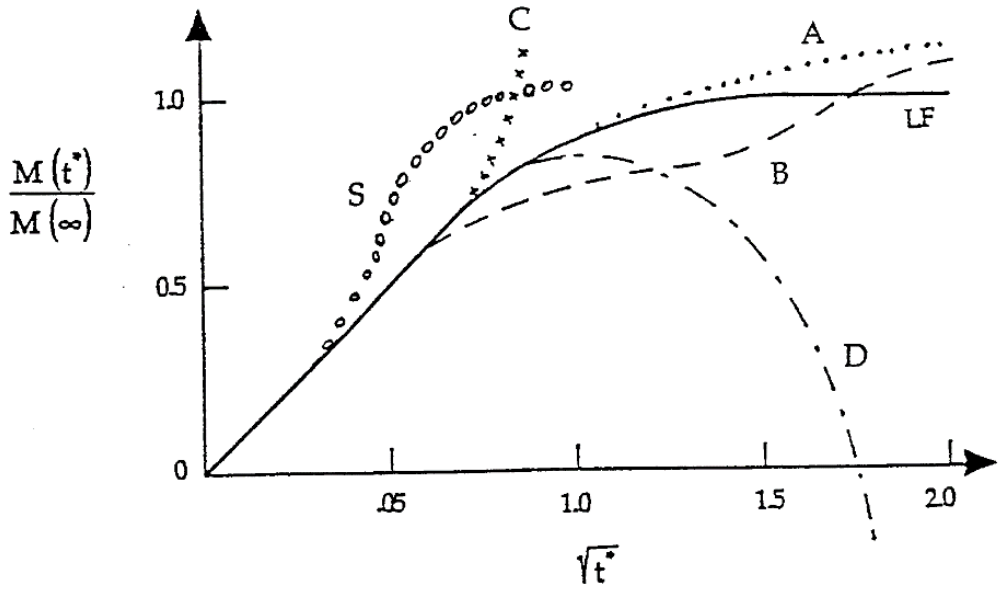

Figure 5.2: Representation of 5 different non-Fickian curves of mass variation during water absorption, where the curve denoted by LF corresponds to linear Fickian diffusion (Weitsman, 1996).

If the process is Fickian, the absorption process will follow curve "LF" in figure 5.2, where it is produced a rapid increase of mass, which will stabilize when the material is saturated. Curve "A" in figure 5.2, which is denoted as "Pseudo-Fickian" ($n > 0.5$), will often have a continuous gradual increase in weight gain and therefore never reach equilibrium (Grayson & Wolf, 1985; Weitsman, 1995). Curve "B" in figure 5.2 is denoted as "Two-stage Diffusion" behavior. Curve "C" in figure 5.2 is associated with rapidly increasing moisture content within the material, which has suffered large deformations, material breakdown, damage growth and mechanical failure. Curve "D" in figure 5.2 corresponds to a weight-loss caused by physical and irreversible chemical damages in the material, and often in context with hydrolysis or the separation of side groups from the polymeric chains. However, curve "C" and "D" corresponds to severe circumstance such as irreversible damages and degradations in the material. Curve "S" in figure 5.2 is usually very rare and corresponds to other types of diffusion (Weitsman, 1995).

6. Materials and Methods

For the experimental part, PLA in virgin and recycled form, and the nanocomposites with 2% of Cloisite 30B^{TM} clay were studied at 37°C. All samples were immersed in a phosphate buffer of pH = 7.4, and all instruments and equipment are listed in appendix 11.1.

6.1 Materials

6.1.1 Polylactic acid (PLA)

The commercial PLA "Ingeo Biopolymer 2003D^{TM}" supplied by NatureWorks LLC^{TM} (USA) was used in this study. It is a thermoplastic resin derived from renewable resources and is particularly designed for use in fresh food packaging and food service ware applications. PLA has a high molecular weight and may be processed without problems in conventional extrusion equipment (NatureWorks). The chemical structure of PLA is illustrated in figure 6.1.

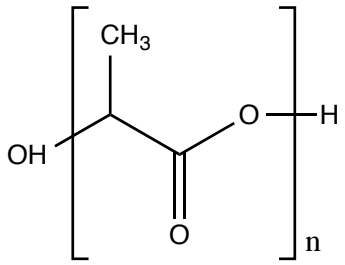

Figure 6.1: Polylactic acid.

6.1.2 Clay

The clay used in this study is Cloisite 30B^{TM}, supplied by Southern Clay Products^{TM} (Texas, USA). Cloisite 30B^{TM} clay is a natural montmorillonite that is organically modified with a quaternary ammonium chloride, in which two of the substituent groups are hydroxyethyl groups. The other two substituents are methyl groups and an organic radical of significant size. The structure of clay is illustrated in figure 6.2 (Ray and Bousmina, 2005).

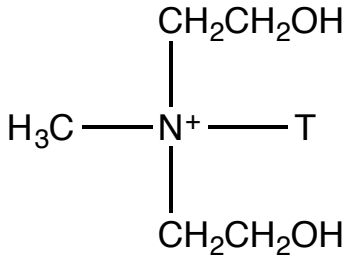

Figure 6.2: Chemical structure of Cloisite 30B^{TM} montmorillonite clay.

6.1.3 Phosphate buffer

A sodium dihydrogen phosphate and disodium hydrogen phosphate buffer with pH = 7.4 was used for immersion of the PLA samples. The immersion buffer was prepared with phosphates and deionized water, and the recipe is given in appendix 11.2.

6.1.4 Obtained materials

Polymer films of virgin and recycled materials were prepared and studied. A mechanical recycling process that includes accelerated ageing, cleaning and extrusion and compression moulding stages obtained the recycled material. The studied materials will further be referred to as:

- **PLAV**: PLA in virgin state
- **PLAV-302**: PLA in virgin state with 2% of clay
- **PLARC:** Mechanically recycled PLA, including a cleaning step
- **PLARC-302:** Mechanically recycled PLA with 2% of clay, including a cleaning step

6.1.5 Trichloromethane

Chloroform was used as the solvent in viscosity measurements of the different materials, and the solutions were prepared in the laboratory. The used chloroform was supplied by Sigma-Aldrich with a purity of 99.8% with ethanol as the stabilizer.

6.2 Methods

A description of the processes and equipment used for the production of the materials described above follows.

6.2.1 Materials obtained by extrusion

PLA and their mixtures with Cloisite 30B^{TM} were extruded with a double screw Rondol Microlab Twin Screw microextruder. Before the extrusion of the wanted materials, pure PLA was run through the machine to clean the screws. This way it was made sure that the material was not contaminated with possible remaining rests stuck inside the extruder.

Before extrusion, the pellets of PLA were crystallised in a vacuum oven at 100°C for 20 minutes. After the crystallisation the pure PLA and the clay were dried in the same oven at 85°C with vacuum, but for two hours. Water must be removed for preventing the material from any possible degradation. If the material contains any water, it will lead to degradation, and therefore it is important to dry the material completely. After two hours in the oven at 85°C, the material was removed and put in a dryer until it was cooled down. By letting the material cool down any absorption of humidity would be avoided.

Finally, the extrusion was carried out with a speed of 60 r.p.m., and with the following temperature profile:

- Application zone: 125°C
- Zone 2: 160°C
- Zone 3: 190°C
- Zone 4: 190°C
- Outlet: 180°C

The extruded material was transferred to a roll of hard paper and let to cool. The extruded material is illustrated in figure 6.3. When the material was cooled down it was cut into little pieces at about 1 cm. The cut material was transferred to a plastic zip-lock bag and stored in a drier to avoid absorption of humidity.

Figure 6.3: Extruded PLA.

The extrusion of the recycled material was performed with the same conditions as for the virgin material. The mechanical recycling will be further explained in section 6.2.3 and 6.2.4.

6.2.2 Manufacturing of polymer films

To obtain the PLA films a hydraulic press, model PL-15, was used. All materials were pre-dried for two hours at 85°C with a constant vacuum.

Approximately 2.6 g material was placed between two polyimide separators that again were placed between two plates of brass with metal spacers to obtain films with the desired thickness of approximately 200 µm. Then the following four steps were executed at 190°C:

1. The plates with the material were placed between the hot plates of the press.

2. The hot plates merged the material without pressure for 5 minutes.
3. The material was degassed by applying pressure (150-200 kg/cm^2) for 20 seconds, then releasing the pressure and reapplying the pressure. This process was repeated for 2 minutes.
4. The plates were placed between the cooling plates of the press and were left there for 5 minutes with a pressure of 150-200 kg/cm^2.

12 films were made for both PLAV and PLAV-302, where half of the films were cut into samples of 4 x 2.5 cm for both PLAV and PLAV-302.

6.2.3 Accelerated and natural ageing

Half of the cut samples were allowed to age naturally for three weeks at room temperature. The microhardness of a PLA with low crystallinity at 37°C changes significantly over time due to physical ageing, a process in which the free volume of the polymer is reduced. This process will alter some of its properties, such as water absorption and hardness. Within this three-week period, it is assumed that a maximum of physical ageing is achieved and that all the materials were in the same state, thus being comparable to each other (Ortega, 2015).

The other half of the films were cut and put into aluminium frames, illustrated in figure 6.4, and subjected to accelerated ageing by ultraviolet light and heat to simulate ageing and degradation that the material generally would suffer from during normal ageing. The films were introduced to a camera Atlas UVCON with eight ultraviolet F40UVB lamps that emit UV radiation at wavelengths between 330 and 280 nm for 40 hours and then subjected to a temperature of 50°C during 480 hours.

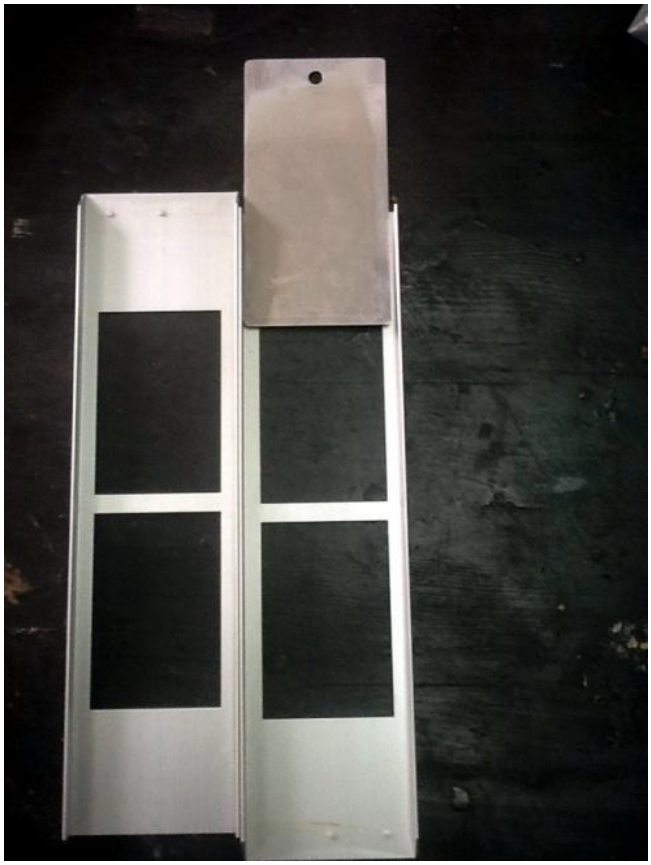

Figure 6.4: Aluminium frames used in the accelerated ageing.

After the accelerated ageing the samples were then cleaned, grounded, extruded and new films were made with the same procedure as explained in section 6.2.1 and 6.2.2. The newly obtained films were exposed to natural ageing for another three weeks.

An IKA A10 mill was used to grind and cut the aged films into tiny pieces, which were re-extruded, under the same conditions given in the procedure outlined in section 6.2.1, to obtain the recycled materials.

The extruded material was again cut into small pieces, to make new films in the press. Once produced, they were cut to the same dimensions mentioned before and allowed to age at room temperature for three weeks before immersing them in the buffer solution so that they could be studied in the same manner and conditions as the virgin material. Accelerated ageing, grinding, extrusion and obtaining new films have been made to simulate the effect of mechanical recycling and reprocessing.

6.2.4 Cleaning - step

If the purpose of PLA is to use it as food packaging application, it is important that the material can endure being cleaned so that there is a possibility of recycling it. Not many studies have documented the process of PLA being cleaned before the mechanical recycling process. According to Chariyachotilert, that based on cleaning conditions from PET processes were able to clean PLA without significant changes in the properties (Chariyachotilert, 2012). The conditions used by Chariyachotilert were utilized in this test. Before cleaning the materials employed in this study, a cleaning test of a sample of recycled PLA was executed, to see if the material could endure it or not. The test was performed under two different conditions:

1. 15 minutes at 85°C with 1 % NaOH and 0.3 % surfactant Triton 100x.
2. 5 minutes at 65°C with 0.5 % NaOH and 0.1 % surfactant Triton 100x.

0.5 g of the sample were added to the solutions and left there for either 5 or 15 minutes depending on the conditions. Then they were rinsed with water and left in water for 5 minutes with circulation. They were dried on a piece of paper and put in an oven with vacuum at 40°C overnight.

One sample that was executed with the first conditions was dried on a piece of paper and left at room temperature overnight. The next day, it was dried in an oven with vacuum at 90°C for 4 hours. The second sample, executed with second conditions, were dried on a piece of paper and dried in an oven with vacuum at 40°C overnight, the same was done for a second sample executed with first conditions.

To check how the cleaning affected the properties of the samples the viscosity of the two samples dried in an oven overnight but with different cleaning conditions were measured using the same procedure as described in 6.2.9, and the results are given in table 11.8 (appendix 11.6). It was chosen to go ahead with the cleaning of the first conditions for the recycled material in this study.

6.2.5 Immersion of samples

The final cut samples were immersed in vials containing phosphate buffer with a pH = 7.4. The phosphate buffer was prepared in the laboratory, and the recipe is given in appendix 11.2. Given

that PLA was studied for the purpose of using it in food packaging, it was decided to use a buffer at physiological pH than for example water that is more different from physiological solutions. In section 5 it was described that the absorption of water and the hydrolytic degradation, does not take place in the same way in acid or neutral mediums as in alkaline mediums. According to some authors, the acidic degradation occurs by cleavage of chain ends, while in alkaline mediums it occurs randomly (de Jong et al., 2001; Proikakis et al., 2006).

Before the immersion of the samples, the thickness of the films was measured with a digital Mega-Check FN de Neuertek micrometer with a precision of ± 1 nm. Five different measurements were taken of each sample at different locations on the sample so an average thickness could be calculated. All samples were weighed before immersion, and in that way, it was possible to track the water absorption. All weights and thicknesses are given in tables 11.1-5 (appendix 11.4).

The volume of the solution in each vial was approximately 100 mL, and it was ensured that the samples were immersed and not floating on the liquid surface in the vials. When the samples had been immersed, they were put in an oven at 37°C.

The timeframe for each material is given in table 6.1 and 6.2. Gravimetric analysis was not done for the virgin material, due to prior studies performed on the virgin material. For each experiment time, three measurements were taken, of which the average was taken as a result and used further on.

Table 6.1: Immersion times for the virgin and recycled material from 2-100 days.

PLAV	PLAV-302	PLARC	PLARC-302
2 days	2 days	2 days	2 days
6 days	6 days	6 days	6 days
13 days	13 days	13 days	13 days
22 days	22 days	22 days	22 days
28 days	28 days	28 days	28 days
44 days	44 days	44 days	44 days
56 days	56 days	56 days	56 days
70 days	70 days	70 days	70 days
84 days	84 days	84 days	84 days
100 days	100 days	100 days	100 days

Importantly, the first day of immersion the measurements were carried out in time intervals given in table 6.2. The reason for carrying out measurements more frequently the first two days is because the significant changes in the mass in the materials occur during the first hours of immersion.

Table 6.2: Immersion times for the recycled materials up until two days.

PLARC (Short times)	PLARC-302 (Short times)
0 days	0 days
10 min	10 min
30 min	30 min
60 min	60 min
90 min	90 min
120 min	120 min
240 min	240 min
360 min	360 min
480 min	480 min
1440 min	1140 min

6.2.6 Gravimetric water absorption

A Mettler AJ100 microbalance with a precision of ± 0.1 mg was used to weigh the immersed samples, straight from taking them out of the buffer, and also one week later after they had been dried in the oven at 40°C. The films were exposed to natural ageing over a period of three weeks before being immersed in the phosphate solution. Natural ageing was executed to be sure that all the samples had been exposed to the same physical ageing. The samples were weighed before immersed, and the initial mass, m_0 was obtained. Thus, the mass variations that occurred in the samples were solely due to the effect of being immersed in the buffer solution. After three weeks samples are weighed, and m_0 is obtained as the initial mass of the dry specimen. The film was then immersed in their corresponding vials.

The film, once submerged, absorbs water but can also suffer a loss of mass due to hydrolysis and dissolution in the liquid. Once the required time was met, the specimen was removed from the vial, dried carefully with paper, to remove any remaining water located at the surface and then weighed. The mass of the sample at that instant is called the humid mass, m_h, and contains the

absorbed water mass, as possible loss of mass from the material degradation, and can be calculated by using equation 6.1.

$$m_h = m_0 + m_{H_2O} - m_{PLA} \quad (6.1)$$

Where m_0 is the initial mass, m_{H2O} is the mass of water absorbed and m_{PLA} is the loss of mass of PLA.

After the samples had been weighed, they were set to dry at 40°C for one week, to enable evaporation of the absorbed water in the sample. The value for the dry sample was obtained, $m_{d,}$. The mass of water absorbed could then be calculated using equation 6.2.

$$m_{H_2O} = m_h - m_d \quad (6.2)$$

The mass loss of PLA could be calculated by using equation 6.3.

$$m_{PLA} = m_0 - m_s \quad (6.3)$$

However, it is considered that at relatively short periods of time the mass loss of PLA is negligible (Engineer et al., 2011), and the final mass of absorbed water can the by calculated using equation 6.4.

$$m_{H_2O} = m_h - m_o \quad (6.4)$$

For further analysis the mass percentage was used and was calculated by using equation 6.5, 6.6 and 6.7.

Water absorbed in mass:

$$\%m_{H_20} = \frac{m_h - m_s}{m_0} \times 100 \tag{6.5}$$

Water absorbed in mass for short times:

$$\%m_{H_20} = \frac{m_h - m_0}{m_0} \times 100 \tag{6.6}$$

Mass loss of PLA:

$$\%m_{PLA} = \frac{m_0 - m_s}{m_0} \times 100 \tag{6.7}$$

6.2.7 Fourier transform infrared spectroscopy (FTIR)

To be able to study the chemical nature of the obtained films, like the processes that occur during the immersion in water and the types of water absorbed, a Nicolet Fourier Transform iS10 infrared spectrophotometer was used. The sampling technique Attenuated Total Reflection (ATR) was used in conjunction with Fourier transforms infrared spectroscopy, FTIR-ATR. This system enables the samples to be examined directly in either the liquid or the solid state, and the surface of the film can be analysed, which is in direct contact with the diamond accessory. As a result, it is possible to obtain spectra that allow studying the effects of water in the material (Cotugno et al., 2001).

The spectra obtained are the result of 16 scans, have a resolution of 4 cm^{-1} and have been conducted between 650-4000 cm^{-1} at room temperature. The software used to collect and process the spectra's is Thermo Scientific™ OMNIC™ Specta Software 9 and OPUS 5.5 software.

6.2.8 Ultraviolet-visible spectroscopy (UV-Vis)

Ultraviolet-visible (UV-Vis) spectroscopy was used to study the effect of hydrolytic degradation in the material. Water causes hydrolysis of PLA, and some of the hydrolysis products can be transferred over to the liquid. The liquid where the samples were immersed was analysed so that the changes produced in the liquid could be observed. A Perkin Elmer Lambda 35 spectrophotometer and Hellma 10mm Quarts cuvettes (100.600QG) was used, and the measurements were carried out at a velocity of 480 nm per minute and transmission between 200 and 800 nm. By the use of UV-Vis spectroscopy, it was intended to follow the hydrolytic degradation process of the polymer by analysing the immersion liquid. UV transmittance spectra of the PLAV and PLARC films were also carried out for samples without immersion (day 0).

6.2.9 Viscosity

The intrinsic viscosity of a polymer can be determined by measuring the time it takes a given volume of a solution of the polymer to fall through a capillary and comparing this time with the time it takes for the pure solvent to fall through the same capillary. The measurements were executed using an Ubbelohde size 1 viscometer with chloroform as the solvent and the following concentrations; 0.01 g/mL, 0.008 g/mL, 0.006 g/mL and 0.005 g/mL. When the viscosity is measured, the temperature, the fact that there are no contaminations, and that the equipment used is completely clean is crucial so that there are no measurement alterations. Steps were taken into account before completing the viscosity measures, like cleaning all the equipment with chromic acid and both solvent and solution were filtrated. The sample of PLA was of approximately 0.25 g, and was dissolved in 25 mL $CHCL_3$, and all measurements were executed at 25°C. The following procedure was performed in the measurements:

1. To avoid possible contaminations, all equipment was cleaned with chromic acid.
2. The solvent is filtered.
3. Weighing and dissolving of the polymer sample.

4. Once the sample is dissolved, the solution is filtered and transferred to a 25 mL flask. Then the solution is diluted with chloroform so that the total volume is 25 mL. The flask is shaken to ensure homogeneity in the solution.
5. The viscometer, flask with solution and solvent are introduced into a water bath at approximately a constant temperature of 25°C.
6. The fall time of the solvent is measured first and then 10 mL of the sample is added to the empty viscometer and the fall time is measured.
7. The sample is then measured with decreasing concentrations, by adding respectively 3, 3 and 4 mL of solvent.

The viscosity was measured for samples of PLARC and PLARC-302 for immersion times of 0, 13, 56 and 84 days. The sample that underwent cleaning test was measured as well.

6.2.10 Thermogravimetric Analysis

Thermogravimetric analysis was performed to determine the thermal stability of PLAV and PLARC with and without Cloisite 30B™ for immersion days 0, 13, 56 and 84. To carry out the analysis, approximately 14 mg of the PLA material were placed in a TGA 2050 thermobalance, from TA Instruments, under a nitrogen atmosphere. The thermobalance is illustrated in figure 6.5. The used gas flow rate was 30 mL/min, where 25 mL/min passed through the oven and 5 mL/min passed through the scale.

Figure 6.5: Thermobalance TGA 2050 of TA Instruments.

7. Results and Discussion

Commercial PLA was purchased to examine the possibility of their application for further use in the packaging industry. The experimental data have been processed in the software OMNIC™ and OPUS or/and Origin®.

7.1 Infrared spectroscopy

ATR-FTIR spectroscopy was used to study and characterise the material. This way the chemical nature of the material, the different types of water absorbed and the changes in both virgin and recycled material, while the material was immersed in the buffer could be determined. The peaks shown in the spectra can be assigned to different absorptions that correspond to vibration modes of the various functional groups in the material. The spectra obtained are the result of 16 scans between 650-4000 cm^{-1} at room temperature with a resolution of 4 cm^{-1}.

7.1.1 Characterisation of the materials without immersion

The spectrum of PLA is illustrated in figure 7.1 and shows the different characteristic bands of PLA. Multiple authors have referenced the bands observed for PLA (Auras et al., 2010; Weng et al., 2013; Meaurio et al., 2006; Carrasco et al., 2010; Kister et al., 1998; Badia et al., 2012). The band at 3502 cm^{-1} is assigned to O-H groups stretching vibrations. 2994, 2946 and 2880 cm^{-1} is assigned to the simple C-H stretching vibrations in CH_2 and CH_3 groups, and the corresponding simple bending vibrations in the methyl groups can be seen in the band at 1457 cm^{-1}. Band at 1747 cm^{-1} is due to stretching vibrations from the C=0 doublebond in the ester groups. 1382 and 1360 cm^{-1} is due to bending vibrations from the C-H bonds. 1266 cm^{-1} is assigned to coupled bending vibrations from the C-H bonds and bending vibrations of C-O-C. This band is related to the amorphous regions. 1207 cm^{-1} is assigned to coupled stretching vibrations of C-O-C and rocking of the CH_3 group and is related to the crystalline regions of the polymer. Stretching vibrations of the C-O-C bonds leads to bands at 1180, 1127 and 1080 and 1045 cm^{-1}. Coupling of the stretching vibrations of the C-C bonds in the back chain, with the rocking of the CH_3 groups, is assigned the band at 956 cm^{-1} and is related to the amorphous regions. The band at 867 cm^{-1} is due to stretching vibrations of the C-COO bonds. 756 cm^{-1} is due to rocking vibration of C=0 doublebonds (Auras et al., 2010; Weng et al., 2013; Meaurio et al., 2006; Carrasco et al., 2010; Kister et al., 1998; Badia et al., 2012).

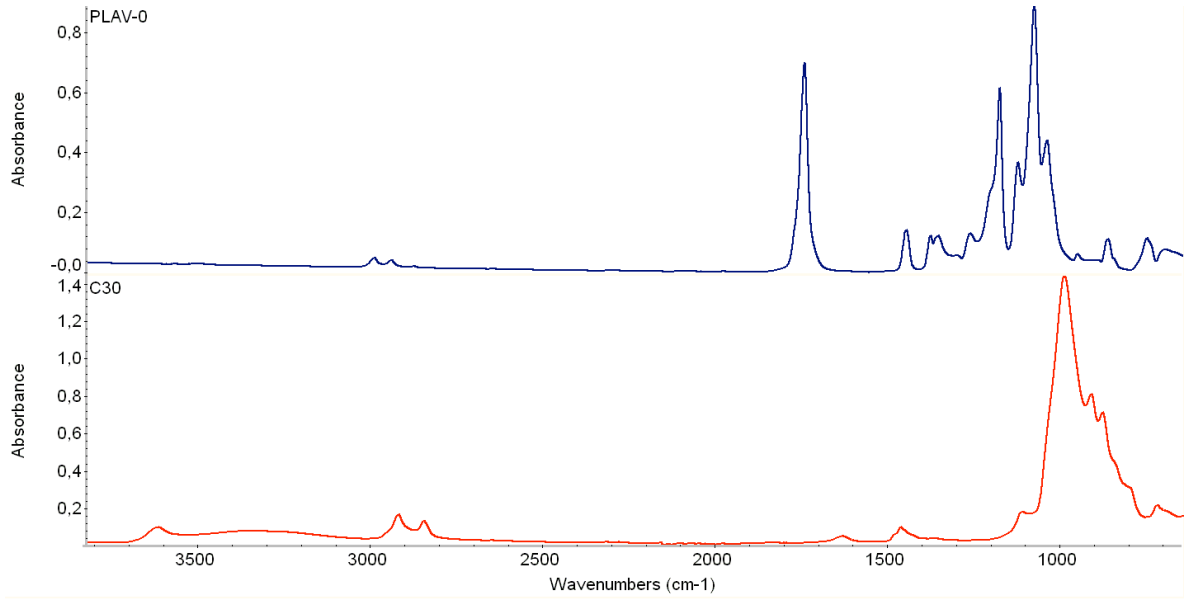

Figure 7.1: FTIR spectra of PLA and montmorillonite Cloisite 30B™ clay (Ortega, 2015).

If the spectrum of clay Cloisite 30B™ is compared to the spectrum of PLA, the most intense bands can be seen at close to 1000 cm^{-1} and corresponds to the siloxane bonds, Si-O-Si. At 2800-3000 cm^{-1} some bands appear that corresponds to the stretching vibrations of the C-H bonds in the organic modification of the clay. Spectra for all materials are presented in figure 11.1-4 (appendix 11.3).

To be able to analyse the spectrum more accurate the differences between PLAV and PLARC has been demonstrated and is illustrated in figure 7.2. The figure shows the characteristic bands of PLA. Because the material is recycled, it can provoke changes in the structure that are important to know about. The figure that illustrates the nanocomposites of PLAV and PLARC with Cloisite 30B^{TM} is presented in table 11.5 (appendix 11.3).

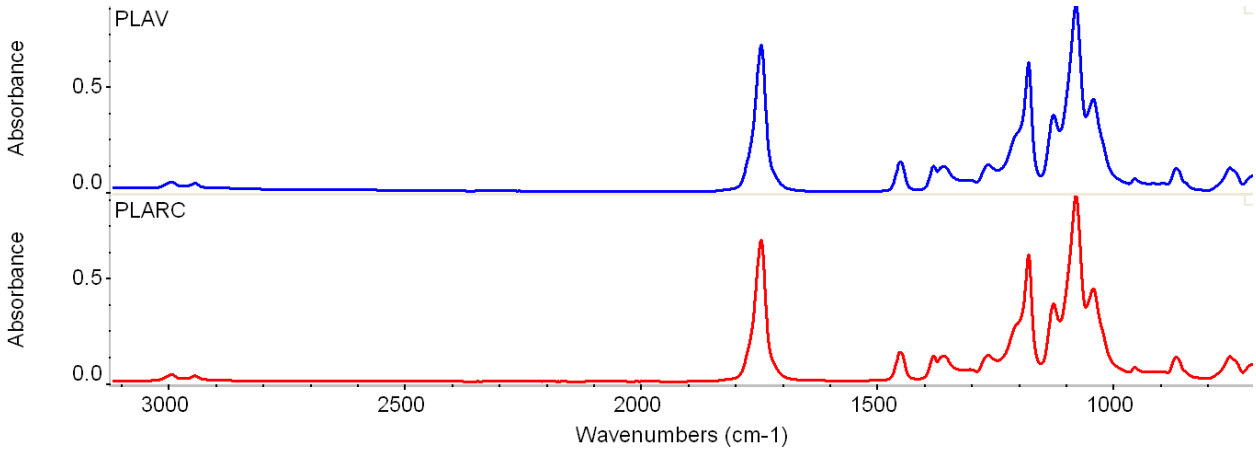

Figure 7.2: FTIR spectra of PLAV (red) and PLARC (blue) at immersion day 0.

In this figure, there is only a minimal difference between the two materials and shows that the recycled material shows the same characteristic bands as the virgin material. To be able to see any difference in the two spectra, the region between 1850-1650 cm^{-1} has been amplified for the both materials and is illustrated in figure 7.3.

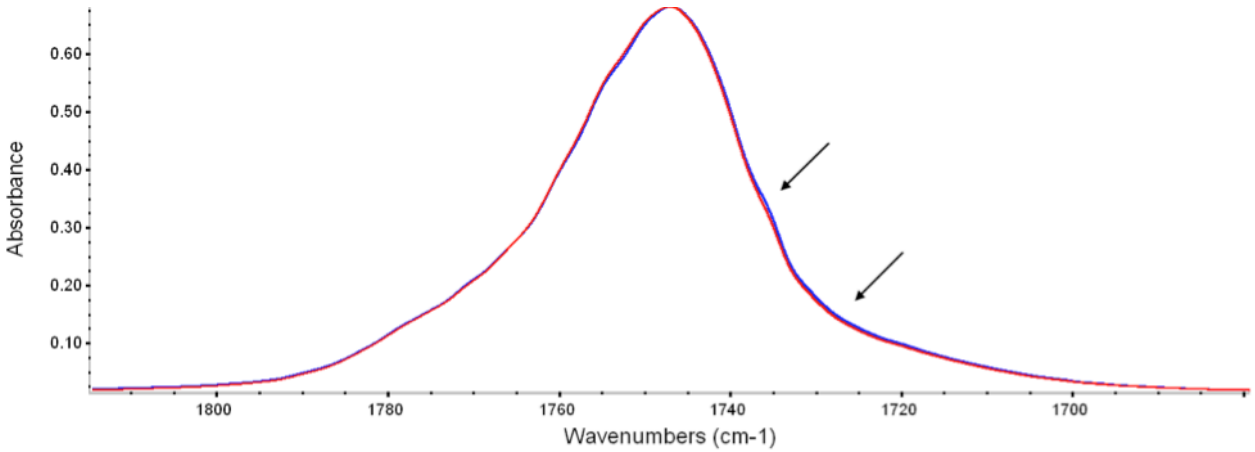

Figure 7.3: Amplification of the spectra of PLAV (red) and PLARC (blue).

In this region of the spectra, it is possible to see some differences, even though they are subtle, in the bands that appear at 1747 cm^{-1} which are due to the C=O doublebonds in the ester groups. This band is a little wider in PLARC than in PLAV. Meaurio et al. have related the changes in these bands with the formation of acidic groups in the polymer chains, which favours the

interaction between these and causes an increased degree of crystallinity in the material. Although subtle, it is also observed a small difference at 1725 and 1735 cm^{-1}, which can be assigned to acid groups in the recycled PLA. These groups are formed as acids primarily as a result of both thermal and photochemical degradation occurring during ageing. The materials have been subjected to simulated ageing and degradation that typically occurs naturally in the materials. Moreover, it can also cause some degradation during the reprocessed by extrusion when it is carried out for mechanical recycling. When the starting materials were characterised, the changes in their structure due to water absorption and the nature of the absorbed water could be studied.

7.1.2 Evolution of the infrared spectroscopy bands with the time of the immersion

The evolution of the bands is minimal at 37°C compared to at higher temperatures. In previous studies done at 58°C, the evolution of the bands has been greater (Ortega, 2015). The differences are minimal, which means that the crystallisation in the polymer and also the degradation, happens a lot faster at 58°C than at 37°C, which has been constated by other authors (Fukushima et al., 2011).

The difference in absorbance between the humid and the dry material was quantified, and the evolution of the bands between 3700 and 3000 cm^{-1} in PLAV-302 from 2-100 days is illustrated in figure 7.4 and for PLAV and PLARC-302 in figure 11.6 and 11.7 respectively (appendix 11.3).

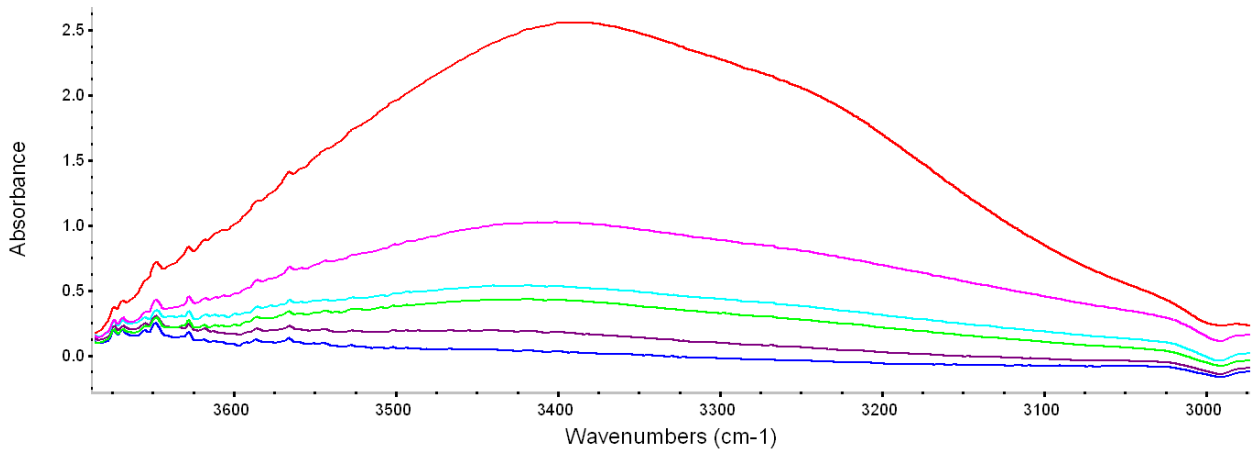

Figure 7.4: The evolution of the bands between 3700 and 3000 cm^{-1} for PLAV-302 for immersion day 2 (blue), 6 (purple), 13 (green), 22 (light blue), 44 (pink) and 100 (red).

A broadband between 3700 and 3000 cm^{-1} that increased with immersion time was observed. This band is related to absorption of water by the material. To obtain more information about the absorbed water, the spectrum of the hydrated material was subtracted to the spectrum of the dry material, and a deconvolution of the differences in spectra was performed. In the deconvolution, the band is decomposed into several bands, which correspond to different types of water, which is absorbed in the material.

The result of the deconvolution that corresponds to the spectrum of PLARC-302 that has been immersed in water during 27 days is illustrated in figure 7.5.

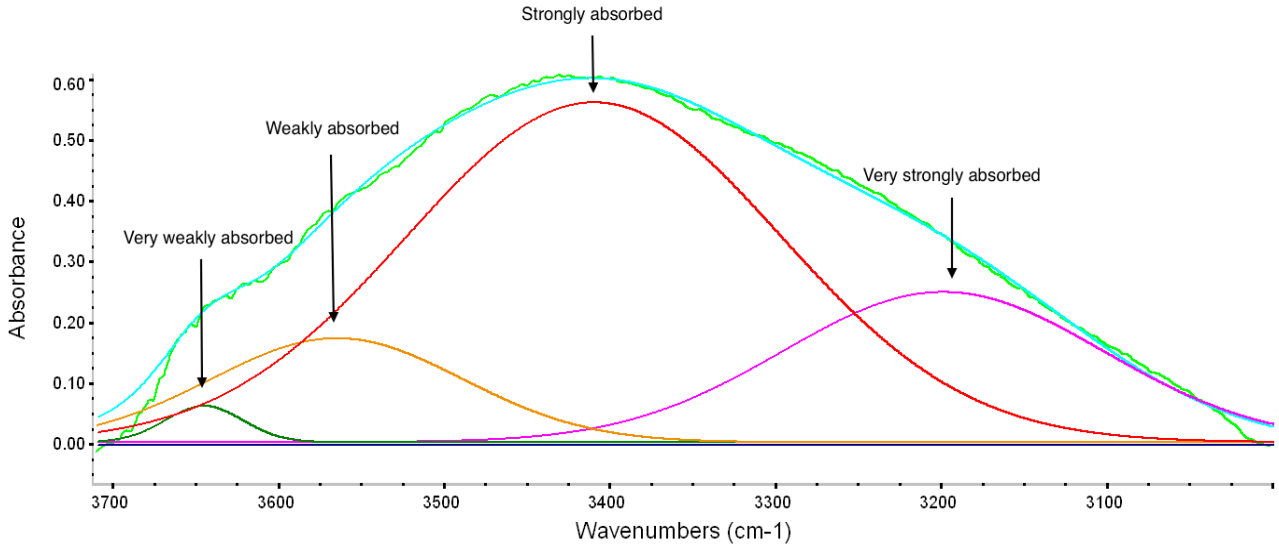

Figure 7.5: Results of the deconvolution of PLARC-302 at immersion day 27.

As indicated above, the spectrum of the unhydrated material was subtracted to eliminate the contribution of the OH-groups in PLA to only obtain information about the water retained at 27 days immersion. The deconvolution was executed by following the model of four states of water, which accounts for the observed bands of OH stretching vibration of absorbed water of the material (3190, 3410, 3567 and 3645 cm^{-1}) (Cotugno et al., 2001; Lasagabáster et al., 2009). This model focuses on the relative distribution of the four types of water molecules, and considers the presence of free and bound water, but it is also believed that water bound to the polymer can be linked in different ways. Depending on their type of interactions, the water can be categorized

into four different types; very weakly, weakly, strongly and very strongly absorbed. Firstly, the bands centered at 3190 and 3410 cm^{-1} are related to strong and very strong interactions between water and polymer respectively. Secondly, the band at 3567 cm^{-1} can be the result of weakly associated water molecules or spontaneously formed dimers. Finally, the band at 3645 cm^{-1} corresponds to very weak interactions between water and polymer or non-associated water that does not establish hydrogen bonds with the polymer. This model was preferred over a simpler model. Another simpler model that only divides the absorbed water in free and bound water was possible to use. Here, the more complex model was preferred because it provides a better description and a better fit with experimental results in similar materials that were examined in this study (Lasagabáster et al., 2009).

The intensity of the interaction of water with the polymer is related to the wavenumber of the stretching vibration of OH bonds. This relation is due to the energy of that link, and that vibration is less when the wavenumber where the band appears is proportional to the energy of the corresponding vibration and when there is a strong hydrogen bonding.

7.1.3 Analysis of the effect of clay and the recycling of the material

The area of the band corresponding to hydration, between 3700-3000 nm, was measured for the corrected and normalized subtractions of the virgin and recycled material with and without montmorillonite clay. The measured area was plotted against immersion days for PLARC and PLARC-302, and the results are illustrated in figure 7.6.

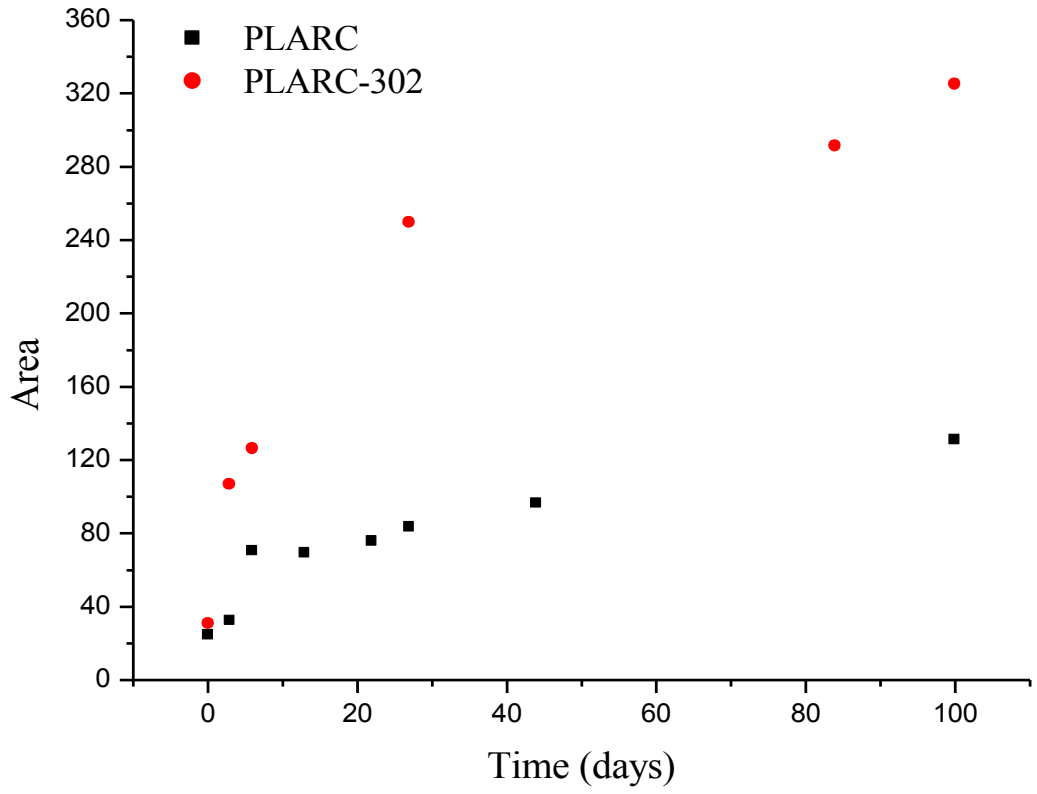

Figure 7.6: Measured area of the band between 3700-3000 nm for PLARC and PLARC-302 over immersion days.

The illustrated effect is that the recycled material with clay has a larger area in this particular band, which again means that it absorbs more water during immersion. Clay is more hydrophilic than the polymer, and therefore it is logical to think that the nanocomposites with clay will absorb more water than just the polymer. Thus, explaining the effect seen in figure 7.6.

To be able to study the effect the recycling process has on the material, the areas of the band between 3700-3000 nm of the recycled material were compared with the virgin material, and are illustrated in figure 7.7.

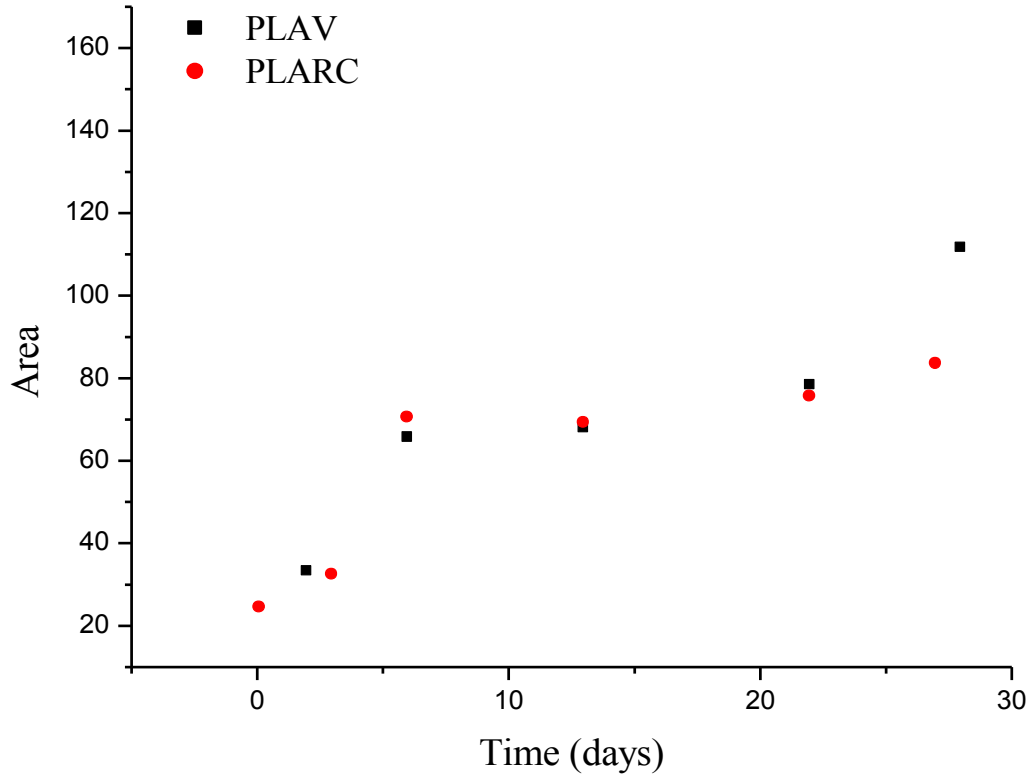

Figure 7.7: Measured area of the band between 3700-3000 nm for PLAV and PLARC over immersion days 0-28.

According to these results, it seems like the recycling process does not have an effect on the absorption of water since the differences are minimal. The FTIR spectrophotometer was unusable for a period when the measurements of the virgin material were being performed, so it's hard to know the effect over a longer period of time, and based on these results it was difficult to conclude with anything.

The figures of the comparison between PLAV-302 and PLARC-302 and PLAV and PLAV-302 of the measured area of the band between 3700-3000 cm^{-1} are given in figures 11.8 and 11.9 respectively (appendix 11.3).

7.2 Study of water absorption by gravimetric analysis

The hydrolytic degradation of PLA begins with water uptake, and as explained in section 5 the behaviour of water absorption of the polymer is uncertain. Possible degradation processes caused by the absorbed water may give rise to the formation of hydrophilic groups and mass loss by hydrolysis and dissolution, which is why the mass loss and the absorption were studied by using gravimetric methods, explained in section 5.2. It is also reasonable to think that this effect is accentuated for the mechanically recycled polymer.

The temperature of 37ºC was chosen as the experimental temperature because it is well below the glass transition temperature (55-60ºC). It also is a temperature that has been studied before, primarily for the purpose of using PLA in biomedical applications, since it is a reference to our body temperature (Höglund et al., 2010).

Clay modifies the structure of the polymer, and the effect of these modifications can lead to changes in the diffusion of water through the polymer or the amount of water absorbed. The water uptake in the polymer and a nanocomposite with 2% Cloisite™ 30B, was observed and compared along with virgin and recycled material without cleaning step. By comparing virgin, recycled, without the cleaning step, and recycled material, the effect of recycling on absorption and how it affects the mechanical properties of the recycled material could be studied. The observed absorption has been compared with a corresponding Fickian diffusion model to obtain information about the diffusion mechanisms and the nature of the effects on the structure caused by clay and mechanical recycling.

7.2.1 Mass variations

The aim was to quantify the mass of absorbed water and mass loss of PLA over specific time intervals. At relatively short times, lower than two days, it has been demonstrated in previous studies that the mass loss of PLA is negligible. Thus, from day two the gravimetric mass loss of PLA and the absorbed water mass was calculated by using equation 6.1-7 and method in section 6.2.6. The results for PLARC are given in table 7.1.

The absorbed water mass for short times was also calculated. The calculations for PLARC are listed in table 7.1, and for PLARC-302 and short times for both materials are presented in tables

11.6 and 11.7 (appendix 11.4). The weighed masses for the materials are given in tables 11.1-4 (appendix 11.4).

Table 7.1: Gravimetric mass loss and absorbed water for PLARC with the associated standard deviation all given in percent for 2-100 days.

Time (days)	m_{PLA-RL} (%)	St.dev (%)	m_{H20} (%)	St.dev (%)
2	0.002	0.033	0.801	0.068
6	-0.027	0.061	0.881	0.114
13	0.010	0.017	0.905	0.069
22	-0.046	0.079	0.949	0.075
28	0.004	0.051	1.066	0.099
44	-0.024	0.042	1.200	0.029
56	-0.103	0.020	1.332	0.086
70	-0.086	0.008	1.549	0.150
84	0.044	0.013	2.059	0.186
100	-0.032	0.029	2.355	0.433

The mass loss presented in table 7.1, are all smaller than their corresponding standard deviation. Therefore, it can be assumed that the loss of PLA is negligible at short time intervals, and small in general when the experiments have been carried out at 37ºC. However, the solution itself can be measured by UV-Vis spectroscopy to get a better perspective of what happens under the immersion of PLA. The evolution of absorbed water in percentage over time for PLARC is illustrated in figure 7.8, with corresponding error bars estimated as the standard deviation, for the differences between the three parallels. The figure of the evolution of absorbed water in PLARC-302 is given in figure 11.10 (appendix 11.4).

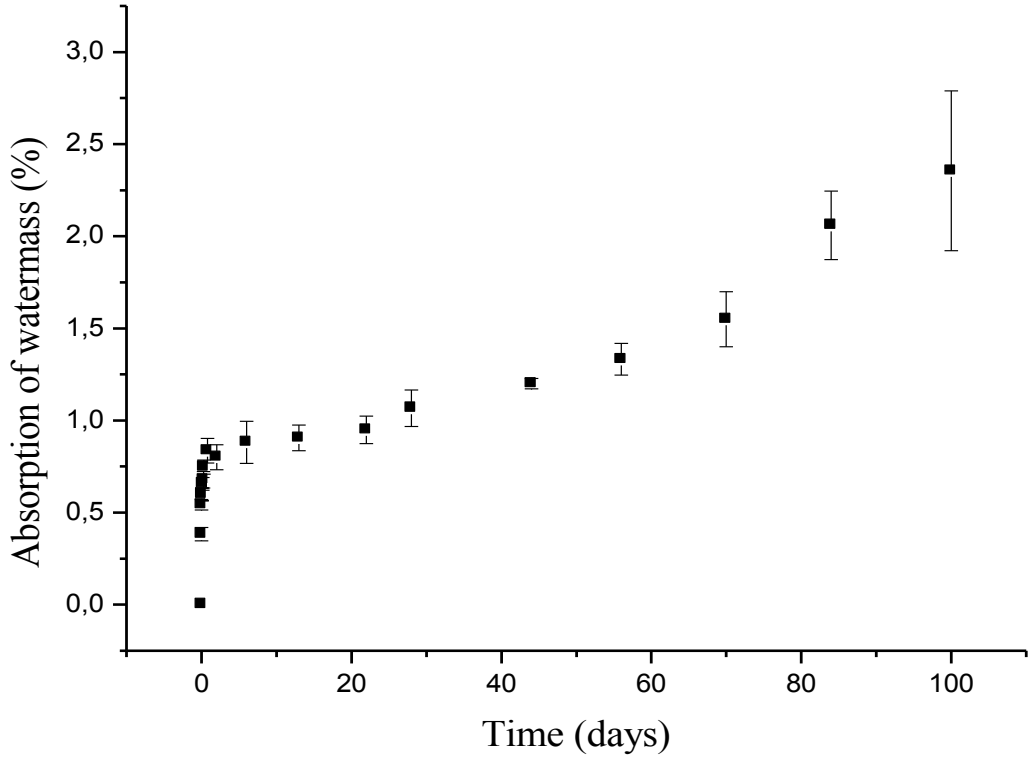

Figure 7.8: Water absorption showed in mass percentage plotted against time from 0-100 days for PLARC, with its associated error bars.

Further, figure 7.8 illustrates a significant increase in the first hours up until one day, where it seems like the water absorption stabilises at around 1% at about ten days. However, it seems like, after around 40 days, the water absorption continues to increase. Thus, the absorption curve illustrates rapid absorption during the first days and then continues to grow more slowly, but it is also observed re-accelerating of the absorption later in the process. This effect may be due to the appearance of hydrophilic groups, such as carboxylic groups, as a result of hydrolysis of the polymer.

The scale was altered to facilitate the view of the stabilisation of the water absorption at 1% and is illustrated in figure 7.9.

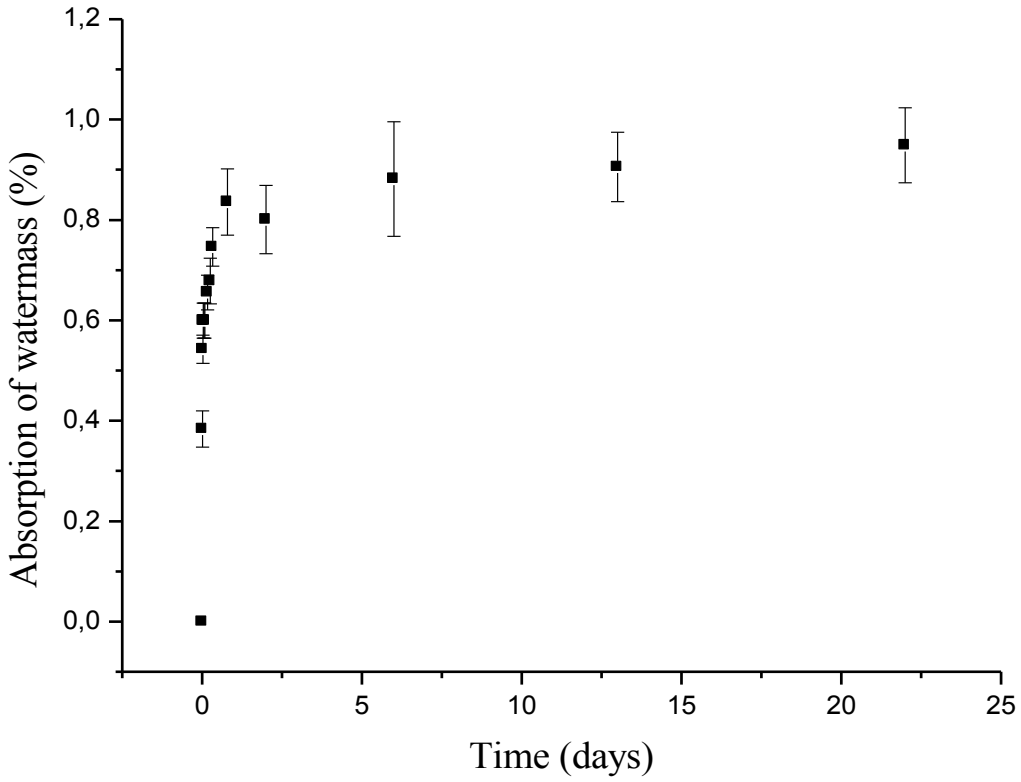

Figure 7.9: Water absorption showed in mass percentage plotted against time from 0-22 days for PLARC, with its associated error bars, facilitating the view of the stabilization at 1%.

At shorter times, the absorption can be explained by the fact that the water occupies the free volume and joins the polymer by Van der Waals forces and hydrogen bonds, and will saturate within a small time frame. The increase of water absorbed observed at longer times can be explained by hydrolysis, thus generating a series of hydrophilic species, such as hydroxyl and carboxyl groups which lead to a gradual water absorption.

The curves of water absorption for the materials have been studied. It can be seen that curves for both PLARC and PLARC-302, for short times, fit neatly into an exponential model of first order, thus indicating that the water absorption could follow a possible Fickian behaviour. So the diffusion coefficient for the materials could be calculated. This study allowed examining the effect the recycling process has on the absorption process. To better illustrate this trend, the water absorption for PLARC is plotted over time and is shown in figure 7.10.

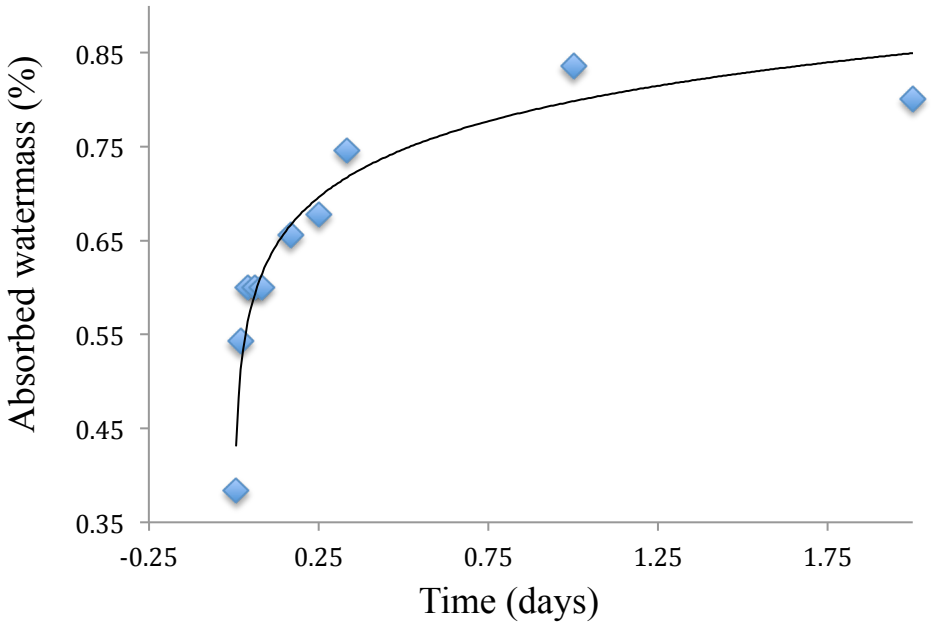

Figure 7.10: Water absorption for PLARC from 0-2 days of immersion.

Agreement with the predicted curve for Fickian behaviour is satisfactory, for short times. To illustrate that the water absorption for PLA does not follow Fickian behaviour over longer periods of time, the water absorption for PLARC was plotted over immersion time from 0-100 days and is illustrated in figure 7.11.

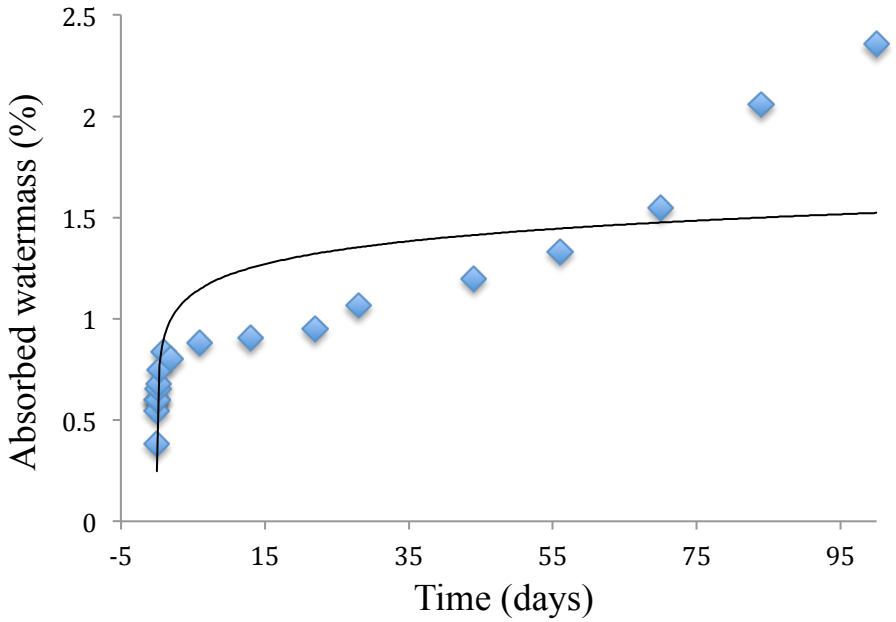

Figure 7.11: Water absorption over time for PLARC from 0-100 days of immersion.

Here the behaviour of PLA at short times has been analysed because the purpose is to use it for packaging in the food industry. Therefore it is logical to think that the analysis should concentrate around the conservation at short times. If the goal is to analyse the immersion over longer time intervals, it is possible to do a study on the waste composting of PLA.

7.2.2 Study of the diffusion model and determination of diffusion constants

Like stated before, it has been assumed Fickian behaviour for up until two days. The diffusion coefficient is defined as the constant proportional to the diffusive phenomenon and is dependent on both the solute and the solvent. The diffusion constants, D, were determined from experimental data by a direct adjustment of the polymer that it follows Fick's second law. D was calculated by using equations 5.1-7 in section 5 and by data given in appendix 11.4 table 11.6 and the measured length and width of samples of 4 and 2.5 cm respectively.

The software Origin® calculates the necessary parameters by using the Levenberg-Marquardt algorithm like explained in section 5, that are required for calculating the diffusion coefficient. The necessary parameters are; the number of terms of wanted series (n), the final mass at equilibrium (M_{inf}) and Tau. The fitted curve of PLARC for different values of n is illustrated in figure 7.12.

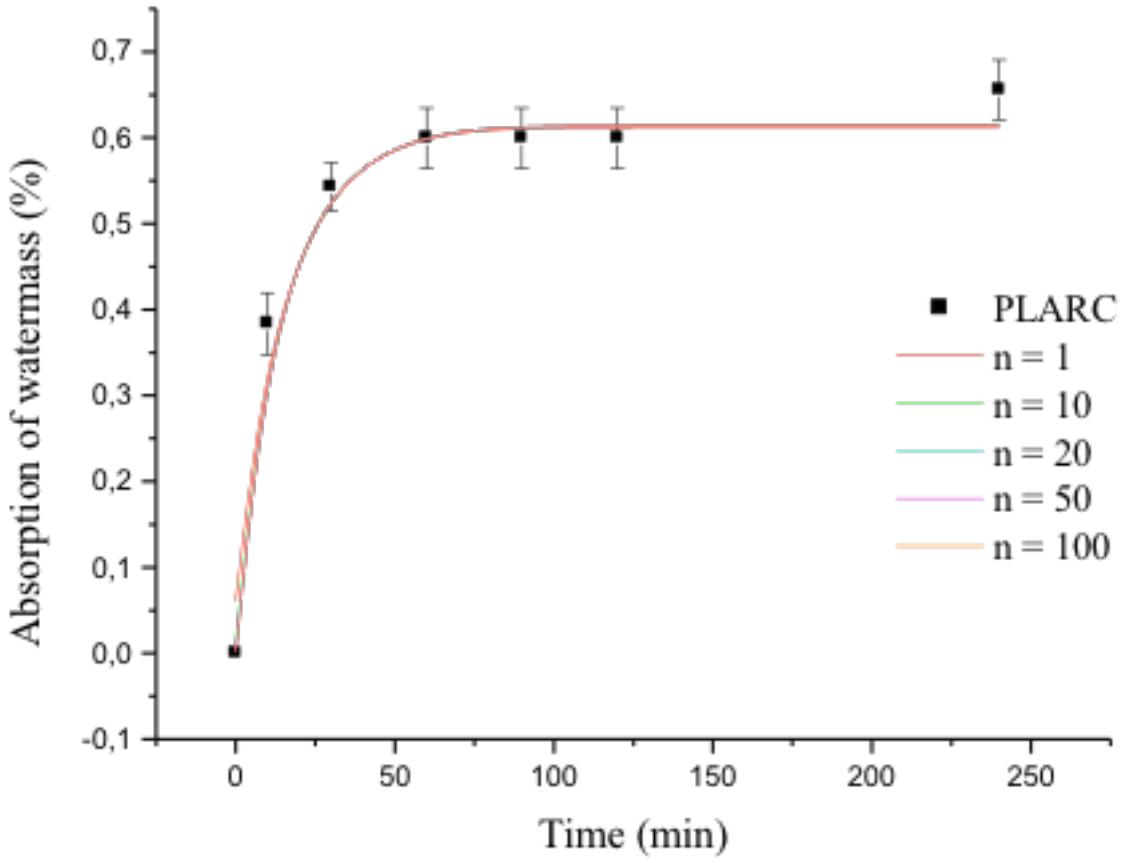

Figure 7.12: Fitted curve of PLARC for different values of n.

The values calculated by Origin® are given in table 7.2 for PLARC, and table 7.3 for PLARC-302.

Table 7.2: Values of the parameters from the adjustment of PLARC calculated in Origin® by using the Levenberg-Marquardt algorithm for different values of n.

n	M_{inf}	τ (min)	R^2	X^2
1	0.61241 ± 0.0179	14.0540 ± 2.5725	0.9801	1.0495
10	0.61403 ± 0.0180	14.1948 ± 2.5859	0.9914	0.4527
20	0.61408 ± 0.0180	14.1999 ± 2.5862	0.9917	0.4373
50	0.61408 ± 0.0180	14.1999 ± 2.5862	0.9918	0.4324
100	0.61408 ± 0.0180	14.1999 ± 2.5862	0.9918	0.4317

Table 7.3: Values of the parameters from the adjustment of PLARC-302 calculated in Origin® by using the Levenberg-Marquardt algorithm for different values of n.

n	M_{inf}	τ (min)	R^2	X^2
1	0.6627 ± 0.0152	35.7325 ± 4.6491	0.9756	5.3903
10	0.6714 ± 0.0164	38.3183 ± 4.7540	0.9860	3.1027
20	0.6717 ± 0.0165	38.3907 ± 4.7568	0.9862	3.0429
50	0.6717 ± 0.0165	38.4128 ± 4.7576	0.9863	3.0241
100	0.6718 ± 0.0165	38.4187 ± 4.7578	0.9863	3.0212

Where X^2 is an indicator of how good the fit is and M_{inf} is the water absorbed at equilibrium. The tables illustrate that for the higher number of terms, the better R^2, and the lower X^2, which means less uncertainty, which improves the fit. When the number of terms is equal to 100, the values are close to constant. For that reason, the parameters used for calculating the diffusion coefficients is the series where n = 100 that has been used.

The diffusion coefficient can then be calculated by using equations 5.1-7, values in table 7.2 for PLARC and table 7.3 for PLARC-302. With the obtained values the diffusion coefficient, D_c could be calculated. D_c for both materials is given in table 7.4.

Further, the effect that montmorillonite clay and the mechanical recycling process has on the diffusion coefficient and absorbed water in the material. The recycled material, including the cleaning step, was analysed and compared with virgin and recycled material from prior studies (Lorenzo, 2015; Ortega, 2015).

Table 7.4: The estimated diffusion constant for PLARC and PLARC-302, the measured thickness of the samples and the calculated values for τ and water absorbed at equilibrium (M_{inf}) with their associated standard deviation.

Material	$M_{inf\,(\%)}$	τ (min)	Thickness (μm)	D (m^2/s)	D_c (m^2/s)
PLARC	0.6141 ± 0.0180	14.1999 ± 2.5862	249 ± 25	$7.3808 \cdot 10^{-12}$	$7.1476 \cdot 10^{-12}$
PLARC-302	0.67175 ± 0.0165	38.4187 ± 4.7578	289 ± 30	$3.6749 \cdot 10^{-12}$	$3.5406 \cdot 10^{-12}$

7.2.3 The effects of mechanical recycling and clay

The absorbed water in the recycled material, which included a cleaning step, has been compared with absorbed water in virgin and recycled PLA, studied in previous projects (Ortega, 2015). The evolution of the absorbed water for all three materials without montmorillonite clay with corresponding error bars is illustrated in figure 7.13. The development of absorbed water in the materials with montmorillonite clay is presented in figure 11.11 (appendix 11.4).

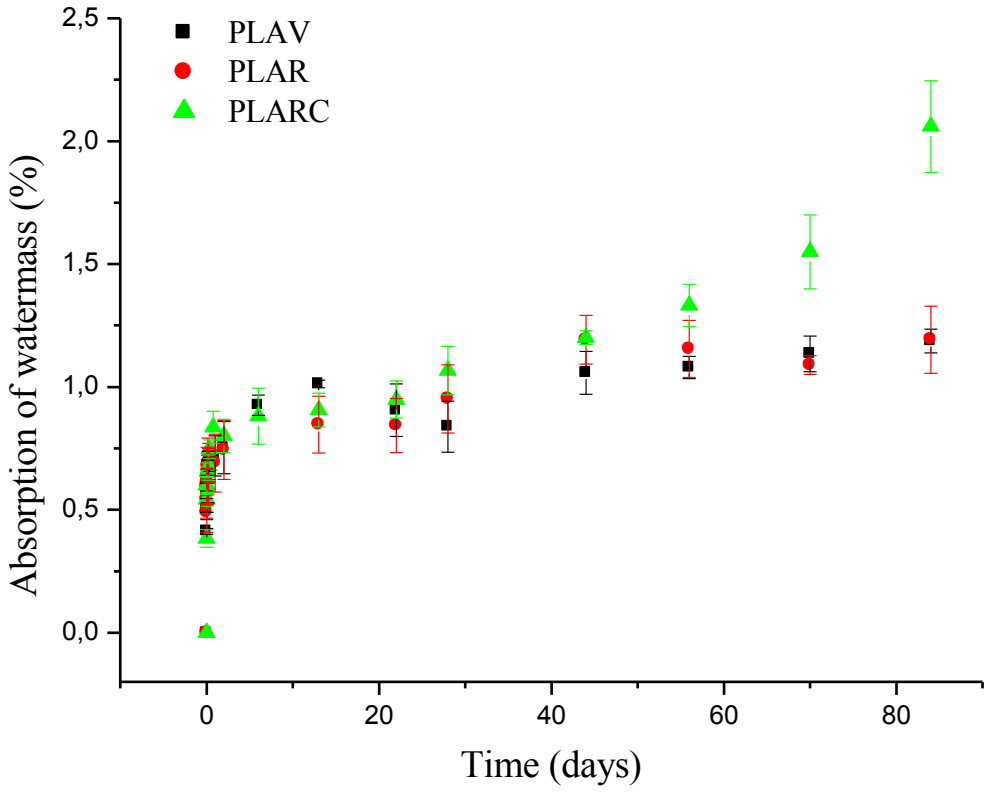

Figure 7.13: Evolution of absorbed water given in mass percentage for PLAV, PLAR, and PLARC with corresponding error bars.

The recycling and recycling including the cleaning step processes do not seem to have a great impact on the absorption of water during immersion for short times, by comparing the materials to the virgin material. Here, there are slight differences between the materials, even though they are small. However, PLARC absorbs more water at longer times, which can be expected due to

degradation in the recycling process with the cleaning step. The cleaning step that the material undergoes is done at a high temperature, 85°C, which can lead to degradation of the material. In alkaline medium, the catalysis of the hydroxyl groups generates low amounts of carboxyl groups in the polymer. Later, these carboxyl groups catalyse the hydrolysis during the immersion of the recycled material, and an autocatalytic process occurs. Thus, the material resists less in water, and more degradation occurs. This hypothesis can be supported by UV transmittance spectra of PLAV, PLAR, and PLARC before immersion, which are illustrated in figure 7.14. The recycled materials, especially PLARC, shows an absorption band centred near 280 nm that has been assigned to carboxyl groups. The figure illustrates that the concentration of –COOH groups, responsible for the posterior autocatalysis, is higher in PLARC than in the two other materials.

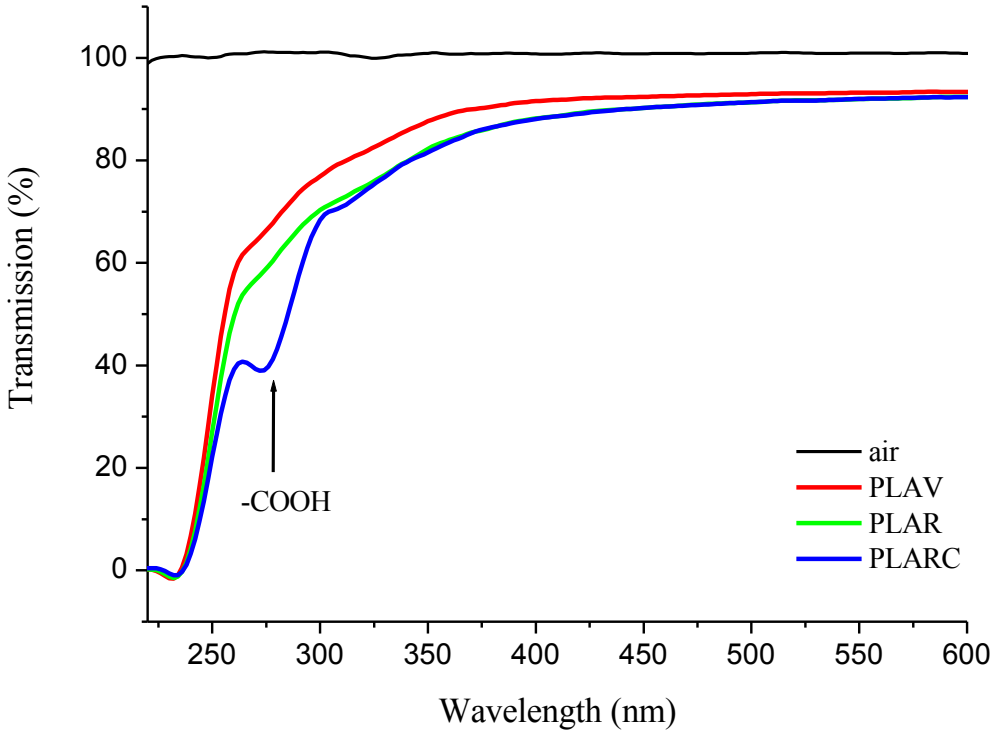

Figure 7.14: UV-Vis transmission spectra of PLAV, PLAR and PLARC at day 0.

The effect of mechanical recycling

To be able to observe the differences in the structure of the recycled material and the effect of the water absorption when the material is recycled and recycled, including the cleaning step, the

absorbed water, the diffusion coefficients and the percentage of absorbed water at equilibrium were compared for PLAV, PLAR, and PLARC. The data for PLAV and PLAR, with and without clay were measured in previous studies (Lorenzo, 2015: Ortega, 2015). The diffusion coeffisients and absorbed water at equilibrium for all materials are given in table 7.5.

Table 7.5: The calculated diffusion constant and the absorbed water at equilibrium with corresponding standard deviation for the materials PLAV, PLAR and PLARC with and without clay.

Material	M_{inf} (%)	St.dev	D_c (m^2/s)
PLAV	0.82	0.04	$8.4 \cdot 10^{-13}$
PLAV-302	0.85	0.04	$3.4 \cdot 10^{-13}$
PLAR	0.69	0.02	$1.3 \cdot 10^{-12}$
PLAR-302	0.97	0.04	$7.3 \cdot 10^{-13}$
PLARC	0.61	0.02	$7.1 \cdot 10^{-12}$
PLARC-302	0.67	0.02	$3.5 \cdot 10^{-12}$

Firstly, to be able to distinguish the differences between the materials, the water absorption over time of PLAV was compared with the one of the PLARC. The relation between the two materials with their corresponding error bars is illustrated in figure 7.15. The figure illustrates that the difference in water absorption is non-significant up until about 45 days. In the virgin material, it seems like the water absorption has reached a maximum at around 1%, whereas in PLARC it seems that after around 45 days the water absorption will continue to increase faster.

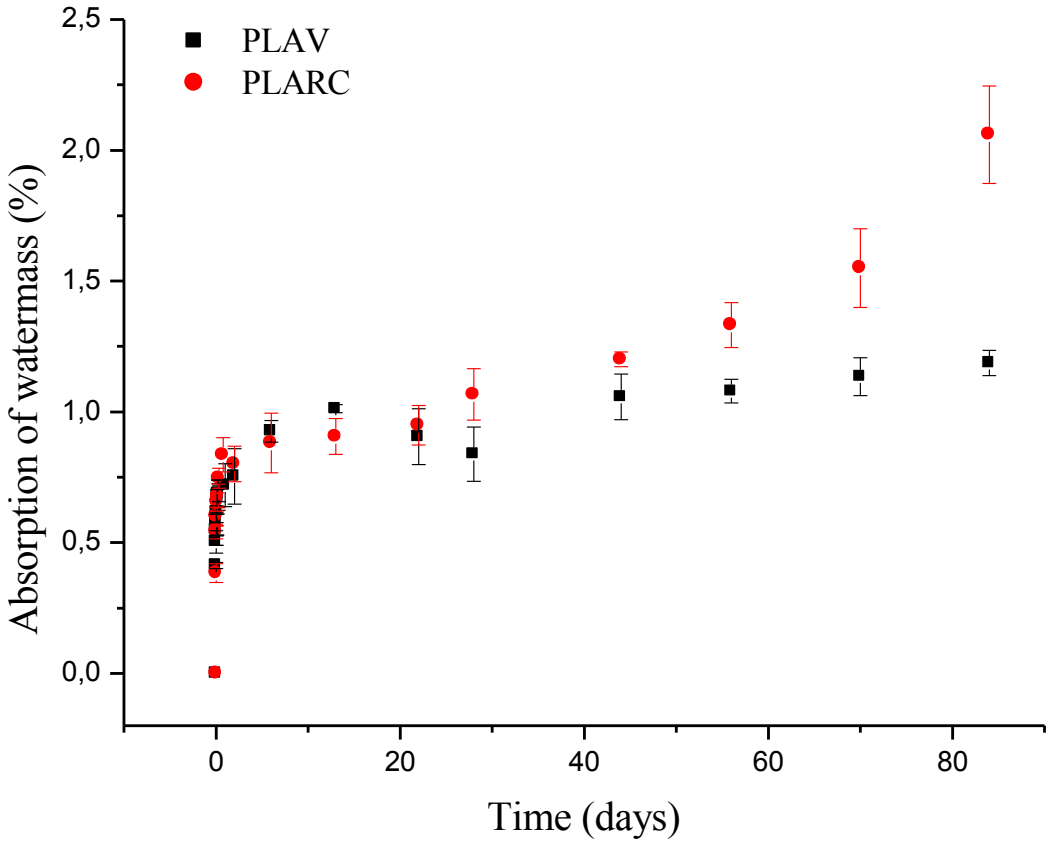

Figure 7.15: Evolution of absorbed water given in mass percentage for PLAV and PLARC with corresponding error bars.

These results are in good agreement with those obtained by using FTIR spectroscopy (figure 7.7).

The comparison of the diffusion coefficients, D_c, between the virgin, the recycled and the recycled, including the cleaning step, materials is illustrated in figure 7.16. In the materials, an increase in the value of the diffusion coefficient can be seen for the recycled material, and an even greater increase when the cleaning step is included. When the material is recycled it causes altering of the molecular structure of the polymer, thus providing faster diffusion of water, and higher diffusion coefficients.

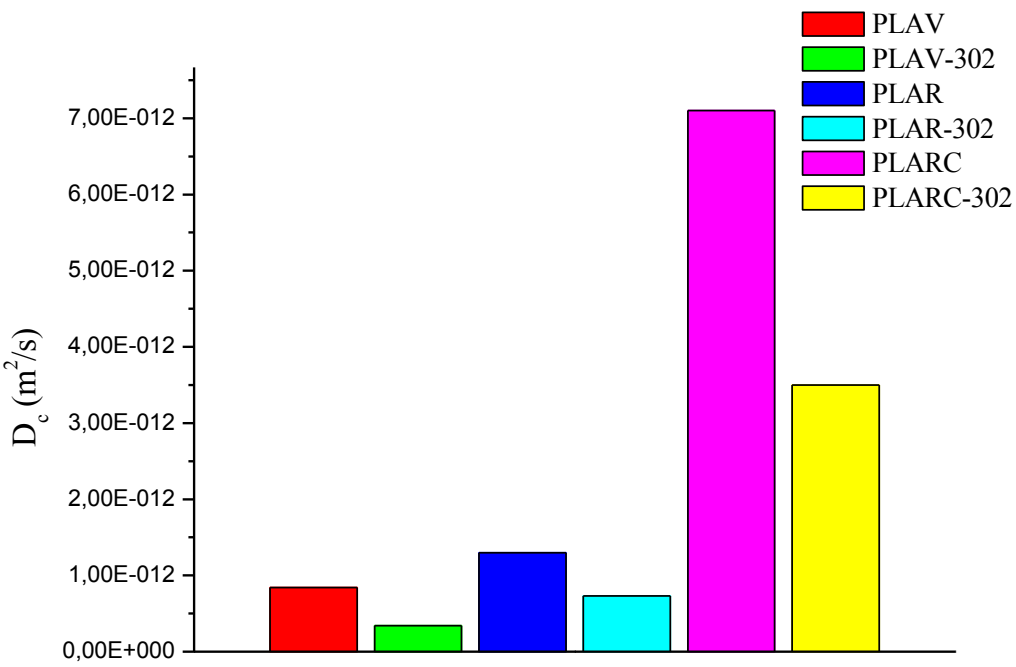

Figure 7.16: The diffusion coefficient, D_c, compared between the materials PLAV and PLAV-302, PLAR and PLAR-302 and, PLARC and PLARC-302.

Recycling may cause bond cleavage and involve the formation of strongly polar and hydrophilic groups, such as –COOH groups in PLA, which facilitate water diffusion through the polymer. This effect will be even greater in the recycling process that includes the cleaning step due to the higher production of carboxylic groups under cleaning step in an alkaline medium, which agrees with prior results showing that the presence of –COOH groups is greater in PLARC (figure 7.14).

The percentages of absorbed water at equilibrium, M_{inf}, were compared for PLAV, PLAR, and PLARC, and are depicted in figure 7.17. Concerning the effect of the recycling process on M_{inf}, even though the diffusion coefficient is higher for the recycled material including the cleaning step, the water absorbed by the different materials are very similar. It must be taken into account that M_{inf} corresponds to water absorbed in the very first stages of the immersion. At longer immersion times, when the absorption does not follow a Fickian behaviour, the amount of absorbed water is clearly higher in the recycled material.

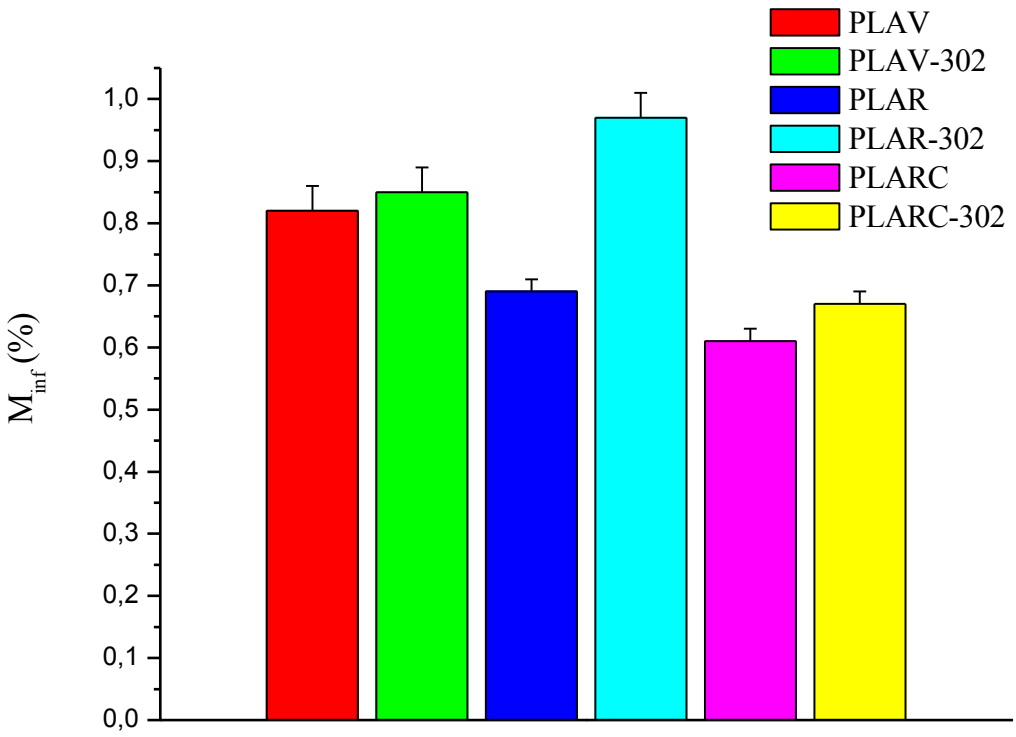

Figure 7.17: The percentage of water absorbed at equilibrium, M_{inf}, compared between the materials PLAV and PLAV-302, PLAR and PLAR-302 and, PLARC and PLARC-302 with associated errorbars.

The effect of montmorillonite clay

To be able to see the effect of montmorillonite clay, the absorption of water in PLARC was compared with the absorption of water in PLARC-302 and are illustrated in figure 7.18. It seems like montmorillonite clay has a greater effect on the water absorption than the recycling process. Like stated above, in PLARC the absorption of water increases over time, but the increase is higher in PLARC-302, with a difference of ~5% in water absorption at 84 immersion days.

Clay is more hydrophilic than the polymer, and therefore it is logical to think that the nanocomposites with clay will absorb more water than just the polymer. Thus, this effect contribute to explain the effect seen in figure 7.18. However, the difference observed at long immersion times is so big that it cannot be fully explained by the absorption of only 2 wt.% of clay. Therefore, it can be proposed that the clay catalyses the hydrolytic degradation of PLA,

producing more hydrophilic groups, which also contributes to the increased water absorption at long immersion times.

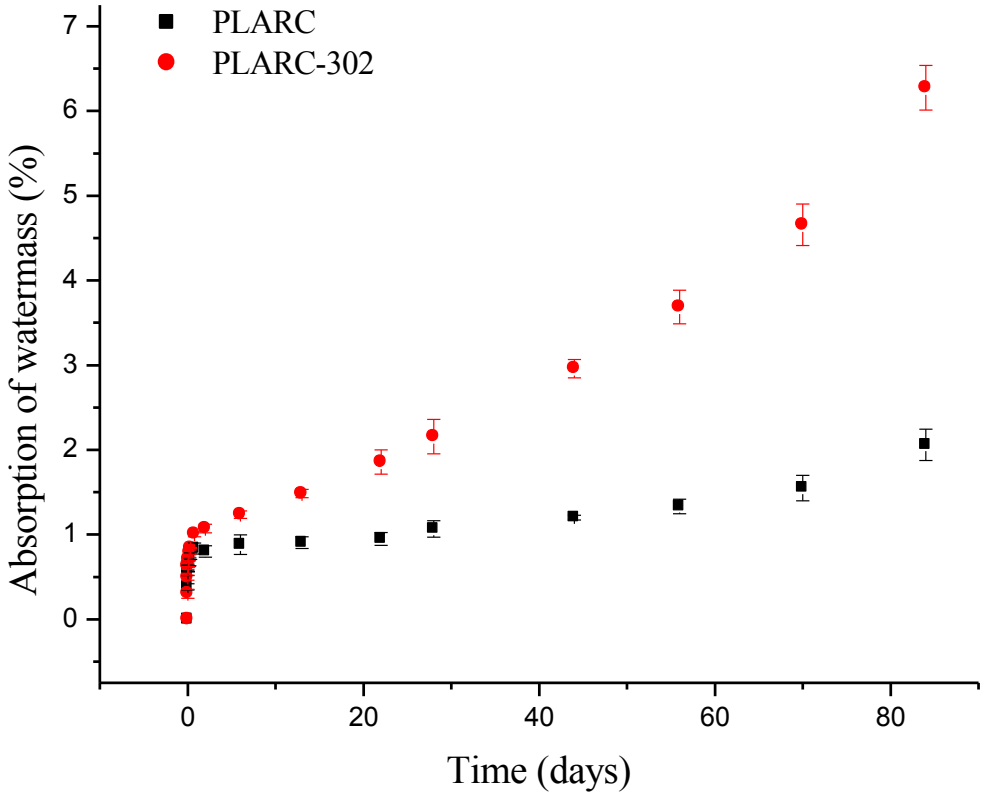

Figure 7.18: Evolution of absorbed water given in mass percentage for PLARC and PLARC-302 with corresponding error bars.

The trend seen in the materials that contain clay is that they will increase the diffusion constant and also the M_{inf}.

Regarding the absorption at short immersion times, more important for the applications of PLA in food packaging, the trend seen in the materials that contain clay is that clay will decrease the diffusion coefficient and increase the M_{inf}. Montmorillonite is a layered silicate, and the clay sheets dispersed in the polymer will function as barriers to water diffusion. When the diffusion coefficient is decreased, it will prevent the passage of water, as well as carbon dioxide and oxygen as a result (Crank, 1975; Roy et al., 2012). When comparing the diffusion coefficient for PLARC with and without montmorillonite clay, the results demonstrate that clay decreases the

value of the diffusion coefficient, which is illustrated in figure 7.16 The percentage of water mass that is absorbed by the material is greater in the presence of clay than without clay. The effect on the absorbed water mass at equilibrium can be explained by considering that the clay is more hydrophilic than the polymer, so it is reasonable to think that the nanocomposites with clay absorb more water than the polymer alone. This effect concurs with studies done by other authors (Roy et al., 2012). The effects on the diffusion coefficients follow the same trend for all three materials, where the materials with clay show lower diffusion coefficients.

The effect that clay has on the absorption of water at equilibrium in the recycled material, including a cleaning step, was studied. The percentage of absorbed water is higher in the material with clay, and the difference between the two materials is illustrated in figure 7.17 for PLAV, PLAR, and PLARC. The same effect for the recycled material, including the cleaning step, can be seen for the virgin and recycled material. The clay augments the percentage of water absorption at equilibrium. However, the increase is tiny, at least for PLAV and PLAR, whereas a little greater in the recycled material. The differences are small in all cases because there is only a 2% of clay.

7.3 Study of the degradation of PLA by UV-Visible spectroscopy of the immersion liquid

When PLA is in contact with water the ester groups in PLA may undergo hydrolysis, which causes the formation of monomers and small oligomers. The immersed materials were analysed by FTIR analysis and to be able to study the effect of hydrolytic degradation further, the immersion liquid was analysed with UV-Vis spectroscopy. The analysis of the liquid can provide valuable information about the chemical processes occurring in the material during immersion in the liquid because some of the monomers and small oligomers formed in the hydrolytic degradation of PLA may migrate to the liquid in which it is immersed.

UV-Vis spectroscopy was used to analyse the liquid in which the samples were immersed. The measurements were performed with a Perkin Elmer Lambda 35 UV-Vis spectrophotometer in the UV-Vis region (800 - 200 nm), where the liquid corresponds to different immersion times for both virgin and recycled material. The spectrophotometer is of a double beam. Therefore a buffer solution was used as a reference.

The immersion liquid of PLAV, PLAV-302, PLARC and PLARC-302 were measured from 2 to 100 days of immersion time. The spectra of the liquid of immersion at 37°C for PLARC are illustrated in figure 7.19. The spectra of the virgin materials with and without clay and for the recycled material with clay are given in figures 11.12-14 (appendix 11.5).

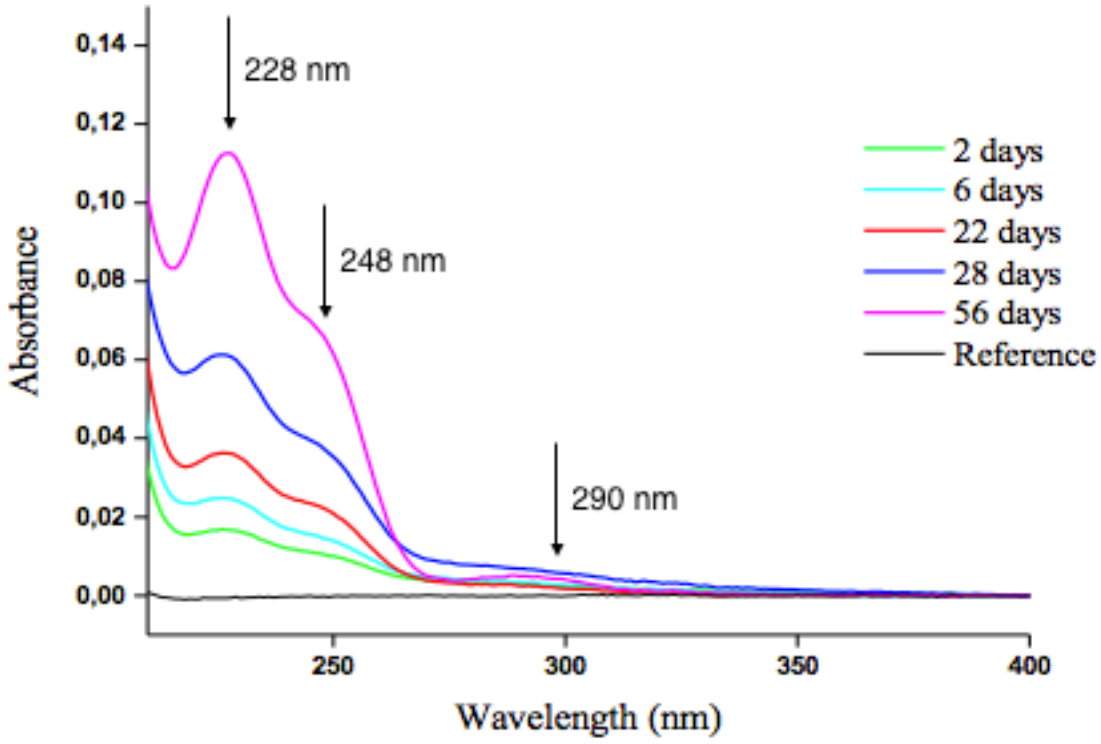

Figure 7.19: Spectra of the immersion liquid of PLARC at 2, 22, 28, 44 and 56 days.

The initial buffer solution does not present any band of absorption, but after immersion of the materials, a series of bands with maximum absorbance at 290, 246 and 228 nm appear. Furthermore, it's observed that the intensity increases with the immersion time. Thus, a detailed analysis of these spectra can give information about the products formed during hydrolytic degradation of the material and on the kinetics of such degradation.

To be able to analyse further information provided by these bands, the spectra of compounds formed during the hydrolysis of PLA, such as lactic acid, has been carried out in another project within the research group (Ortega, 2015). Lactic acid has two absorption bands: one at about 215 nm and another around 280 nm. Additionally, other researchers that have been working with PLA have studied what other products that may be the reason for the bands outlined above. Thus, by dissolving PLA in benzene, Gupta and Deshmukh concluded that an absorption band appears at 280 nm, which could be due to breakage of ester bonds with subsequent formation of –COOH groups at the chain ends (Gupta and Deshmukh, 1982). Lalla and Chugh dissolved PLA in chloroform and concluded that the absorption band that appears at 240 nm corresponds to

ester bonds in the polymer. These ester groups may be linked to oligomers that emerge from the PLA during hydrolysis (Chugh and Lalla, 1990). Furthermore, Stevels et al., assigned the same band at 240 nm to the cyclic dimer of lactic acid (Stevels et al., 1996). Finally, peaks corresponding to the presence of montmorillonite clay in the polymer have been reported to result in absorption bands between 230-300 nm (Bocchini and Frache, 2013).

7.2.1 Effect of recycling and clay

To be able to analyse the effect recycling can have on the hydrolytic degradation of PLA, the evolution of the bands at 228, 248 and 290 nm over immersion time was studied. The evolution of the bands in the liquid at 228 nm for the recycled material, which included the cleaning step, was compared with the virgin material.

In figure 7.20 the evolution of the bands appearing at 228 nm is illustrated for PLAV and PLARC. In the figure, only PLARC has corresponding error bars, when PLAV was only measured with one parallel. It is important to consider that the absorbance is small for both materials, which corresponds to slow processes resulting in the dissolution of small amounts of material, making the noise in the measurement crucial concerning the magnitude of the measures. However, the results appear to indicate that the leaching is more important in the recycled material, at least in the first stages of the immersion.

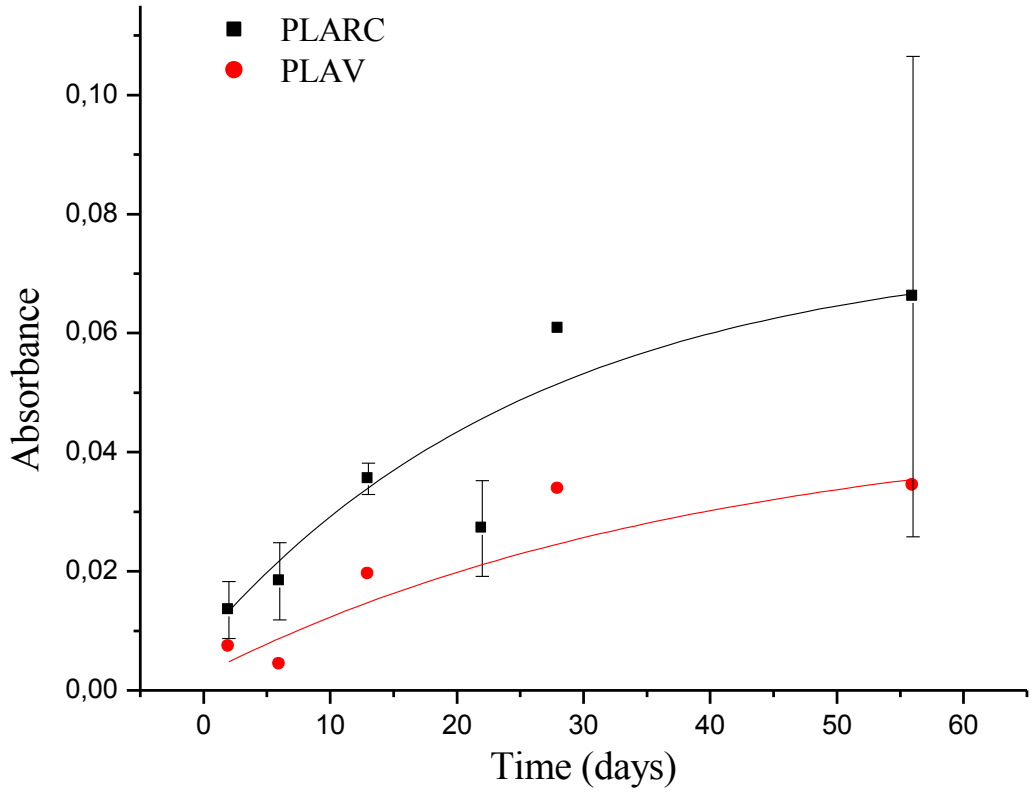

Figure 7.20: Evolution of the band at 228 nm in PLAV and PLARC over immersion time with corresponding first order decreasing exponential fit.

In figure 7.21, the evolution of the bands appearing at 228 nm is illustrated for PLARC and PLARC-302, with corresponding error bars. Here, no significant effect can be seen in the absorbance in the two materials, and it doesn't seem like the clay have a too substantial effect on the absorbance in the immersion liquid.

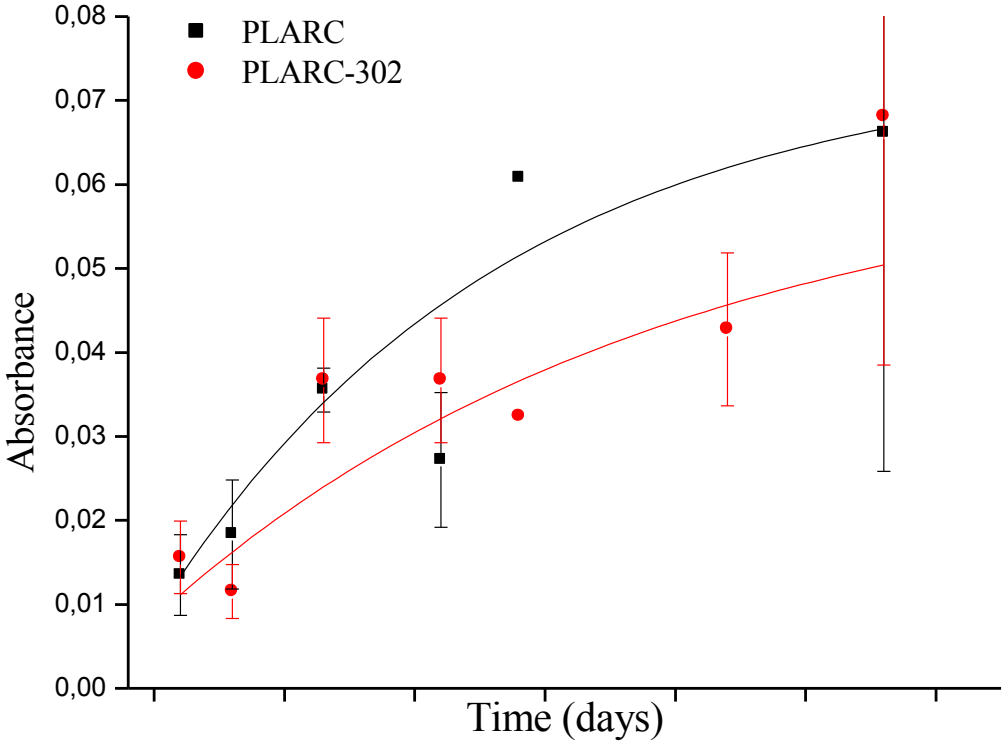

Figure 7.21: Evolution of the band at 228 nm in PLARC and PLARC-302 over immersion time with corresponding first order decreasing exponential fit.

The evolution of the bands at 246 for the plot of PLARC and PLARC-302 and the plot of PLAV and PLARC are presented in figures 11.15 and 11.16 respectively (appendix 11.5).

7.4 Viscosity measurements

The intrinsic viscosity was measured so that the effect of the hydrolytic degradation in the molecular weight in the polymer in the recycled material at different immersion times at 37°C could be studied. The viscosity was measured in a chloroform solution, and the method is described in section 6.2.9. The viscosity of PLARC and PLARC-302 were measured for immersion times 0, 13, 56 and 84 days, and calculated by using equation 4.1-5. The representation of PLARC is illustrated in figure 7.22. The numeric viscosity is given in table 11.9 (appendix 11.6).

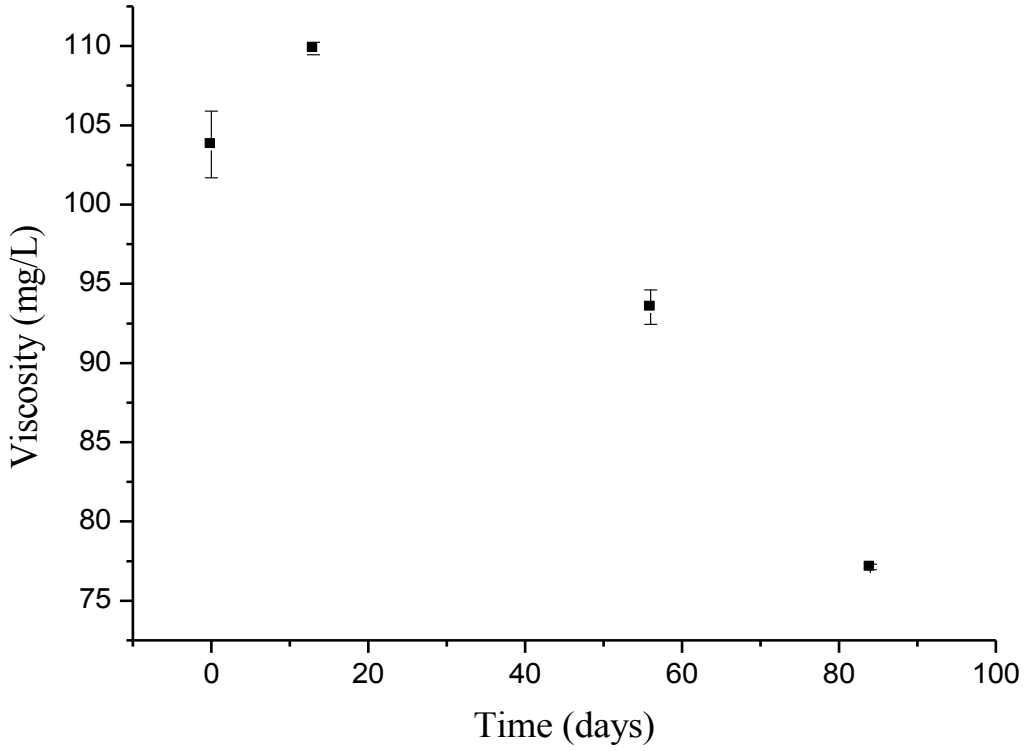

Figure 7.22: Evolution of the viscosity of PLARC at 37°C.

It can be seen in the first days that the viscosity in the material is increasing but, at after around 15 days the viscosity will decrease, this is accurate for both with and without clay. The increase in viscosity is from 0-13 days can be due to error in the measurements, but the error is minimal when the uncertainties are considered. It can also be due to structural changes in the material. The decrease in viscosity is due to the occurrence of hydrolysis during immersion time. The

intrinsic viscosity corresponds to a loss of the average molecular weight of the polymer that dominates at higher time intervals, which is reduced by hydrolysis. The ester groups in PLA undergo hydrolysis in the presence of water, thus being degraded, generating carboxyl and hydroxyl groups as well as smaller molecules, which increase the intermolecular forces between the chains, as it is explained in more detail in section 5. Degradation of the polymer depends on several factors, mainly pH and temperature. To prevent autocatalysis, the immersion was performed in a buffer solution with a pH equal to 7.4. When the immersion is conducted in a neutral pH solution, neutral hydrolytic degradation will occur. Under hydrolytic degradation under controlled pH, the cleavage of the molecule chain is divided into two stages (Auras et al., 2010). In the first stage, during the first days of immersion, backbiting cleavage will occur, and does not lead to immense changes in the molecular weight, thus not affecting the intrinsic viscosity in a high degree. In the second stage, random chain cleavage occurs that affects the longitude of the chains, thus affecting the molecular weight that again affects the intrinsic viscosity, which concurs with the results obtained here (Ray and Bousmina, 2005).

To study the effect of clay present in the recycled material, the evolution of the viscosity in PLARC was compared with the evolution of the viscosity in PLARC-302. The comparison is illustrated in figure 7.23.

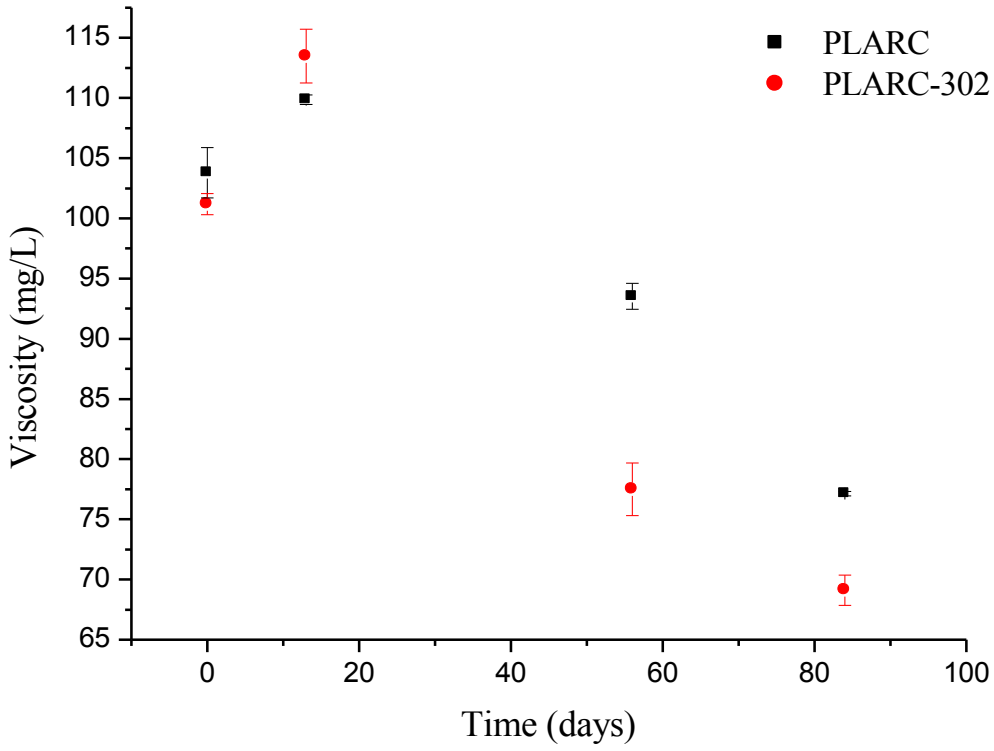

Figure 7.23: Evolution of the viscosity in PLARC and PLARC-302 measured at 25°C.

The viscosity of PLARC-302 is somewhat smaller than for PLARC, besides from immersion day 13, but when compared with error bars for PLARC, the difference in viscosity is non-significant. The addition of clay into PLA will decrease the viscosity of the nanocomposites, and is caused by the degradation of the PLA/MMT nanocomposites (Hwang et al., 2013). The degradation may be because the preparation of nanocomposites with organically modified layer silicates provides increased biodegradability. This effect may be because these silicates act as catalysts for the degradation by the presence of terminal hydroxyl groups in their sheets, which can initiate hydrolytic degradation in polymers (Auras et al., 2010; Ray and Okamoto, 2003; Paul and Robeson, 2008).

The evolution of the measured viscosity of the materials PLARC was compared with measured values of PLAV and PLAR from prior studies, to investigate the effect of recycling, when a cleaning step is included (Moreno, 2015). The evolution of the viscosities of all three materials is

illustrated in figure 7.24 without error bars to facilitate the view of the evolution. The evolution with the corresponding error bars is included in figure 11.17 (appendix 11.6).

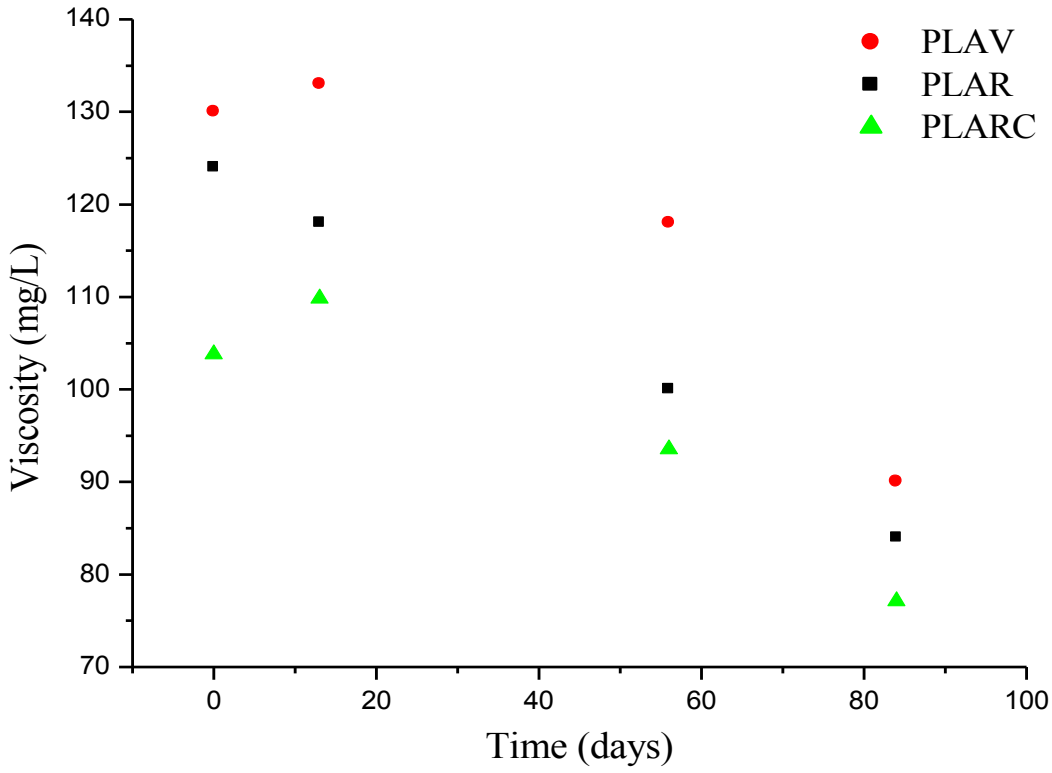

Figure 7.24: Comparison of the evolution of viscosity of virgin, recycled and recycled, including the cleaning step, materials at 0, 13, 56 and 84 days.

What can be seen in the material at day 0, without immersion, is that the viscosity of the recycled material, including the cleaning step, is lower than the recycled, which again is less than the virgin material. This decrease in viscosity is probably because of the degradation that occurs when the material is subjected to the accelerated ageing and the cleaning step. The accelerated ageing simulates ageing and the degradation in the material during use. Extrusion of the aged material, which is carried out in the recycling process, is also likely to lead to degradation material because of its exposition to high temperatures and shear stress, which can cause breakage of the polymer chains. Furthermore, it can be seen that both the recycled and recycled, including the cleaning step, material degrades somewhat faster than the virgin material during immersion. This decrease in viscosity may be because the material is more degraded from the beginning after the recycling process, than PLAV. Prior degradation can generate reactive groups, like –COOH groups, which can increase water absorption and catalyse hydrolytic

degradation of the recycled PLA. The recycled material, including the cleaning step, degrades even faster than the recycled material without the cleaning step, although the differences are small. Cleaning the material can lead to further degradation, and possibly generating more reactive groups, thus causing further hydrolytic degradation of PLA. Furthermore, it is possible that the process weakens the structure of PLA, thus making it more susceptible to thermo-mechanical degradation.

Overall, the intrinsic viscosity measurements indicate that the immersion in water will lead to hydrolytic degradation, meaning, chain breakage resulting in a decrease of average molecular weight and viscosity. The viscosity of the recycled material including the cleaning step is slightly inferior compared to the recycled material, which again is slightly inferior compared to the virgin material. This effect is due to the occurrence of degradation during ageing and reprocessing. For the material prepared with MMT clay the intrinsic viscosity is slightly inferior to the material without, due to the presence of terminal hydroxyl groups in their structure, which can initiate hydrolytic degradation.

7.5 Thermogravimetric analysis

Thermogravimetric analysis was performed to obtain information about the thermal degradation produced in the materials at different times of immersion. The thermograms of PLARC for immersion day 0, 13, 56 and 84 are illustrated in figure 7.24.

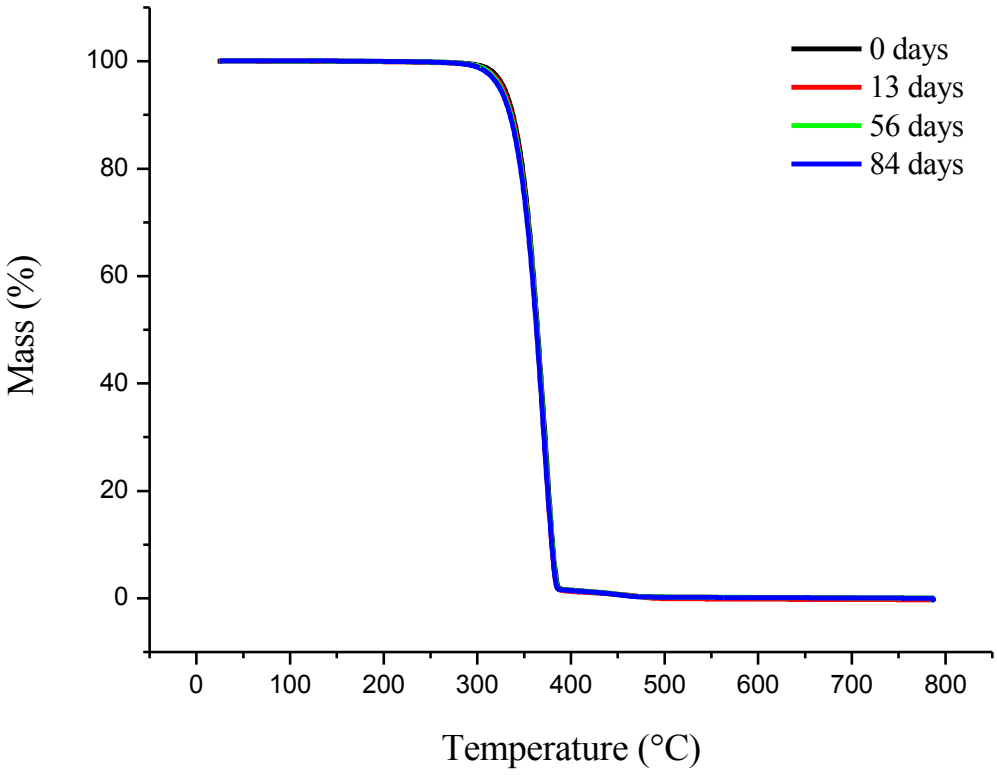

Figure 7.24: Thermograms for PLARC immersed at day 0, 13, 56 and 84.

To appreciate the variation presented at different days of immersion, an extension of the TGA was performed. The extension is illustrated in figure 7.25.

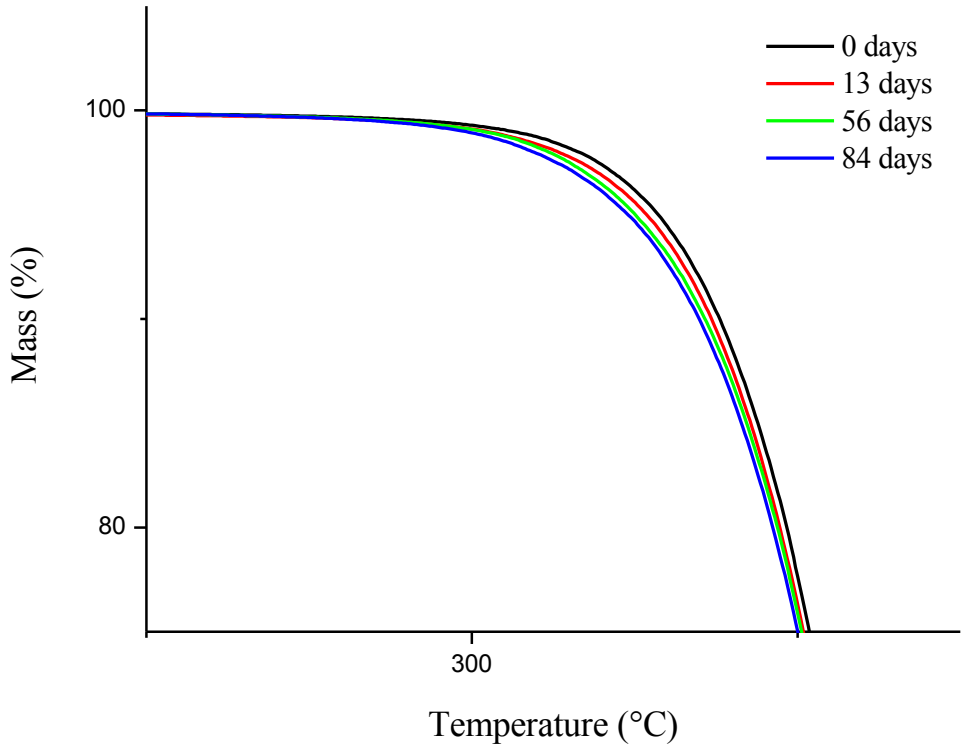

Figure 7.25: Amplification of the thermograms for PLARC immersed at day 0, 13, 56 and 84.

The figure illustrates that PLARC without immersion, day 0, has a higher thermal stability than the submerged material. The thermal stability does not change significantly over the days of immersion in the PLARC material. However, higher immersion time corresponds to a slight decrease in thermal stability. This small decrease in stability is due to hydrolytic degradation produced during immersion, causing a reduction in the average molecular weight of the polymer as discussed in section 7.4. The behaviour represented in figure 7.25 is consistent with the results in section 7.4, where the material presented a slight decrease in viscosity, and therefore in the average molecular weight, during the first days of immersion and decreasing more rapidly with time.

The same amplification of the thermograms of PLARC was done for PLARC-302 for immersion days 0, 13, 56 and 84, and is presented in figure 7.26. The full-size thermograms for PLARC-302 are shown in figure 11.18 (appendix 11.7).

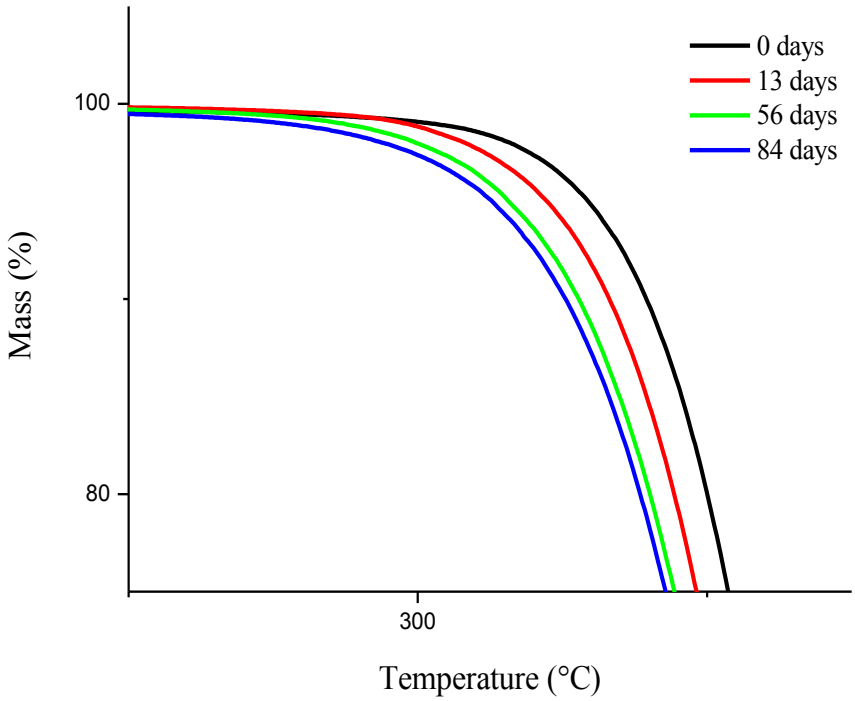

Figure 7.26: Amplification of thermograms of PLARC-302 for immersed at day 0, 13, 56 and, 84.

For the recycled material with montmorillonite clay, it can be seen a difference in the thermal stability already from immersed day 13. The decrease in thermal stability is increasing with immersion time, like for the recycled material without clay.

Figure 7.27 illustrates the evolution of the temperature that produces a mass loss of 5, 10 and 50% (T5, T10 and, T50) and the temperature where the mass loss occurs at maximum speed (TMAX) in PLARC.

The figure illustrates that the behaviour is similar to what was presented in the TGA diagram in figure 7.25. Even though the differences are subtle, the figure shows that the temperatures are reducing, as immersion days get higher. Thus, meaning that the degradation increases, which is seen in previous results.

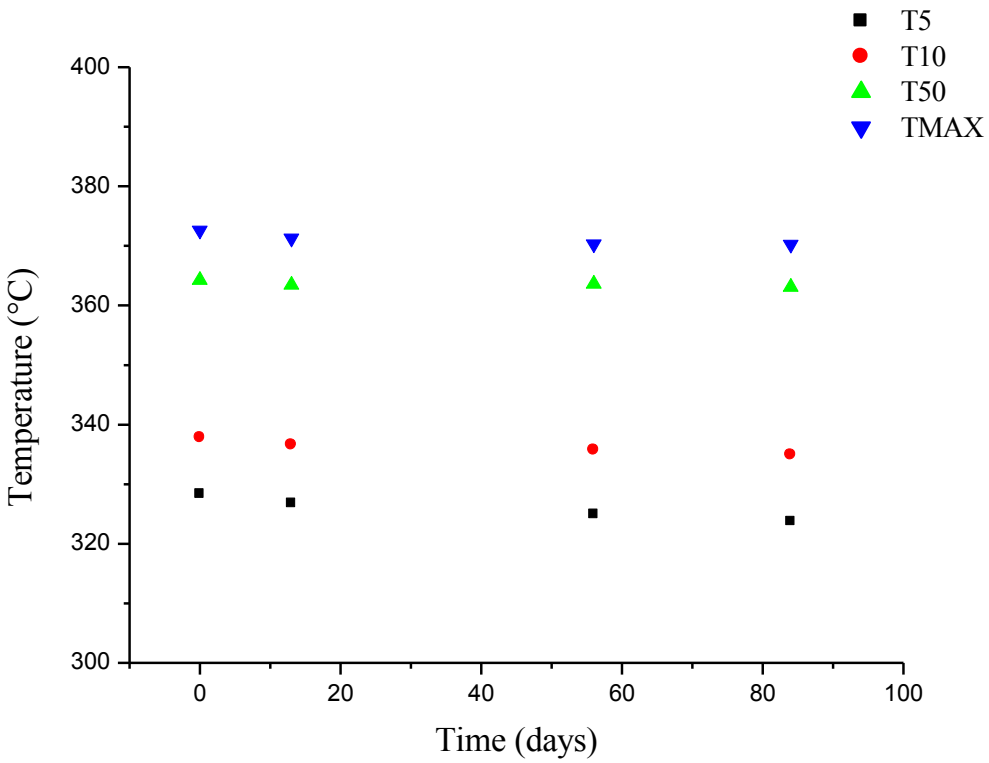

Figure 7.27: TGA Diagram of the temperature that produces a mass loss of 5, 10 and 50% and where the mass loss occurs at maximum speed for PLARC for immersed days 0, 13, 56 and 84.

To see the effect the mechanical recycling process has on the thermal stability of the material, the thermal stability of the recycled material, including the cleaning step, was compared to the thermal stability of the recycled and virgin materials from previous studies (Moreno, 2015). The stability hardly varies during the first days of immersion. The mass loss at 5%, T5, was compared between the materials to facilitate how the recycling process affects the thermal stability. The comparison is illustrated in figure 7.28 and presents that the stability of the recycled material always is slightly less than that of the virgin material. It also shows that the stability of the recycled material, including the cleaning step, is slightly less than the recycled material without the cleaning step, which concurs with results from viscosity measurements in section 7.4.

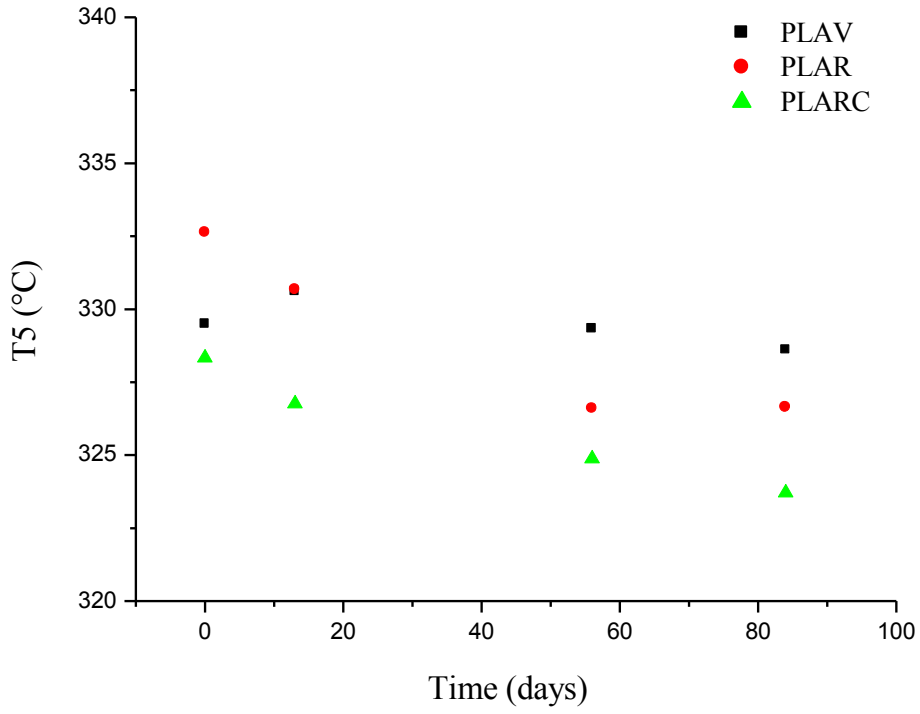

Figure 7.28: Evolution of the temperature that produces a mass loss of 5%, T5, for materials PLAV, PLAR, and PLARC.

Figure 7.29 illustrates the evolution of the temperature that produces a mass loss of 5, 10 and 50% (T5, T10 and, T50) and the temperature where the mass loss occurs at maximum speed (TMAX) in PLARC-302.

The figure illustrates that the behaviour is similar to what was presented in the TGA diagram in figure 7.26, which shows differences in stability, with decreasing stability with increasing immersion time. The decrease in thermal stability is higher for PLARC-302 than for PLARC. Thus, meaning that the degradation is larger in PLARC-302, which concurs with results from section 7.4.

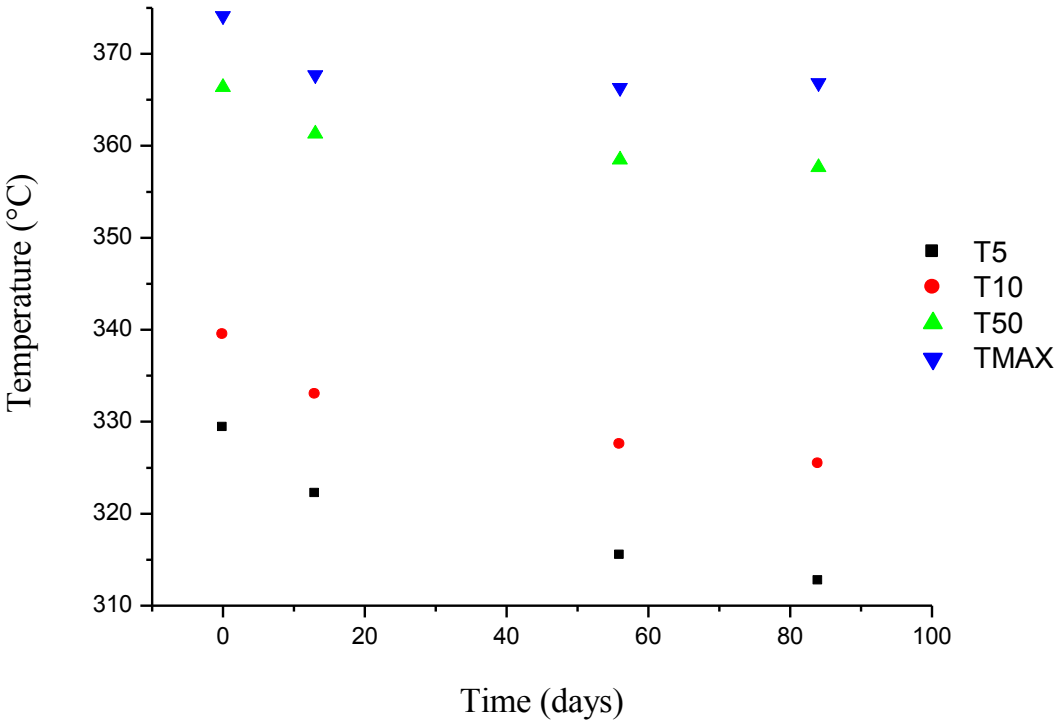

Figure 7.29: TGA Diagram of the temperature that produces a mass loss of 5, 10 and 50% and where the mass loss occurs at maximum speed for PLARC-302 for materials immersed during 0, 13, 56 and 84 days.

To be able to see the effect the montmorillonite clay has on the thermal stability of the material, it was compared with the material without clay.

The presence of clay in the polymer may catalyse hydrolytic degradation in the nanocomposites, which was explained in section 7.4. Thus, explaining why there is a more rapid degradation in the material with montmorillonite clay and that the stability continues to decrease.

The mass loss at 5%, T5, was compared between PLARC and PLARC-302 to facilitate how the presence of clay in the polymer affects the thermal stability. The comparison is illustrated in figure 7.30 and presents that the stability of the recycled material with clay is always slightly less than that of the recycled material without clay, which concurs with results from viscosity measurements in section 7.4.

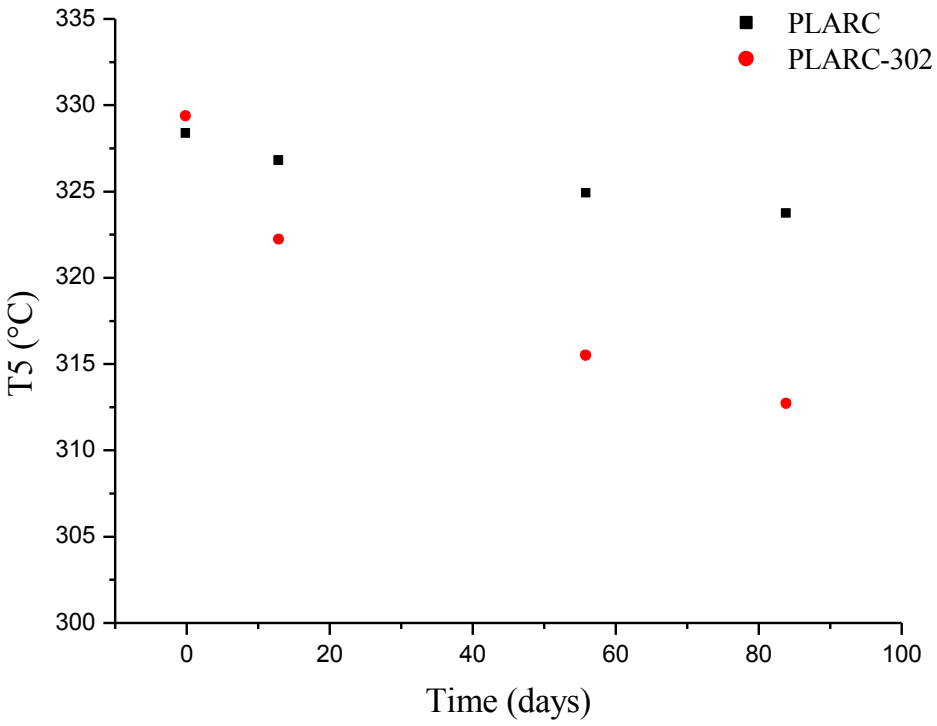

Figure 7.30: Evolution of the temperature that produces a mass loss of 5%, T5, for materials PLARC and PLARC-302.

The thermal stability of the material is reduced with immersion time due to degradation. Small differences in stability can be seen in the recycled material and the virgin material. However, recycling, including the cleaning step, also show slight inferior thermal stability to the recycled material without the cleaning step. A 2% clay present in the polymer will cause a faster degradation and therefore, a decreased thermal stability compared to the material without clay.

8. Conclusions and future work

PLA is a biopolymer produced from renewable sources with excellent mechanical properties and easy processing. PLA has the disadvantage that it is currently not recycled for reuse, but instead sent to composting. Being a polymer obtained from food sources, it is questionable to use it as a material for a single use. The ability to reuse and recycle PLA should have clear environmental, social and economical benefits.

The main application of PLA is in food packaging, making it necessary to have excellent resistance to hydrolytic degradation because it is in continuous contact with moist food. If resistance to hydrolytic degradation of the recycled material were much lower than that of the virgin material, the possible application of mechanical recycling would be questionable. Therefore, the overall object of this project was to study and compare the behaviour of the polymer in virgin and recycled state on the absorption of water and, therefore, the hydrolytic degradation.

The resistance to hydrolytic degradation in PLA was studied by FTIR analysis, as well as UV-Vis spectroscopy, thermogravimetric analysis, gravimetric analysis and viscosity measurements.

When analysed by FTIR spectroscopy, interactions between the water and the polymer was established, it follows that there are four types of associations: very strongly bound water, strongly bound, weakly bound and very weakly bound (or free). The area of the band corresponding to hydration exhibited that, while the recycling process did not have a significant effect on the water absorption, the montmorillonite clay did.

UV-Vis spectroscopy of the liquid where the PLA samples were immersed showed the appearance of bands with maxima at 290, 248 and 228 nm. These bands revealed the existence of products such as oligomers of low molecular weight, lactide, and lactic acid, which are formed during the hydrolytic degradation. The UV-Vis measurements indicate that the absorbance increase with immersion time. Further, UV-Vis spectroscopy shows that the recycling process does not significantly affect the absorbance, nor does the presence of clay in the material. But due to the magnitude of deviations in the measurements, it's hard to conclude anything.

The gravimetric analysis of virgin and recycled materials showed that at short absorption times, water occupies the free volume and joins the polymer by hydrogen bonds and Van der Waals forces. However, the observed increase in absorption at longer times can be explained by the phenomenon of hydrolysis, resulting in the generation of hydrophilic species in the material, which make the absorption gradually increase.

The diffusion coefficients obtained by the Fickian fit of the water absorption were lower in the virgin and recycled materials than in the recycled material including the cleaning step. The diffusion coefficients were calculated to be $8.4 \cdot 10^{-13}$, $1.3 \cdot 10^{-12}$ and $7.1 \cdot 10^{-12}$ m^2/s, for the virgin, recycled and recycled, including the cleaning step, materials without clay respectively. For the materials with clay, they were calculated to be $3.4 \cdot 10^{-13}$, $7.3 \cdot 10^{-13}$, and $3.5 \cdot 10^{-12}$ m^2/s for PLAV-302, PLAR-302 and PLARC-302 respectively. The water absorption at equilibrium does not show a significant difference between the three materials.

The measured intrinsic viscosity indicates that the immersion in water causes hydrolytic degradation in the material that results in a decrease of the average molecular weight. The degradation is much more pronounced in the material with montmorillonite clay than in the material without clay, which may be because the silicates in the clay act as catalysts for the hydrolytic degradation. The recycled material including the cleaning step has a slightly lower viscosity and therefore a lower average molecular weight than the recycled material and the virgin material, because of degradation during ageing, reprocessing and also the exposure to the alkaline medium in which it was cleaned. Furthermore, degradation is faster in the recycled material than in the virgin material, due to the previous degradation, favouring their hydrolytic degradation during immersion.

Thermogravimetric analysis indicates that the thermal stability decreases with immersion time due to degradation. Small differences in stability can be seen in the recycled material and the virgin material. However, recycling, including the cleaning step also show slight inferior thermal stability to the recycled material without the cleaning step. Clay present in the polymer will cause faster degradation and therefore reduced thermal stability compared to the material without clay.

The results obtained by the different techniques used to measure degradation are mutually consistent. The presence of clay in the material results in less diffusion of water into the material,

acting as a barrier. Finally, recycling causes a slight degradation of the virgin material, and when the cleaning step is included it also causes a small degradation concerning the recycled material without the cleaning step, but the influence is not of high magnitude.

These results appear to show that the properties of the mechanically recycled samples of PLA depend on the steps included in the recycling process. When no demanding cleaning steps are included, the recycled material shows a behaviour very similar to that observed in the virgin material, thus indicating that this recycled material can be used in packaging. When a demanding cleaning step is included in the recycling process, the recycled material shows degradation and a decrease in the resistance to hydrolysis, although the worsening is not severe. These results support the feasibility of the mechanical recycling of PLA.

As a consequence of the results obtained during this thesis, ideas for future research has emerged related to the study of mechanically recycling PLA. First, it would be interesting to expand the information regarding hydrolytic degradation of PLA by employing additional techniques such as X-Ray Diffraction or Differential Scanning Calorimetry. Secondly, the effect of hydrolytic degradation on other material properties such as optical properties and mechanical stability could be characterised. Thirdly, the effect of temperature on the kinetics of hydrolysis could be studied by measuring at different temperatures below the glass transition temperature. Finally, it would be interesting to examine the effect that recycling has on the composting of PLA.

9. Social and environmental impact

The use and demand of plastics have significantly increased over the last years. Conventional plastics are petroleum derivatives that are non-biodegradable, which means that they can be highly contaminating the environment. Many of the synthetic plastics, made from fossil fuels, are recyclable but non-biodegradable and therefore they pose a significant contamination risk when a part of them goes to the ecosystem without control of it. These conventional plastics may have a degradation time up to hundreds of years, and along with shortages and increased pricing of fossil fuels it has led to the development of biodegradable materials.

In recent years the use of biodegradable bioplastics obtained from renewable sources has grown. Given its excellent properties and reduction in production costs, they have become competitors of conventional plastics and are expected to continue its growth worldwide in the years to come (European Bioplastics, 2013).

In biological decomposition of bioplastics, they are reduced to simpler substances such as water and carbon dioxide by microorganisms, which implies a much smaller environmental impact than that of conventional plastics. An important compound that has aroused considerable interest, especially in the sector of food packaging, is poly (lactic acid), which is the studied material in this project.

An important issue is whether or not these bioplastics can be mechanically recycled. If mechanical recycling is possible, it will provide a second life for these materials, optimizing and justifying their use. Here, it has been emphasized the effect that mechanical recycling has on PLA and its nanocomposites with Cloisite 30B™ montmorillonite clay when the goal is to use the bioplastic in food packaging. Since the purpose is to use the bioplastic in food packaging, its most valuable property is its resistance to hydrolytic degradation, since humidity usually is present in food.

The mechanical recycling of plastics, which includes the process of collecting, sorting, purification and mechanically reprocessing the post-consumption plastic waste, currently accounts for a significant reduction of emission of CO_2 and other gases will help decrease waste ending up as landfill. Recycling also provides savings in raw materials and energy, and can also contribute to society by generating a large number of jobs.

10. Expenses

The costs of this study were determined by taking into account the costs of the used equipment and raw materials, as well as personnel costs. The study was carried out in the Department of Industrial Chemical Engineering and Environment at Escuela Técnica Superior de Ingenieros Industriales at Universidad Politécnica de Madrid, and its duration was of 7 months, from January 2016 until July 2016.

10.1 Personnel cost

The personnel costs were determined by considering that the internal tutor of the study, an external tutor, and the master student forms the team implicated.

For the student, the following prices for the performed workload were estimated, and the total cost of the student is given in table 10.1:

- A price of 6 €/hours
- Total working hours to be 30 hours/week over a period of 7 months

Throughout the study the internal tutor has offered his advice, when needed, and helped to achieve goals, the estimated prices for the tutor follows, and the total cost is given in table 10.1:

- A price of 30 €/hours
- Total working hours to be 3 hours/week over a period of 7 months

The external tutor has complemented the main tasks of the internal tutor while helping the student in the laboratory, and with processing results. The estimated price for the external tutor follows, and the total cost is given in table 10.1:

- A price of 25 €/hours
- Total working hours to be 2 hours/week over a period of 7 months

Table 10.1: The estimated total cost for the student, internal tutor and external tutor over the project time period of 7 months.

Personnel	Cost (€)
Student	5040
Internal tutor	2520
External tutor	1400
Total cost (€)	8960

10.2 Materials and Equipment cost

The material costs are associated with the materials used in this study like reagents and solvents such as phosphates, acetone, starting plastics, as well as glassware, plastic vials, and polyimide. The main materials used are PLA Ingeo Biopolymer 2003D™ and Cloisite™ 30B montmorillonite clay, and it's estimated to 300 €. The total cost of materials is estimated to be **800 €**.

Further, the cost of the equipment used is estimated. To be able to estimate the cost of the equipment, the life expectancy, for all equipment, is set to a certain amount of working hours. The operation cost of the equipment has been estimated by using equation 10.1.

$$Operation\ cost = \frac{Equipment\ costs}{Life\ expectancy} \cdot Use \tag{10.1}$$

The cost of operational for all equipment, with the total cost of operation of all equipment, is given in table 10.2.

Table 10.2: Operational cost for all equipment used

Equipment	Equipment cost (€)	Life expectancy (h)	Use (h)	Cost of use (€)
Extruder	24000*	10000	10	24
Hydraulic press	5000*	10000	30	15
Analytical balance	8000*	10000	25	20
FTIR Spectrophotometer	23000*	10000	16.5	37.95
UV-Vis Spectrophotometer	21000*	10000	20	42
Vacuum-oven at 40°C	5000*	10000	3072	1536
Oven at 37°C	1500*	20000	2904	217.8
Cryogenic mill	2500*	10000	6	1.5
Micrometer	1000*	10000	4	0.4
Total equipment cost (€)	-	-	-	1894.65

* : Internal prices from Universidad Politécnica de Madrid.

10.3 Indirect cost

Indirect costs also had to be considered, which include electricity, water, heating and other utilities. These costs are estimated to a 25% of the total cost of the study and are determined to be by using equation 10.2 and 10.3.

$$Indirect\ costs = 0.25 \cdot Total\ cost \quad (10.2)$$

$$Total\ cost = Personnel\ costs + Material\ and\ equipment\ costs + indirect\ costs \quad (10.3)$$

When the indirect costs had been determined, the total cost of the study could be calculated, and the value is given in table 10.3.

Table 10.3: Total cost of study determined by personnel costs, material and equipment costs and indirect costs

Concept	Cost (€)
Personnel costs	8960
Material and equipment cost	2695
Indirect costs	3885
Total cost of study (€)	15540

The cost breakdown is illustrated in figure 10.1.

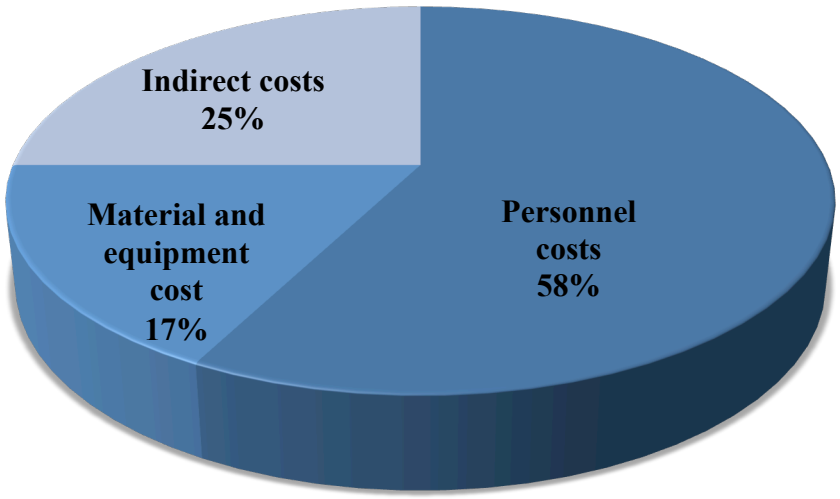

Figure 10.1: Cost distribution.

References

Andreopoulos, A.G., Hatzi, E.C., Doxastakis, M., 1999. *Synthesis and properties of poly(lactic acid).* Journal of Materials Science: Materials in Medicine; 10 (1); pp. 29-33.

Auras, R., Lim L.T., Selke, S., Tsuji H., 2010. *Poly(lactic acid): Synthesis, Structures, Properties, Processing and Applications*. Ed. Wiley, USA.

Badia, J.D., Santonja-Blasco, L., Martínez-Felipe, A., Ribes-Greus, A., 2012. *Hygrothermal ageing of reprocessed polylactide.* Pol Deg & Stab, 97; pp.1881-1890.

Balik, C.M., 1996. *On the Extraction of Diffusion Coefficients from Gravimetric Data for Sorption of Small Molecules by Polymer Thin Films.* Macromolecules; 29 (8); pp. 3025–3029.

Bastioli, C., 2005. *Handbook of biodegradable polymers*, Rapra Technology Limited.

Beall, G.W. and Powell, C.E., 2011. *Fundamentals of Polymer-Clay Nanocomposites.* Cambridge University Press, New York, pp. 1-3.

Belgacem, M.N. & Gandini, A., 2008. *Monomers, Polymers and Composites from Renewable Resources.* 1st ed. Elsivier Ltd, Oxford, UK.

Benninga, H. (Ed), 1990. *A history of Lactic Acid Making.* Kluwer Academic Publishing, Boston, London, Dordrecht.

Bocchini, S. And Frache, A., 2013. *Comparative study of filler influence on polylactide photooxidation.* Express Polymer Letters; 7 (5); pp. 431-442.

Bonsignore, P.V., 1995. *Production of high molecular weight polylactic acid*. US Patent 5470944.

Carrasco, F., Pagès, P., Gámez-Pérez, J., Santana, O.O., Maspoch, M.L., 2010. *Processing of poly(lactic acid): Characterization of chemical structure, thermal stability and mechanical properties.* Polymer Degradation and Stability; 95; pp. 116-125.

Chan, C.C., Lee, Y. C., Lam, H., Zhang, X-M., 2004. *Analytical Method Validation and Instrument Performance Verification.* John Wiley & Sons, Hoboken, New Jersey.

Chariyachotilert, C., Joshi, S., Selke, S.E.M., Auras, R., 2012. *Assessment of the properties of poly(L-lactic acid) sheets produced with differing amounts of postconsumer recycled poly(L-lactic acid).* Journal of Plastics Film & Sheeting; 28 (4); pp. 314-335.

Chugh. N. N. and Lalla J. K., 1990. *Effects of morphology, conformation and configuration on the IR and Raman spectra of various poly(lactic acid).* Indian Drugs; 27 (10); pp. 516-522.

Cole-Parmer, 2015. *Seeing the Light: An Overview of Visible and UV-VIS Spectroscopy*. [Online] Available at: http://partners.coleparmer.com/techinfo/techinfo.asp?htmlfile=Overview_Visible_UV_VIS_S 82 pectroscopy.htm&ID=1396 [Accessed: 15 March 2016].

Cotugno, S., Larobina, D., Mensitieri, G., Musto, P., Ragosta, G., 2001. *A novel spectroscopic approach to investigate transport processes in polymers: the case of water-epoxy system.* Polymer; 42; pp. 6431-6438.

Crank, J., 1975. *The Mathematics of Diffusion*. 2nd ed.; Oxford University Press: New York; pp. 47-48.

Datta R, Henry M. 2006. *Lactic acid: recent advances in products, processes and technologies: a review.* J Chem Technol Biotechnol*;* 81; pp.1119–129.

de Jong, S.J., Arias, E.R., Rijkers, D.T.S., van Nostrum, C.F., Kettenes-van den Bosch, J.J., Hennink, W.E., 2001. *New insights into the hydrolytic degradation of poly(lactic acid): participation of the alcohol terminus*. Polymer; 42; pp. 2795-2802.

Dept. of Chem and Biochem, UC, 2007. *Handbook for Organic Chemistry Lab: 9th Edition.*

Dorgan, J. R., Lehermerier, H., Mang, M., 2000. *Thermal and rheological properties of commercial-grade poly(lactic acid)s.* J Polym Environ 2000; 8; pp. 1–9.

Dusselier, M., Van Wouve, P., Dewaele, A., Jacobs, P.A., Sels, B.F., 2015. *Shape-selective zeolite catalysis for bioplastics production*. Sci; 349 (6243); pp. 78-80.

Engineer, C., Parikh, J., Raval, A., 2011. *Effect of copolymer ratio on hydrolytic degradation of poly(lactide-co-glycolide) from drug eluting coronary stents.* Chem Eng Res Des; 89 (3); pp. 328–334.

European Bioplastics, 2013. *Bioplastics facts and figures; 2013.* [Online] Available at: http://www.corbion.com/media/203221/eubp_factsfigures_bioplastics_2013.pdf [Accessed 26.01.2016].

European Bioplastics, 2014. [Online] Available at: http://en.european-bioplastics.org/blog/2014/12/11/bioplastics-production-capacities-to-grow-by-more-than-400-by-2018/ [Accessed: 20.11.2015].

European Bioplastics. *Mechanical Recycling.* [Online] Available at: http://www.european-bioplastics.org/bioplastics/waste-management/recycling/ [Accessed 20.11.2015].

Franco Urquiza, E.A. and Maspoch Rulduá, M.L., 2009. *Estructura de las arcillas utilizadas en la preparación de nanocompuestos poliméricos.* Ingenierías; 44; pp. 35-41.

Fukushima, K., Tabuani, D., Dottori, M., Armentano, I., Kenny, J.M., Camino, G., 2011. *Effect of temperature and nanoparticle type on hydrolytic degradation of poly(lactic acid) nancomposites*. Polymer Degradation and Stability; 96; pp. 2120-2129.

Gabbott, P., 2008. *Principles and Applications of Thermal Analysis*. USA: Blackwell publishing, 1st ed.

Garlotta, D., 2001. *A Literature Review of Poly(Lactic Acid).* J Pol Env; 9 (2). **Grayson, M. A. & Wolf, C. J., 1985.** *Diffusion of Water in Carbon Epoxy Composites.* Proceedings of the Fifth International Conference on Composite Materials (ICCM-5) TMS.

Griffiths, P.R., De Haseth, J.A., 2007. *Fourier Transform Infrared Spectrometry.* 2nd edition, John Wiley & Sons, Hoboken, New Jersey.

Grim, R.E., 1968. *Applied clay mineralogy*. McGraw-Hill Book Co., New York; 596.

Grizzi, I., Garreau H., Li, S., Vert, M., 1995. *Hydrolytic degradation of devices based on poly(D,L-lactic acid) size-dependence.* Biomaterials; 16; pp. 305-311.

Gruber, P. and O'Brien, M., 2005. *Polylactides "NatureWorks® PLA*". Biopolymers Online.

Guggenheim, S. & Martin, R.T., 1995. *Definition of clay and clay mineral: Joint report of the AIPEA nomenclature and CMS nomenclature committees*. Clays and Clay Minerals; 43 (2); pp. 255-256.

Gupta, M.C. and Deshmukh, V.G., 1982. *Thermal oxidative degradation of poly-lactic acid*. Colloid and Polymer Science; 260; pp. 514-517.

Gupta, B., Revagade, N., Hilborn, J., 2007. *Poly(lactic acid) fiber: An overview.* Prog Polym Sci; 32 (4); pp. 455–482.

Hakkarainen, M., 2001. *Aliphatic polyesters: abiotic and biotic degradation and degradation products.* Adv Polym Sci; 157; pp. 113-38.

Hartmann, M.H., 1998. *Biopolymers from Renewable Resources.* D.L. Kaplan (Ed.) Springer-Verlag, Berlin, pp. 367-411.

Hatakeyama, T. and Quinn, F.X., 1994. *Thermal Analysis: Fundamentals and Applications to Polymer Science.* National Institute of Materials and Chemical Research, John Wiley & Sons: Chichester, UK.

Helfenbein, D., 2011. *Development of recycling of PLA sheet into PLA pellets without undergoing chemical process*. Atlanta, GA.

Henton, D. E., Gruber, P., Lunt, J., Randall, J., 2005. *Polylactic acid technology. Natural Fibers, Biopolymers, and Biocomposites*. Taylor & Francis, Boca Raton, FL; pp. 527-577.

Hwang, S., Yang, J. and Hu, C., 2013. *Effects of clay loading on the structure, mechanical, rheological properties of microcellular foams of PLA/MMT nanocomposites*. University of Science and Technology, Taiwan.

Höglund, A., Hakkarainen, M., Albertsson, A.C., 2010. *Migration and Hydrolysis of Hydrophobic Polylactide Plasticizer*. Biomacromolecules; 11 (1); pp. 277.83.

Jamshidian, M., Tehrany, E.A., Imran, M., Jacquot, M., Desobry, S., 2010. *Poly-Lactic Acid: Production, Applications, Nanocomposites, and Release Studies*. Compr Rev Food Sci F; 9 (5); pp. 552-571.

Kister, G., Cassanas, G., Vert, M., 1998. *Effects of morphology, conformation and configuration on the IR and Raman spectra of various poly(lactic acids)s.* Polymer, 39 (2); pp. 267-273.

Kojima, Y., Kawasumi, M., Usuki, A., Okada, A., Fukushima, Y., Kurachi, T., Kamigaito, O., 1993. *Mechanical properties of nylon 6-clay hybrid.* J Mat Research; 8 (05); pp.1185-1189.

Kristić, V., 2005. *Catalizadores de Rh-soportado y su aplicación en la hidrogenación de crotonaldehído*. PhD, Universidad de Cantabria.

Lan, T. and Pinnavaia, T.J., 1994. *Clay-Reinforced Epoxy Nanocomposites.* Chem Mater; 6; pp. 2216-2219.

Lasagabáster, A., Abad, M.J., Barral, L., Ares, A., Bouza, R., 2009. *Application of FTIR spectroscopy to determine transport properties and water-polymer interactions in polypropylene (PP)/poly(ethylene-co-vinyl alcohol) (EVOH) blend films: Effect of poly(ethylene-co-vinyl alcohol) content and water activity*. Polymer; 50; pp. 2981- 2989.

Liu, C.H., Ni, X.H., Pu, Y., Yang, Y.L., Zhou, F., Zuzolo, R., Wang, W.B., Masilamani, V.,

López-Mayorga, O., 2012. *Espectroscopia Ultravioleta/Visible. Experimentales para la Determinación de Estructuras de Biopolímeros*. Universidad de Granada. [Online] Available at:

http://www.ugr.es/~olopez/estruct_macromol/index_archivos/Page559.html Métodos [Accessed: 13.03.2016].

Lorenzo, S.R., 2015. *Degradación hidrolítica y absorción de agua en poli(ácido láctico) virgen y reciclado*. Bachelor thesis in Chemical Engineering, ETSII-Universidad Politécnica de Madrid.

Lu, Y., An, L., Wang, Z.G., 2013. *Intrinsic Viscosity of Polymers: general Theory Bases on a Partially Permeable Sphere Model*. Macromolecules; 46; pp. 5731−5740.

Lunt, J., 1998. *Large scale production, properties and commercial applications of polylactic acid polymers.* Polym Deg Stab; 59; pp. 145–152.

Lyulin, A.V., Davies, G.R., Adolf, D.B., 2000. *Brownian dynamics simulation of dendrimers under shear flow*. Macromolecules; 33; pp. 3294–3304

McMurry, J., 2008. *Organic chemistry.* 7th edition ed. London: Thomson.

McNaughton, J.L. and Mortimer, C.T., 1975. *Differential Scanning Calorimetry*. London, The Perkin-Elmer Corp; pp. 44.

Meaurio, E., López-Rodríguez, N., Sarasua, J.R., 2006. *Infrared Spectrum of Poly(L-Lactide): Application to Crystallinity Studies.* Macromolecules; 39; pp. 9291-9301.

Melk, L., 2011. *Thermal Analysis of Hard Ceramics*. Master of Science in Engineering Technology Materials Technology, Luleå University of Technology.

Meneghetti, P. and Qutubuddin, S., 2006. *Synthesis, thermal properties and applications of polymer-clay nanocomposites*. Thermochimica Acta; 442 (1-2); pp. 74-77.

Merdas, I., Thominette, F., Tcharkhtchi, A., Verdu, J., 2002. *Factors governing water absorption by composite matrices.* Compos Sci Technol; 62; pp. 487–92.

Moreno, J., 2015. *Estudio de la degradación hidrolítica de poli(ácido láctico) virgen y reciclado.* Bachelor thesis in Chemical Engineering, ETSII-Universidad Politécnica de Madrid.

Najafi, N., Heuzey, M.C., Carreau, P.J., Wood-Adams, P.M., 2012. *Control of thermal degradation of polylactide (PLA)-clay nanocomposites using chain extenders.* Polym Degrad Stab; 97 (4); pp. 554-565.

Nampoothiri, K. M., Nair, N.R., John, R.P., 2010. *An overview of the recent developments in polylactice (PLA) reserach.* Bioresource Technology; 101; pp. 8493-8501.

NatureWorks LLC, *Renewing Ingeo: End-of-Life Options.* [Online] Available at:

http://www.natureworksllc.com/the-ingeo-journey/end-of-life-options.aspx [Accessed 29.04.2016].

NatureWorks. IngeoTM Biopolymer 2003D Technical Data Sheet. [Online] Available at: http://www.natureworksllc.com/~/media/Technical_Resources/Technical_Data_Sheets/TechnicalDataSheet_2003D_FFP-FSW_pdf.pdf [Accessed: 16.03.2016].

Nogueira, P., Ramirez, C., Torres, A., Abad, M.J., Cano, J., Lopez, J., et al., 2001. *Effect of water sorption on the structure and mechanical properties of an epoxy resin system*. J Appl Polym Sci; 80; pp. 71–80.

Obaje, S.O., Omada, J.I., Dambatta, U.A., 2013. *Clays and their Industrial Applications: Synoptic Review.* Int J of Sci and Tech; 3 (5).

Ortega, E.P., 2015. *Estudio de la absorción de agua en la degradación hidrolítica de un nanocomposite del poli(ácido láctico) reciclado*. Bachelor thesis in Chemical Engineering, ETSII-Universidad Politécnica de Madrid).

Owen, T., 1996. *Fundamentals of UV-visible spectroscopy*. Primer, Agilent Technologies, Germany; pp. 9-35.

Paul, D.R. and Robeson, L.M., 2008. *Polymer nanotechnology: Nanocomposites.* Polymer; 49 (15); pp. 3187-3204.

Paul, M.A., Delcourt, C., Alexandre, M., Degée, P., Monteverde, F., Dubois, P., 2005. *Polylactic/montmorillonite nanocomposites: study of the hydrolytic degradation.* Polym Degrad Stab; 87; pp. 535-542.

Plastics Europe, 2015. *Plastics – the Facts 2015; An analysis of European plastics production, demand and waste date.* [Online] Available at: http://www.plasticseurope.org/Document/plastics---the-facts-2015.aspx [Accessed: 26.06.2016].

Plastics Recyclers Europe. *Mechanical Recycling*. [Online] Available at: http://www.plasticsrecyclers.eu/mechanical-recycling [Accessed: 29.04.2016].

Perstorp Winning Formulas. *Bioplastics – Making biopolymers the perforance plastics of choice for a more sustainable future.* [Online] Available at: https://www.perstorp.com/products/plastic_materials/bioplastics?Filterlevel0=Capa&Filterlevel1=Bioplastics [Accessed at 20.11.2015].

Proikakis, C.S., Mamozuelos, N.J., Tarantili, P.A., Andreopoulos, A.G., 2006. *Swelling and hydrolytic degradation of poly(D,L-lactic acid) in aqueous solutions.* Polymer Degradation and Stability; 91; pp. 614-619.

Ray, S.S. and Okamoto, M., 2003. *Polymer/layered silicate nanocomposites: a review from preparation to processing.* Prog Polym Sci; 28 (11); pp. 1539-1641.

Ray, S.S. and Bousmina, M., 2005. *Biodegradable polymers and their layered silicate nanocomposites:* in green the 21st century materials word. Prog. Mater. Sci.; 50; pp. 962-1079.

Ray, S.S., 2010. *Nanocomposites, in Poly(Lactic Acid): Synthesis, Structures, Properties, Processing, and Applications* (eds R. Auras, L.-T. Lim, S. E. M. Selke and H. Tsuji), John Wiley & Sons, Inc., Hoboken, NJ, USA.

Remar, 2011. *Bioplásticos.* [Online] Available at: http://www.modernanavarra.com/wp-content/uploads/Bioplasticos.pdf [Accessed: 20.11.2015] Remar, Red de energía y Medio Ambiente.

Rizwan, A., Alfano, R.R., 2012. *Optical Spectroscopic Characteristics of Lactate and Mitochondrion as New Biomarkers in Cancer Diagnosis: Understanding Warburg Effect*. SPIE Proceedings, 8220; 82200Y.

Roy, P.K., Hakkarainen, M., Albertsson, A.C., 2012. *Nanoclay effects on the degradation process and product patterns of polylactide*. Polymer Degradation and Stability; 97; pp. 1254-1260.

Royal Society of Chemistry, 2009. *Ultraviolet - Visible Spectroscopy (UV)* [Online] Available at: http://www.rsc.org/learn-chemistry/resource/download/res00000282/cmp00001304/pdf [Accessed:13.03.2016].

Schliecker, G., Schmidt, C., Fuchs, St., Kissel, T., 2003. *Characterization of a homologous series of$_{D,L}$-lactic acid oligomers; a mechanistic study on the degradation kinetics in vitro.* Biomaterials; 24 (21); pp. 3835–3844.

Siracusa, V., Rocculi, P., Romani, S., Rosa, M.D., 2008. *Biodegradable polymers for food packaging: a review*. Trends in Food Sci & Tech; 19; pp. 634-643.

Soles, C.L., Chang, F.T., Bolan, B.A., Hristov, H.A., Gidley, D.W., Yee, A.F., 1998. *Contributions of the nanovoid structure to the moisture absorption properties of epoxy resins.* J Polym Sci Pol Phys; 36; pp. 3035–48.

Soroudi, A. & Jakubowicz, I., 2013. *Recycling of bioplastics, their blends and biocomposites: A review.* Europ Polym J; 49; pp. 2839-2858.

Starkova, O., Buschhorn, S.T., Mannov, E., Schulte, K., Aniskevich, A., 2013. *Water transport in epoxy/MWCNT composites. European Polymer Journal*; 49; pp. 2138-2148.

Stevels, W.M., Ankoné, M.J.K., Dijkstra, P.J., Feijen, J., 1996. *Kinetics and Mechanism of L-Lactide Polymerization Using Two Different Yttrium Alkoxides as Initiators*. Macromolecules; 29; pp. 6132-6138.

Stuart, B.H., 2005. *Infrared Spectroscopy: Fundamentals and Applications.* John Wiley & Sons; pp. 8-24.

Södegård, A. & Stolt, M., 2002. *Properties of lactic acid based polymers and their correlation with composition.* Prog Polym Sci; 27; pp. 1123-1163.

Taubner, V. & Shishoo, R., 2001. *Influence of processing parameters on the degradation of poly(L-lactide) during extrusion*. J Appl Polym Sci; 79 (12); pp. 2128-35.

Thomas, S. & Pothan, L.A., 2008. *Natural Fibre Reinforced Polymer Composites from Macro to Nanoscale.* Old City Publishing: Philadelphia; pp. 455-56.

Van de Weert, M., Hering,J.A., Haris, P.I., 2005. *Methods for Structural Analysis of Protein Pharmaceuticals: Fourier transform infrared spectroscopy* W. Jiskoot, D.J.A. Crommelin (Eds.) vol. 3, AAPS Press, Arlington; pp. 131–166.

Visakh, P.M., Thomas, S., Chandra, A.K., Mathew, A.P., 2013. *Advances in Elastomers II – Composites and Nanocomposites.* Springer Heidelberg New York Dordrecht London; pp. 167.

Wagner, H.L., 1985 *The Mark-Houwink-Sakurada Equation for the Viscosity of Linear Polyethylene.* National Bureau of Standards, Gaithersburg, J Phys Chem Ref Data; 14 (2).

Warrington, S.B., Höhne, G.W.H., 2008. *Thermal Analysis and Calorimetry*. Ullmann's Encyclopedia of Industrial Chemistry.

Weitsman, Y.J., 1995. *Effect of Fluids on Polymeric Composites – A review*. Office of Naval Research Arlington, Virginia, The University of Tennessee.

Weng, Y.X., Jin, Y.J., Meng, Q.Y., Wang, L., Zhang, M., Wang, Y.Z., 2013. *Biodegradation behaviour of poly(butylene adipate-co-terephtalate) (PBAT), poly(lactic acid) (PLA), and their blend under soil conditions.* Polymer Testing; 32; pp. 918-926.

William Reusch, 2013. *Visible and Ultraviolet Spectroscopy.* [Online] Available at: https://www2.chemistry.msu.edu/faculty/reusch/VirtTxtJml/Spectrpy/UV-Vis/spectrum.htm [Accessed: 13.03.2016].

XIAO, L., Wang, B., Yang, G., Gauthier, M., 2012. *Poly (lactic acid)-based biomaterials: synthesis, modification andapplications.* INTECH Open Access Publisher.

Zhou, J., Lucas, J.P., 1999. *Hygrothermal effects of epoxy resin. Part I: The nature of water in epoxy.* Polymer; 40; pp. 5505–12.

Åmand, L.E., Tullin, C.J., 1997. *The Theory Behind FTIR analysis*. Department of Energy Conversion, Chalmers University of Technology.

11. Appendices

11.1 Instruments

All instruments are listed by model and production company.

Hardware

Production company	*Model*
Rondol	Microlab Twin Screw Extruder
IQAP LAP	Hydraulic press PL-15
Atlas UVCON	F40UVB
Mettler Toledo	Analytical balance AJ100
Thermo Fisher Scientific	Nicolet iS10 FTIR Spectrophotometer
Perkin Elmer	Lambda 35
Shel Lab	Vacuum-oven
Memmert	Oven
IKA	A10 Cryogenic mill
Neuertek	Mega-Check FN
TA Instruments	TGA 2050

Software

Production company	*Model*
Origin®	6.1
Thermo Scientific™	OMNIC™ Specta Software 9
OPUS	5.5

11.2 Buffer

Phosphate buffer used for immersion of samples

0.05	M	Phosphat buffer
22	g	Na_2HPO_4
12	g	NaH_2PO_4
5	L	Deionized H_2O

11.3 FTIR analysis

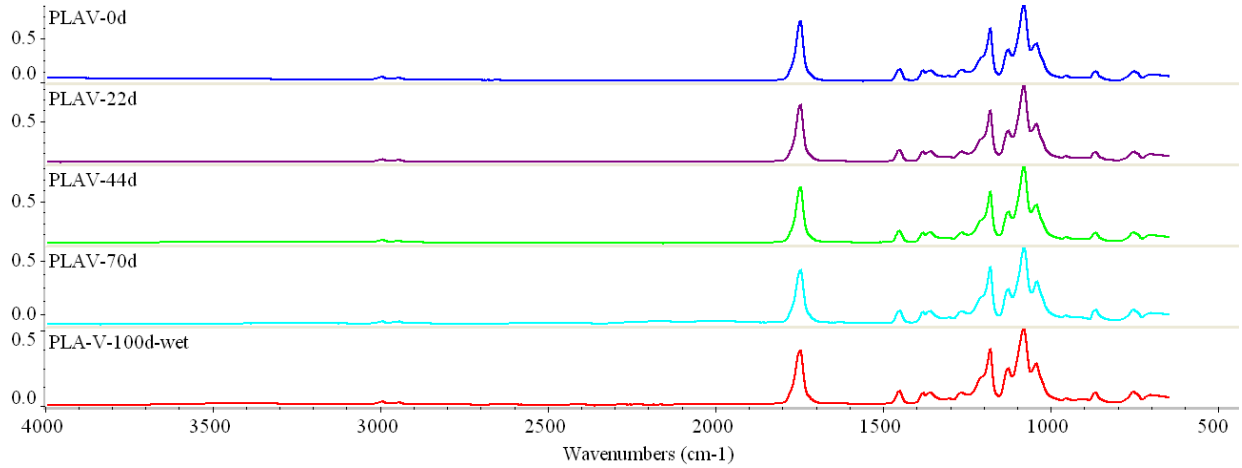

Figure 11.1: FTIR spectra for PLAV at day 0, 22, 44, 70 and 100.

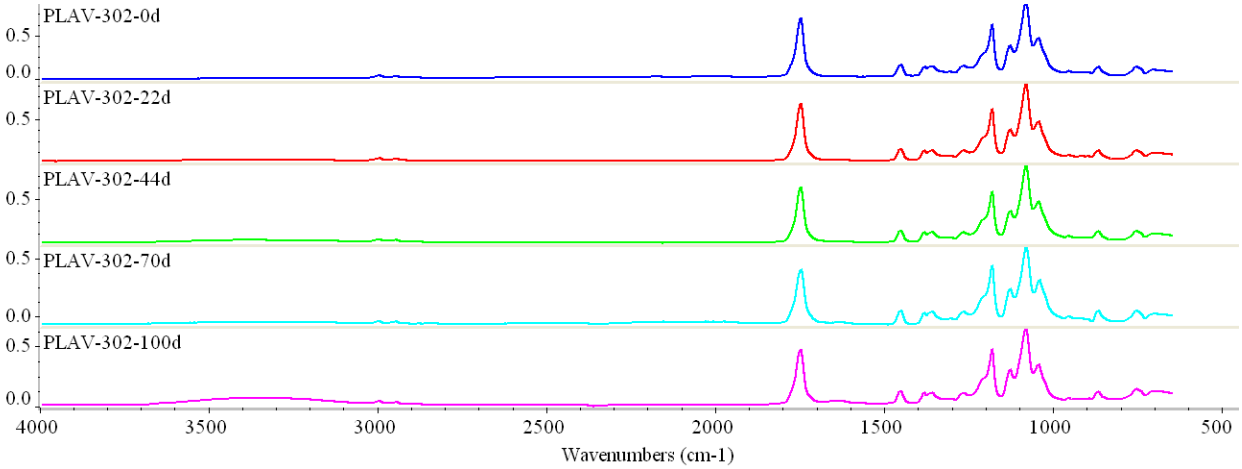

Figure 11.2: FTIR spectra for PLAV-302 at day 0, 22, 44, 70 and 100.

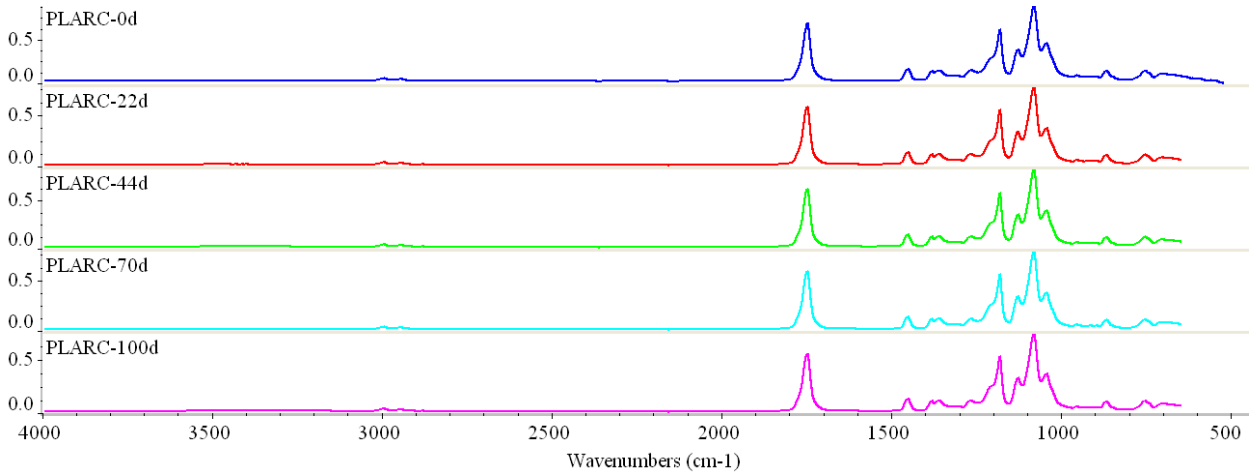

Figure 11.3: FTIR spectra for PLARC at day 0, 22, 44, 70 and 100.

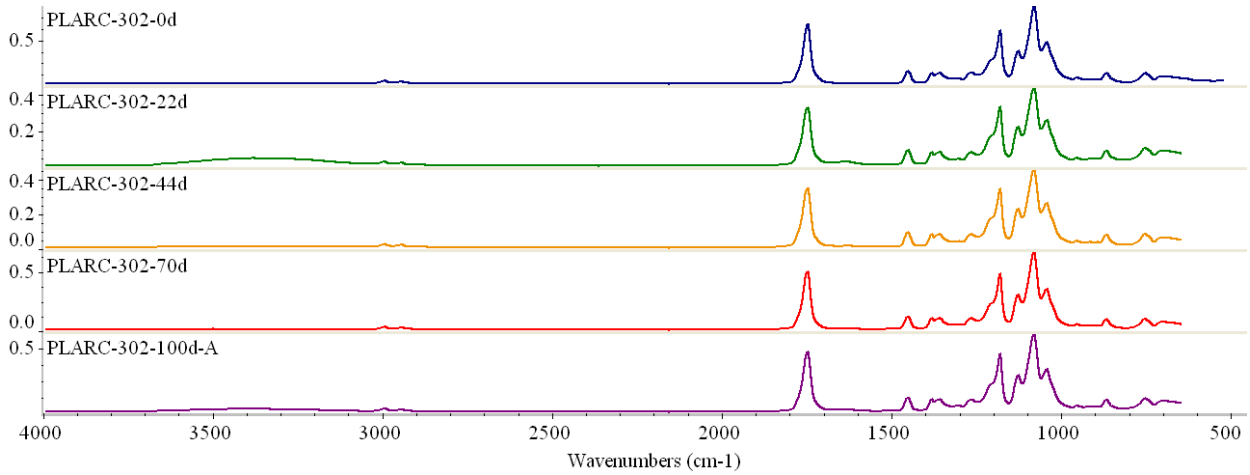

Figure 11.4: FTIR spectra for PLARC-302 at day 0, 22, 44, 70 and 100.

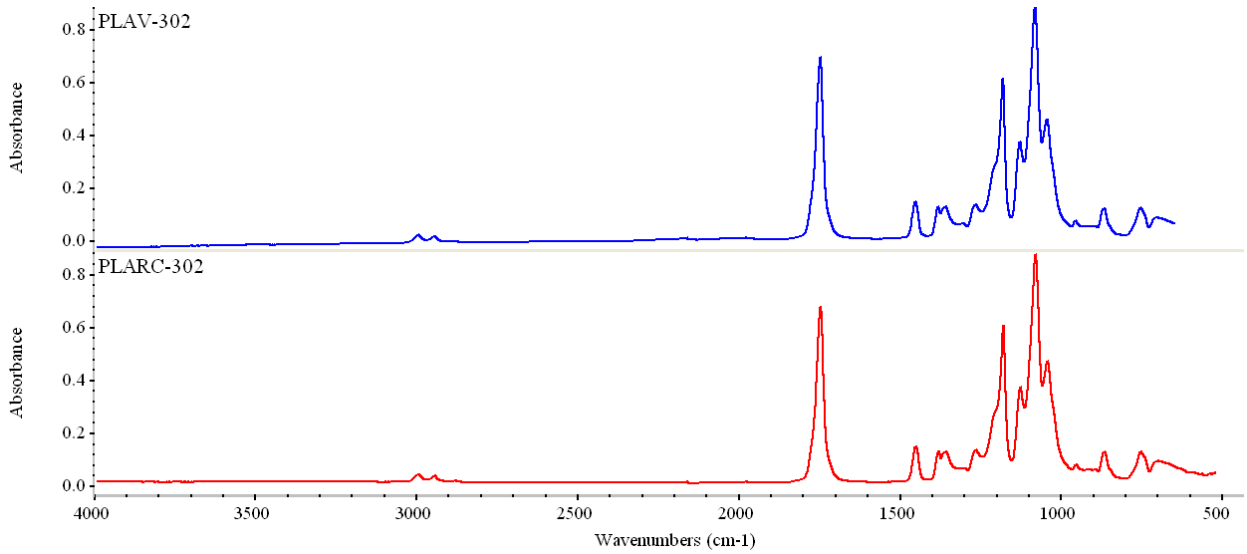

Figure 11.5: Comparison of the spectra of PLAV-302 and PLARC-302 at immersion day 0.

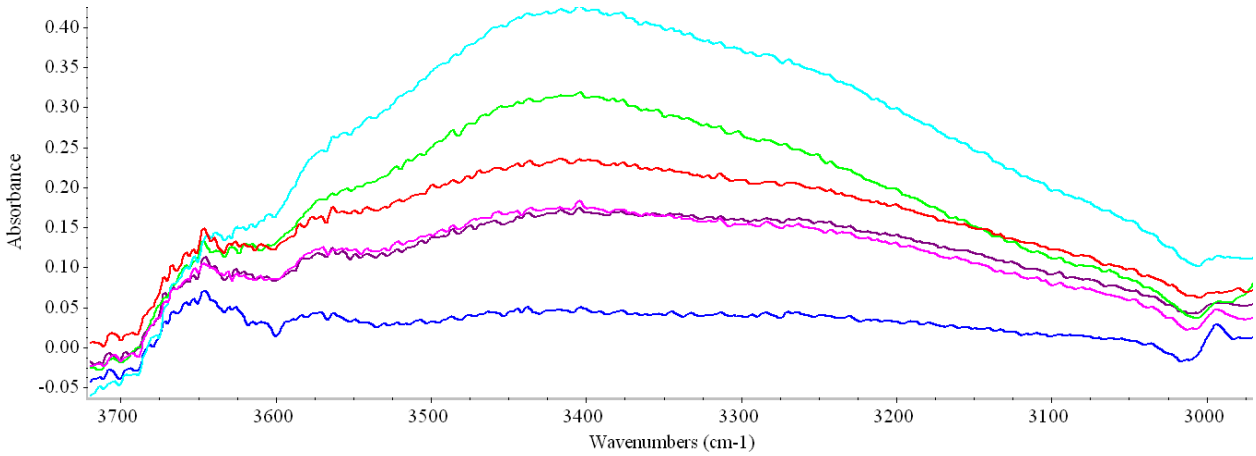

Figure 11.6: The evolution of the bands between 3700 and 3000 cm^{-1} for PLAV for immersion day 2 (blue), 6 (purple), 13 (pink), 22 (red), 44 (green) and 100 (light blue).

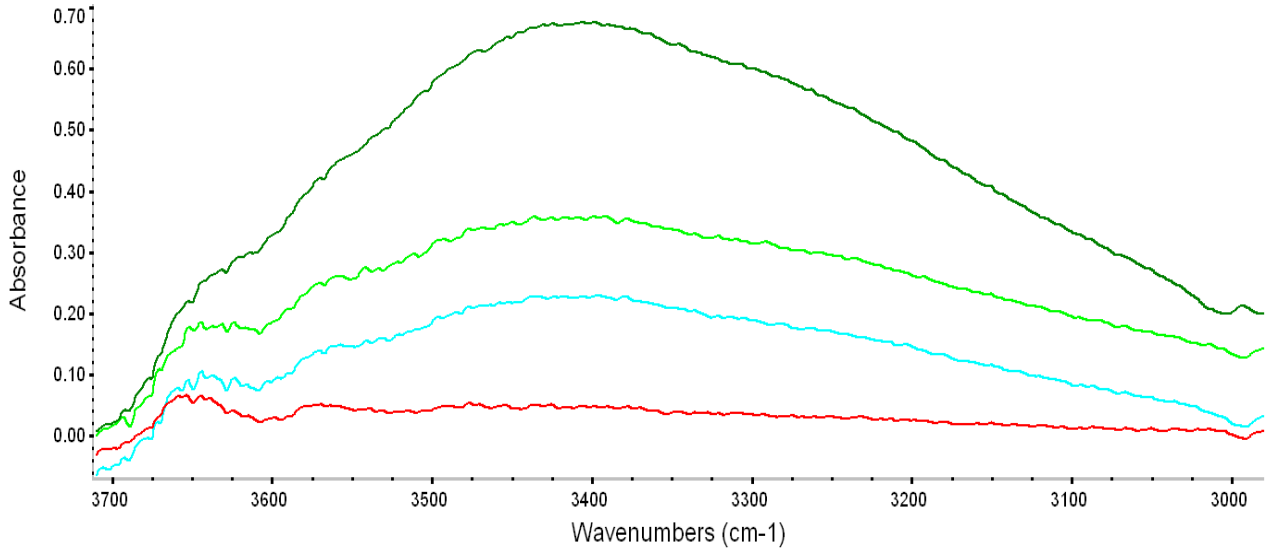

Figure 11.7: The evolution of the bands between 3700 and 3000 cm^{-1} for PLARC-302 for immersion day 2 (red), 22 (light blue), 44 (light green) and 100 (dark green).

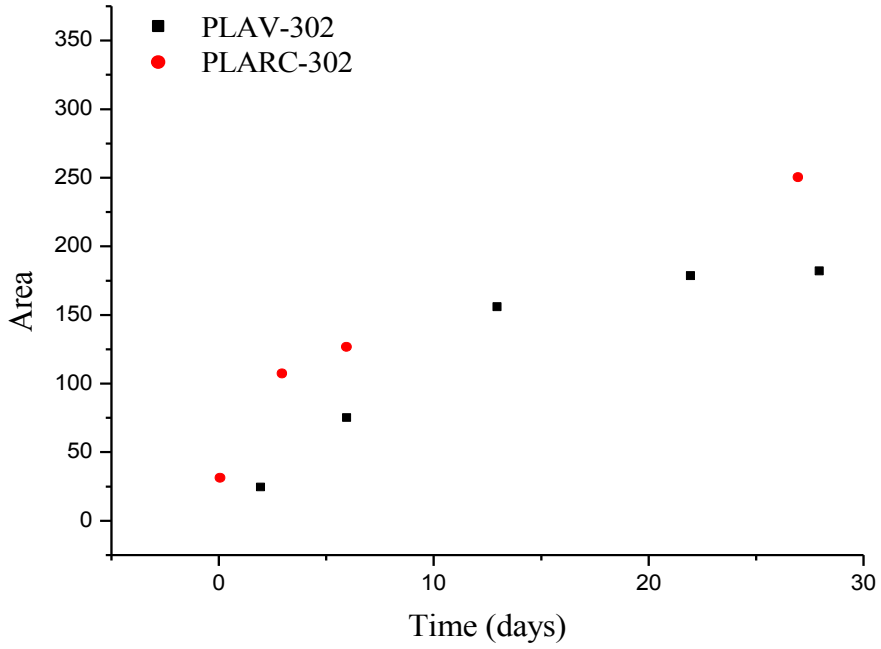

Figure 11.8: Measured area of band between 3700-3000 nm for PLAV-302 and PLARC-302 over immersion days.

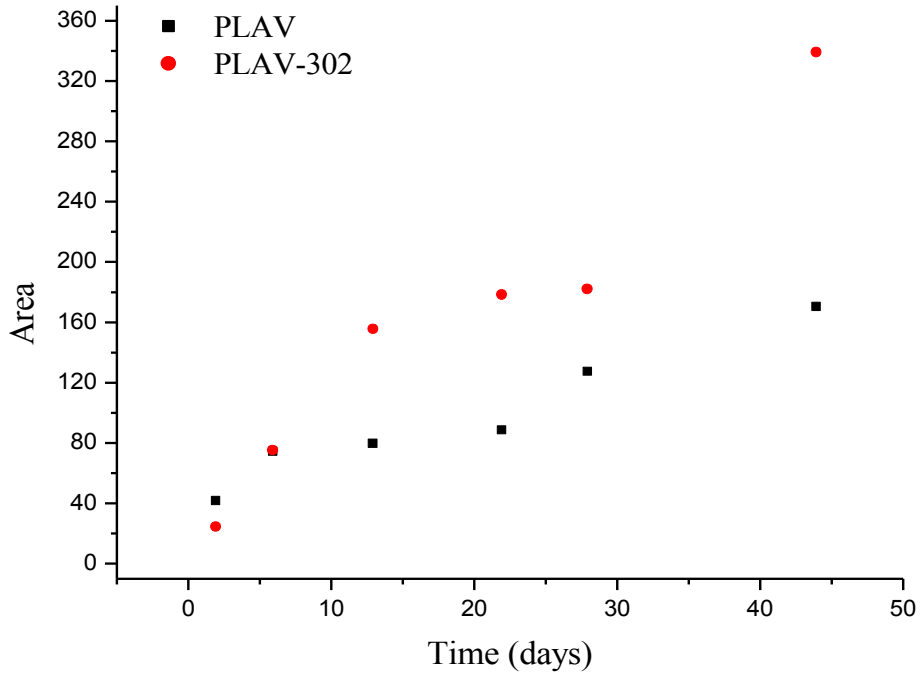

Figure 11.9: Measured area of band between 3700-3000 nm for PLAV and PLAV-302 over immersion days.

11.4 Gravimetric analysis

Table 11.1: Weighed masses of PLARC and PLARC-302 at immersion time up until 2 days.

	PLA-RL			PLA-RL302		
t (min)	**m_{P1} (g)**	**m_{P2} (g)**	**m_{P3} (g)**	**m_{P1} (g)**	**m_{P2} (g)**	**m_{P3} (g)**
0	0.3306	0.2675	0.2831	0.4358	0.3710	0.3566
10	0.3320	0.2685	0.2841	0.4370	0.3720	0.3579
30	0.3325	0.2689	0.2846	0.4378	0.3729	0.3584
60	0.3327	0.2691	0.2847	0.4387	0.3732	0.3588
90	0.3327	0.2691	0.2847	0.4385	0.3733	0.3588
120	0.3327	0.2691	0.2847	0.4388	0.3733	0.3589
240	0.3329	0.2692	0.2849	0.4390	0.3736	0.3591
360	0.3330	0.2693	0.2849	0.4393	0.3740	0.3593
480	0.3332	0.2694	0.2852	0.4395	0.3741	0.3596
1440	0.3336	0.2697	0.2853	0.4403	0.3746	0.3602

Table 11.2: Weighed masses before immersion for PLARC and PLARC-302, where the time is the intended immersion time.

	PLA-RL			PLA-RL302		
Days	**m_{P1} (g)**	**m_{P2} (g)**	**m_{P3} (g)**	**m_{P1} (g)**	**m_{P2} (g)**	**m_{P3} (g)**
2	0.3306	0.2675	0.2831	0.4358	0.3710	0.3566
6	0.4366	0.3309	0.3174	0.3807	0.2849	0.3459
13	0.2574	0.3240	0.3385	0.3120	0.4234	0.3866
22	0.4275	0.3634	0.2883	0.3269	0.2465	0.3836
28	0.3177	0.3656	0.2894	0.4230	0.3598	0.3946
44	0.3406	0.2963	0.4129	0.3793	0.3210	0.3868
56	0.2916	0.3570	0.3242	0.2903	0.3305	0.3928
70	0.3433	0.3876	0.3210	0.4455	0.3053	0.2969
84	0.4157	0.3673	0.3476	0.3681	0.3751	0.3573
100	0.2540	0.2586	0.3578	0.3078	0.4469	0.3349

Table 11.3: Weighed masses of PLARC and PLARC-302 at immersion time from 2-100 days

	PLA-RL			PLA-RL302		
Days	**m_{P1} (g)**	**m_{P2} (g)**	**m_{P3} (g)**	**m_{P1} (g)**	**m_{P2} (g)**	**m_{P3} (g)**
2	0.3336	0.2695	0.2852	0.4408	0.3748	0.3603
6	0.4411	0.3338	0.3200	0.3856	0.2886	0.3502
13	0.2598	0.3271	0.3412	0.3163	0.4297	0.3923
22	0.4319	0.3671	0.2910	0.3336	0.2507	0.3910
28	0.3213	0.3697	0.2921	0.4331	0.3674	0.4027
44	0.3448	0.2998	0.4181	0.3912	0.3304	0.3983
56	0.2957	0.3624	0.3287	0.3017	0.3433	0.4068
70	0.3495	0.3937	0.3259	0.4676	0.3195	0.3107
84	0.4237	0.3742	0.3554	0.3906	0.3981	0.3810
100	0.2596	0.2639	0.3682	0.3327	0.4846	0.3651

Table 11.4: Weighed masses of PLARC and PLARC-302 at immersion time from 2-100 days, after the samples had been dried for 1 week at 40°C.

	PLA-RC			PLARC-302		
Days	**m_{P1} (g)**	**m_{P2} (g)**	**m_{P3} (g)**	**m_{P1} (g)**	**m_{P2} (g)**	**m_{P3} (g)**
2	0.3307	0.2675	0.2830	0.4359	0.3710	0.3565
6	0.4367	0.3312	0.3173	0.3808	0.2850	0.3461
13	0.2574	0.3240	0.3384	0.3118	0.4232	0.3866
22	0.4275	0.3639	0.2883	0.3271	0.2465	0.3838
28	0.3176	0.3658	0.2893	0.4230	0.3599	0.3948
44	0.3406	0.2963	0.4132	0.3795	0.3211	0.3871
56	0.2919	0.3573	0.3246	0.2908	0.3306	0.3932
70	0.3436	0.3879	0.3213	0.4456	0.3057	0.2973
84	0.4155	0.3671	0.3475	0.3680	0.3752	0.3575
100	0,2541	0,2586	0,3580	0,3080	0,4471	0,3353

Table 11.5: Measured thicknesses for the samples used for the immersion at short days, from 0-2 days, executed at 5 different positions on each parallel sample.

	PLARC			PLARC-302		
Nr.	**1**	**2**	**3**	**1**	**2**	**3**
1	248	273	220	235	255	331
2	289	231	254	271	302	303
3	235	263	212	256	270	323
4	222	272	218	262	275	315
5	278	259	260	302	323	319

Table 11.6: Gravimetric massloss and absorbed water for PLARC-302 with the associated standard deviation all given in percent for 2-100 days.

Time (days)	$m_{PLA-RL302}$ (%)	St.dev (%)	m_{H20} (%)	St.dev (%)
2	0.002	0.026	1.071	0.050
6	-0.040	0.016	1.237	0.044
13	0.037	0.033	1.484	0.047
22	-0.038	0.033	1.856	0.143
28	-0.026	0.025	2.158	0.203
44	-0.054	0.023	2.959	0.109
56	-0.101	0.071	3.687	0.199
70	-0.096	0.064	4.657	0.243
84	-0.018	0.042	6.274	0.263
100	-0.076	0.039	8.438	0.439

Table 11.7: Absorbed water for PLARC and PLARC-302 from 10 min - 1 day with their associated standard deviation all given in percent.

	PLARC		PLARC-302	
Time (min)	m_{H20} (%)	St.dev (%)	m_{H20} (%)	St.dev (%)
10	0.384	0.036	0.303	0.053
30	0.543	0.028	0.492	0.029
60	0.600	0.035	0.625	0.037
90	0.600	0.035	0.619	0.002
120	0.600	0.035	0.651	0.035
240	0.656	0.035	0.712	0.019
360	0.678	0.045	0.790	0.028
480	0.746	0.038	0.842	0.007
1440	0.836	0.066	1.004	0.031

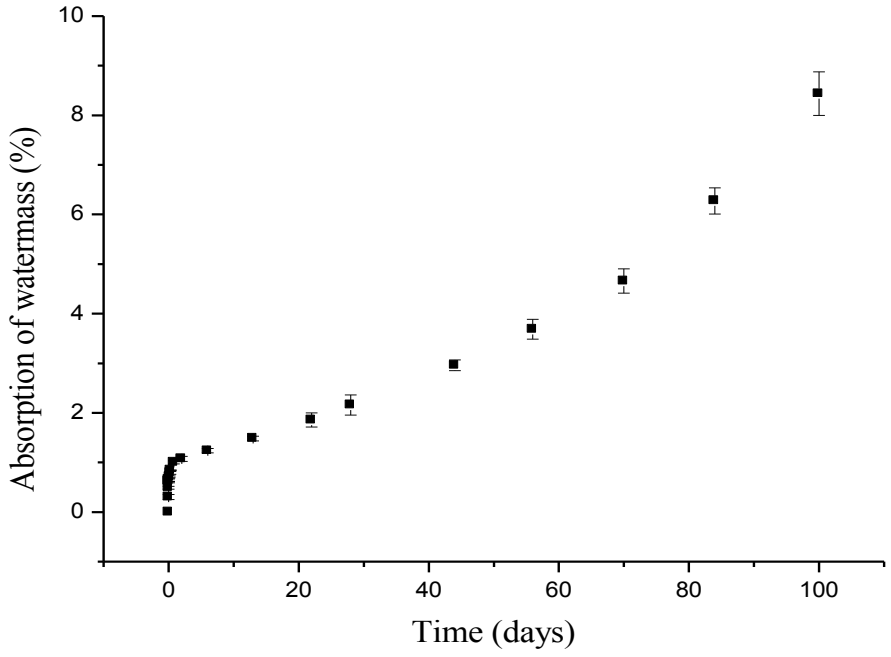

Figure 11.10: Water absorption showed in mass percentage plotted against time from 0-100 days for PLARC-302, with its associated error bars.

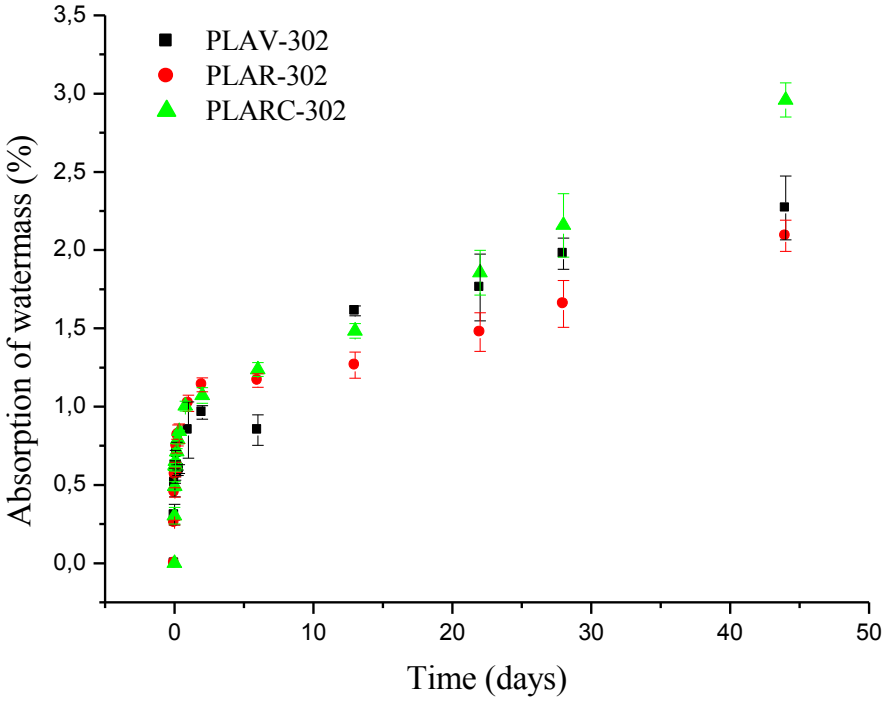

Figure 11.11: Evolution of absorbed water given in mass percentage for PLAV-302, PLAR-302, and PLARC-302 with corresponding error bars.

11.5 UV-Vis spectroscopy

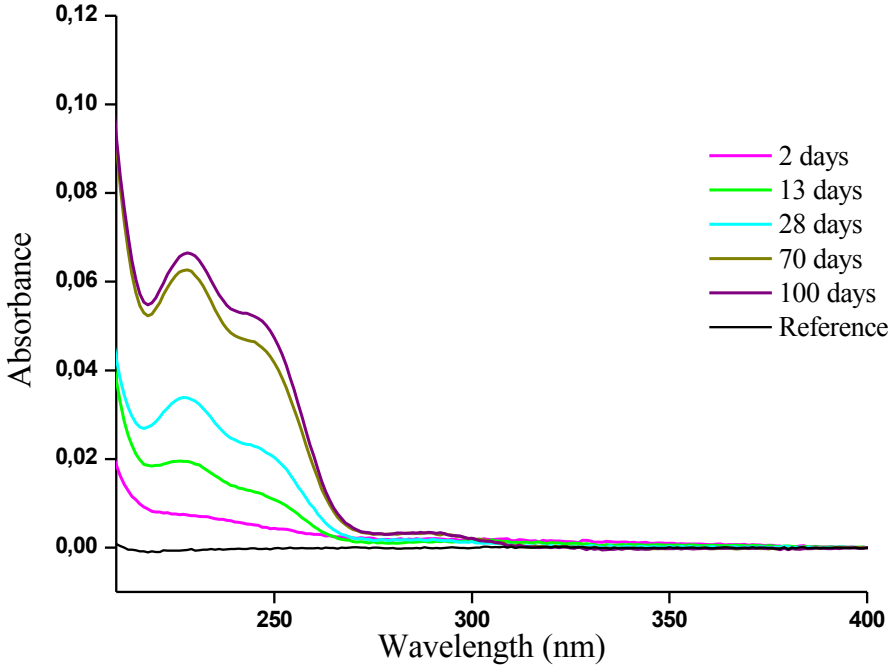

Figure 11.12: Spectra of the immersion liquid of PLAV at 2, 22, 28, 44 and 56 days.

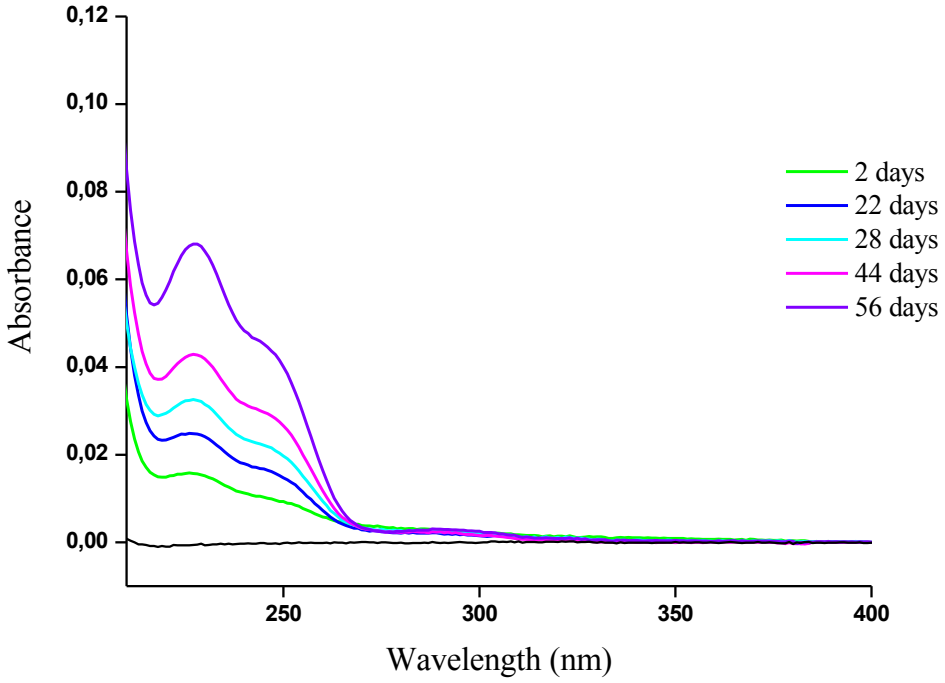

Figure 11.13: Spectra of the immersion liquid of PLARC-302 at 2, 22, 28, 44 and 56 days.

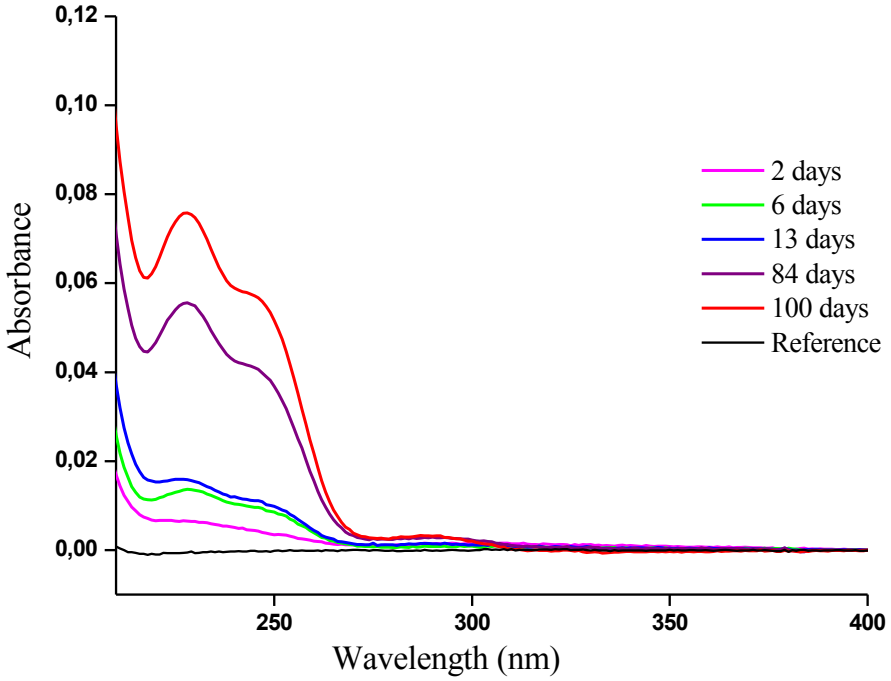

Figure 11.14: Spectra of the immersion liquid of PLAV-302 at 2, 22, 28, 44 and 56 days.

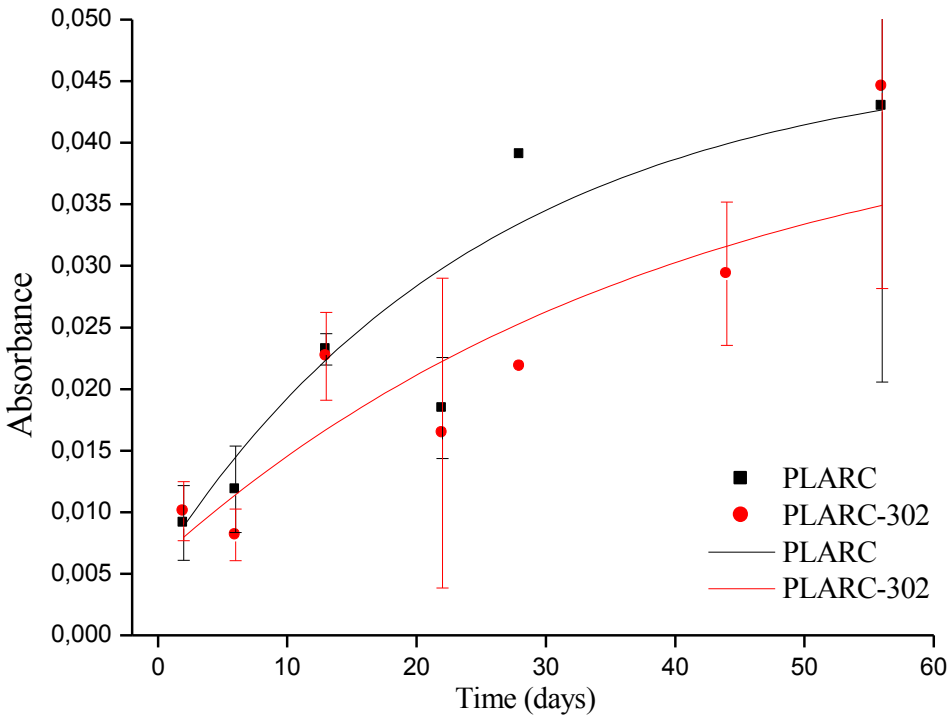

Figure 11.15: Evolution of the band at 246 nm in PLARC and PLARC-302 over immersion time with corresponding first order decreasing exponential fit.

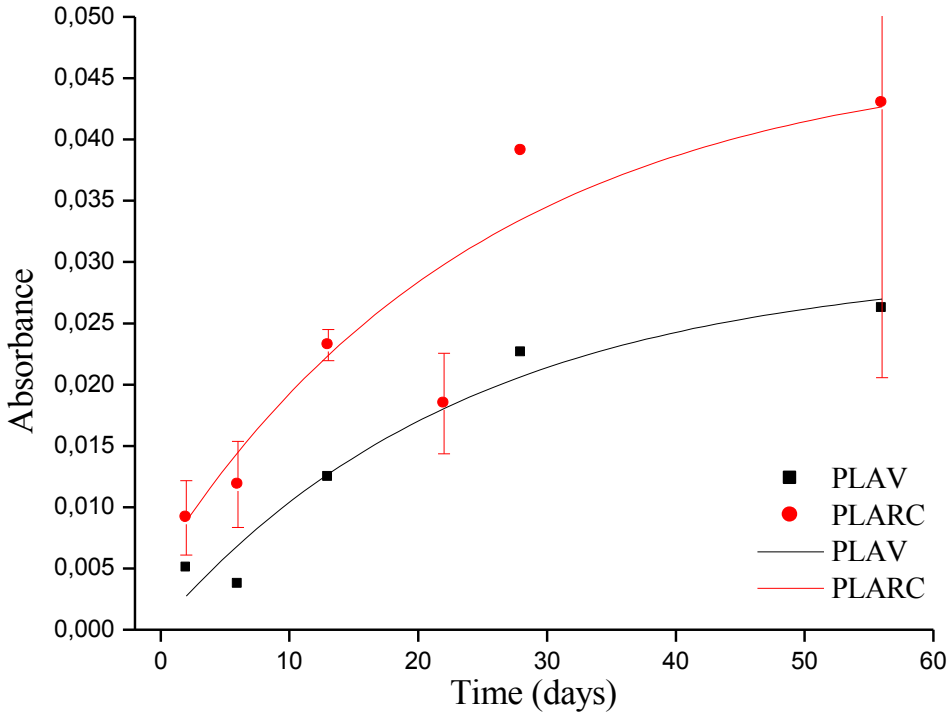

Figure 11.16: Evolution of the band at 246 nm in PLAV and PLARC over immersion time with corresponding first order decreasing exponential fit.

11.6 Viscosity

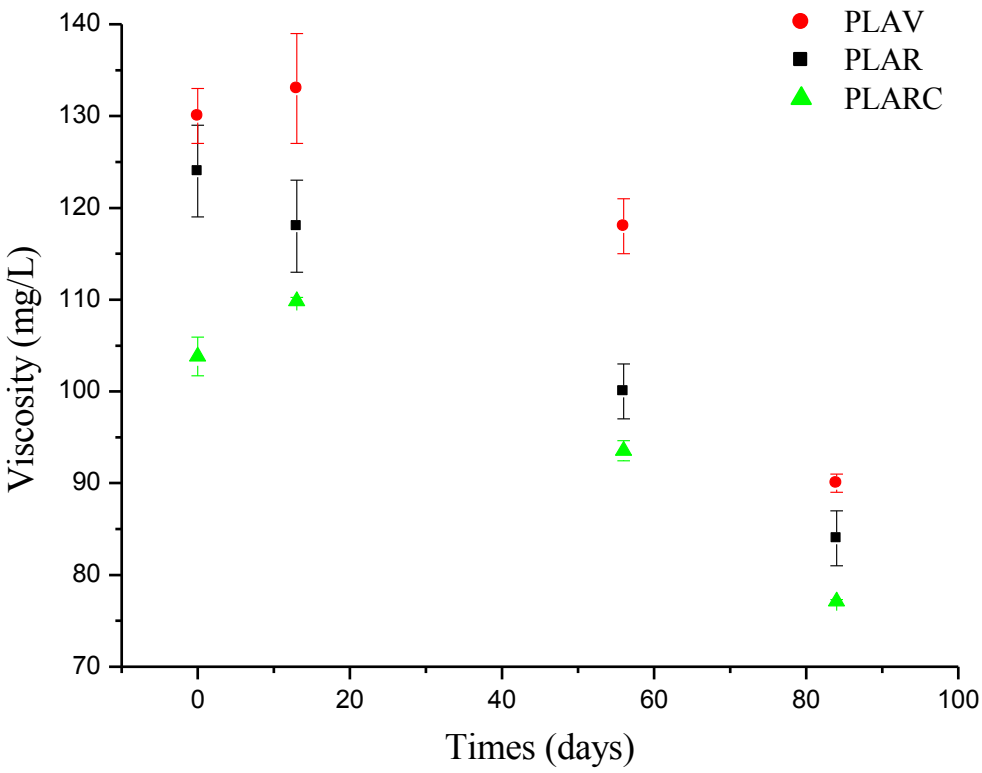

Figure 11.17: Comparison of the evolution of viscosity of virgin, recycled and recycled-cleaned materials at 0, 13, 56 and 84 days.

Table 11.8: Viscosities for test-samples of PLAR in cleaning-step with corresponding standard deviation, where the first condition was as following; 15 minutes at 85°C with 1 % NaOH and 0.3 % surfactant Triton 100x. Second condition: 5 minutes at 65°C with 0.5 % NaOH and 0.1 % surfactant Triton 100x.

Sample	Viscosity (mg/L)	St.dev
First condition, dried in oven at 40°C over night	118.8	1.2
Second condition, dried in oven at 40°C over night	122.5	2.2

Table 11.9: Measured viscosities at 25°C for PLARC and PLARC-302 of immersion days 0, 13, 56 and 84 with corresponding standard deviation.

Sample	Viscosity (mg/L)	St.dev
PLARC		
0 days	103.8	2.1
13 days	109.9	0.3
56 days	93.5	1.1
84 days	77.1	0.2
PLARC-302		
0 days	101.8	0.9
13 days	113.5	2.2
56 days	77.5	2.2
84 days	69.1	1.3

11.7 Thermogravimetric Analysis

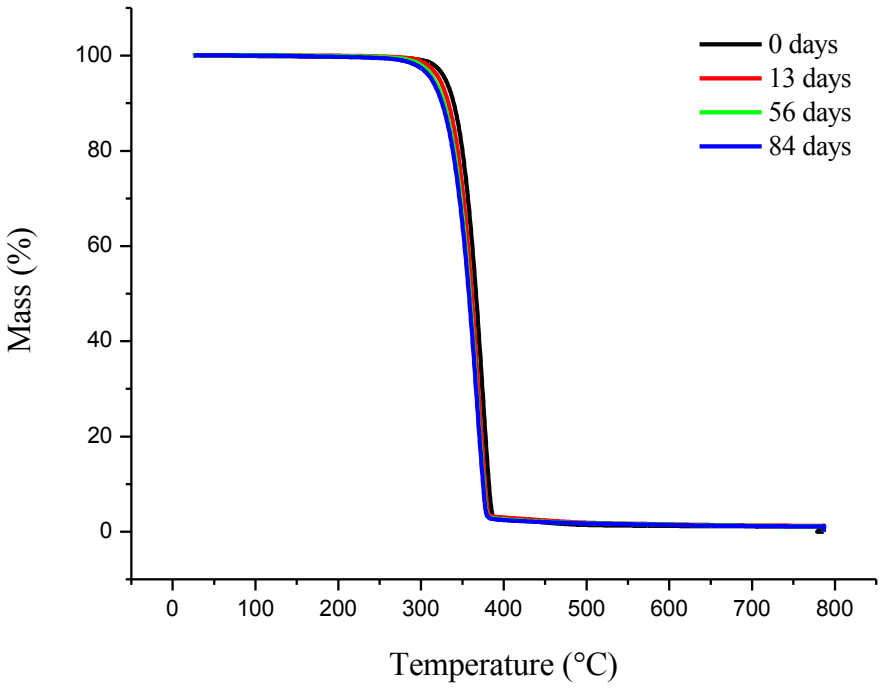

Figure 11.18: Thermograms for PLARC-302 immersed at day 0, 13, 56 and 84.